Methane Production from Natural Gas Hydrates

Impact of Temperature on CH_4 -CO_2 Exchange rate in Hydrate Bearing Sandstone

A Master´s Thesis in Reservoir Physics

By

Truls Hamre Håheim

Department of Physics and Technology

University of Bergen

Norway

I. Summary

Dissociation by pressure depletion, thermal stimulation and/or injection of inhibitors are three known methods for gas production from natural gas hydrates. Challenges concerning these production methods are water and sand production as well as a potential loss of geo-mechanical stability, which may cause subsidence and landslides. A fourth production scheme, studied in this thesis, is based on the exchange process taking place when methane hydrate is introduced to the more thermodynamically stable guest molecule carbon dioxide. Sequestration of CO_2 in hydrate follows as an added benefit to released methane gas.

This thesis investigates experimentally the impact of temperature on CH_4-CO_2 exchange within hydrate-bearing sandstone. All experiments have been conducted at the Department of Physics and Technology, University of Bergen. The experimental work performed covered three main procedures; 1) methane hydrate formation in consolidated sandstone cores, 2) exchange between methane stored in hydrate and injected liquid carbon dioxide, and 3) hydrate dissociation either by depressurization or thermal stimulation.

Time and effort was used on improving the hydrate laboratory with regards to safety, more accurate measurements, and ease of use. To achieve this goal, new instruments and solutions were implemented, service on old equipment was carried out, and new tubing systems were implemented where needed.

Methane hydrate was successfully formed in eleven Bentheim sandstone cores with similar initial water saturation (S_{wi}=0.4) and brine salinity (0.1 wt%), providing equal initial conditions for the CH_4-CO_2 exchange process. Repetitiveness in post hydrate results were observed at equal initial properties. A consistent trend was also observed where increased initial water saturations (S_{wi}>0.6) and increased salinity (3.5 wt%) resulted in a decrease in hydrate saturation when compared with earlier experimental results.

Following the completed hydrate formation, six CH_4-CO_2 exchange experiments were conducted at two different temperatures (4° C and 9.6° C). Liquid carbon dioxide was injected into the core at a slow rate (1.2ml/h) and effluent, composition and mass were measured. A spontaneous exchange process was proven in several experiments, consequently producing methane from the solid hydrate and sequestrating carbon dioxide. Based on the experimental results there is a strong indication towards an increase in both exchange rate as well as total methane recovery with an increase in temperature, especially when close to the equilibrium line where the hydrate is less stable.

A new approach of adding heat to the system was tested by co-injecting carbon dioxide with a potential catalyst for CH_4-CO_2 exchange; methyldiethanolamine (MDEA) or monoethanolamine (MEA). Injection of these liquids post pure CO2 injection and CH_4-CO_2 exchange showed no enhanced recovery of methane from hydrate. A modified setup was designed where MEA could be injected by a separate pump and therefore be introduced ahead of the carbon dioxide. A high methane recovery was observed at a high recovery rate. This was most likely due to melting of the hydrate which can be verified by observation of water in the production line.

Dissociation of both pure and mixed hydrate (CH_4 and CO_2) by thermal stimulation with a stepwise increase in temperature showed different equilibrium temperatures. The mixed hydrate dissociated at a range of higher temperatures, compared to pure methane hydrate. This verifies presence of carbon dioxide and the increase in stability for a mixed hydrate where carbon dioxide is present.

II. Acknowledgements

First and foremost I would like to express my gratitude to Professor Arne Graue for giving me the opportunity to work with the challenging and fascinating topic of natural gas hydrates.

I am grateful for the guidance, knowledge and good spirits provided by Associate Professor Geir Ersland, whom has been a true inspiration.

I would like to thank Phd students Lars Petter Haugen and Knut Arne Birkedal for being more than helpful and patient both in the laboratory work as well as during data analysis.

The knowledge and time provide by Professor Bjørn Kvamme is greatly appreciated.

I am also grateful for the collaboration with my dear friend and laboratory partner Reza Houssainpour. Thank you for sharing your knowledge and your great spirits! To all of my fellow students at the reservoir physics group and IFT, thank you for creating a great student environment.

I would furthermore like to express my gratitude to my family, and especially my mom and dad, for being supportive, loving and kind.

Last but not least a big thank you to all of my dear friends!

Bergen, June 17. 2013

Truls Hamre Håheim

Table of Contents

III. Preface

The future outlook concerning global energy demand is pointing towards a necessity for new and cleaner energy resources. Global sustainability in terms of energy cover topics like greenhouse gases, climate change, alternative energy resources and handling of carbon dioxide emission (Jung et al., 2010). A population growth is expected in the decades to come, as well as an increase in energy demand as there today is 1.3 billion people lacking electricity (IEA, 2012). In parallel, environmental considerations for a more global sustainability are a high priority and a necessity. Scarcities of conventional energy resources as well as a retreat in nuclear energy in some countries result in a demand for a new energy system. This could lead to a shift and an adaption in the economics towards unconventional energy commodities (Strauss, 2012). The oil and gas industry could hold a key role in this transition and become the main driver of change with its experience and technological advantages. As the figure below illustrate, the energy resource outlook points towards an increase in unconventional gas. Natural gas hydrates could potentially be a major part of this segment in the future. If the production method based on an exchange process is achievable in terms of profit in the future, where the injected greenhouse gas carbon dioxide is stored and methane produced, it would be a step in the right direction of meeting the demand of a cleaner energy.

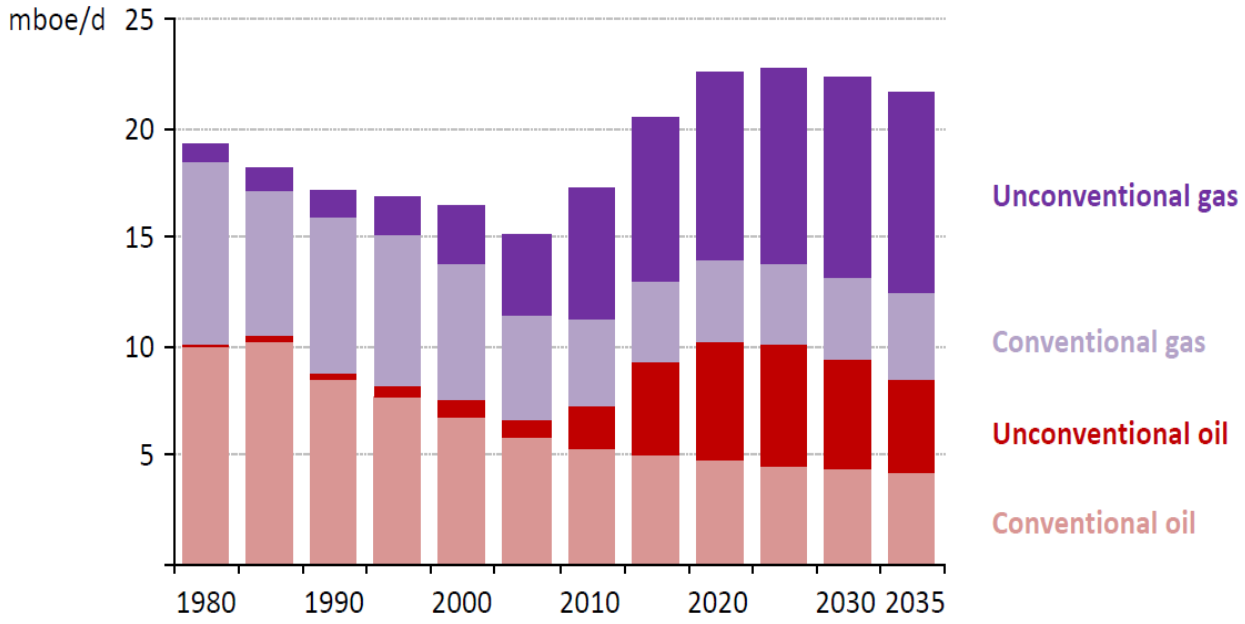

Figure III-I: US oil and gas production in the past, present and anticipated future (IEA, 2012). The graph illustrates an increase in production of unconventional gas in the years to come. Natural gas hydrates may be a participant in this segment.

IV. Introduction

Natural gas hydrates are ice-like compounds often referred to as burning ice. Methane encaged by water molecules in the solid state of hydrate is compressed, and the global amount of methane present in the earth in hydrates is vast. Hydrate may form where gas and water are both present under high pressure and low temperature conditions. Such conditions may be found in permafrost regions, as well as in sub-marine sediments on continental margins. Estimates of global energy content are uncertain but several suggest that methane in gas hydrate carry energy in the same order of magnitude as conventional fossil fuels combined. Due to the vast amount of energy stored in natural gas hydrates there is, and has been, a great interest in research and development so that this resource will come to be a conventional resource in the future, providing relatively clean energy as well as meeting the future energy demand.

Hydrate research can historically be divided into three eras; 1) as a scientific curiosity, 2) a man-made problem in gas and oil transportation and 3) as a potentially vast energy resource present in nature. Gas hydrates were first discovered in 1810 by Sir Humphrey Davy in the laboratory and were mainly regarded as a scientific curiosity (E.D. Sloan et al., 2007). When transportation of gas in pipelines under high pressure and low temperature was achieved in 1934, hydrate growth occurred at temperatures above the ice point resulting in plugging of the pipeline. Hydrate plugs can potentially act as a projectile, as the pressure difference increase, causing great harm both to equipment and personnel. Immense resources have and still are used to prevent hydrate formation in pipelines (E.D. Sloan et al., 2007). When occurrence of hydrates in nature was proposed in the late 1960s a new source of potential energy was born. Today great challenges still prevent economically viable gas production from natural gas hydrate deposits. Production techniques proposed are based on dissociation of the hydrate, where depressurization of the hydrate reservoir, thermal stimulation, or injection of inhibitors are possible methods. Depressurization is the most promising technique, or a combination of the three methods. But regardless of which of these methods used, great challenges like water production, sand production, and geo-mechanical instabilities will be present. An alternative production method, which this thesis investigates, is to inject carbon dioxide into the natural gas hydrate reservoir. The carbon dioxide is, at a wide range of temperatures, more thermodynamically stable than methane, subsequently triggering a spontaneous exchange where methane is released and carbon dioxide stored within the solid hydrate. This production method prevents water and sand production since the hydrate remains solid, and therefore also preventing geo-mechanical instabilities. Though this production method clearly has

encouraging abilities, there are still great concerns regarding the exchange rate and the total recovery of methane, consequently questioning the economical viability of this production method.

The Department of Physics and Technology at UIB have studied the CH_4-CO_2 exchange process as a potential natural gas hydrate production method for many years. Previous in-house studies consist of verification of CH_4-CO_2 exchange and hydrate formation patterns in porous sandstones by MRI visualization (Graue et al., 2006), the effects of boundary conditions on formation and dissociation kinetics (Birkedal, 2009), impact of brine salinity and initial brine saturations (Husebø, 2008), measurements of gas permeability and non-Darcy flow in gas-water-hydrate systems (Ersland, 2008) and impact of temperature on the methane recovery after exchange (Bringedal, 2011). By continuing research on natural gas hydrate and improving the experiments for more accurate measurements more data will be available for further knowledge on this subject.

The five chapters presented in this thesis are meant to provide insight to natural gas hydrates. Chapter one consists of basic theory relevant to the experimental procedures and results presented in chapter two and three, before conclusions and future work in chapter four. Chapter five provides formulas used for calculations.

Part 1

Introduction on Natural Gas Hydrates

1 Natural Gas Hydrates

This chapter will provide an introduction on natural gas hydrate (NGH). Topics that will be discussed are the characteristics of NGH and its constituents, its potential as an energy resource, the different production schemes and challenges concerning methane production from NGH. This thesis is based on a CH_4-CO_2 exchange process as a production method, and therefore there will be emphasis on this subject when discussing NGH. The theory will mainly be founded on the book "Clathrate Hydrates of Natural Gases" by E. Dendy Sloan and Carolyn A. Koh (E.D. Sloan et al., 2007), and is recommended for further reading.

1.1 Natural gas hydrates (NGH)

Natural gas hydrates are ice like crystalline solids formed by water and natural gas, and are often referred to as burning ice. Given the required conditions, high pressure and low temperature, water molecules will interconnect in an open structure and encage gas molecules to provide stability to the clathrate structure. This trapped natural gas, mostly methane in great abundance in nature (Hester et al., 2009), is referred to as a guest molecule or a hydrate former, and is of great interest due to its energy potential.

1.1.1 The water molecule

Water is the main component in hydrate and its special properties, such as the structure of the water molecule, provides the foundation of hydrate formation. It is a colorless liquid, with an unusual high boiling point at 100° C and a melting point at 0°C. Water is at its most dense between 0° C and 4° C, and as a unique result water will expand upon freezing, making ice float on liquid water.

The water molecule has a nonlinear structure consisting of one oxygen atom (O) in a covalent bonding with two hydrogen atoms (H). The oxygen atom has eight electrons, with the electronic configuration $1s^2 2s^2 2p^4$, and each hydrogen atom has an electronic configuration $1s^1$. The bent structure of the water molecule has an angle of 105° (Daintith et al., 2010). The shared electrons with the protons give the molecule two positive charges, and the lone pair electrons give the molecule two negative charges (E.D. Sloan et al., 2007). This results in a molecule with four charges and a permanent dipole. The aligning of the hydrogen and oxygen atom, caused by the attraction of the positive pole on one molecule to a negative pole on the nearby molecule, is called a hydrogen bond. Each water molecule is then attached to four other water molecules arranged tetrahedrally around the central molecule, as illustrated in

Figure 1-1, by donating two and accepting two hydrogen bonds (E.D. Sloan et al., 2007). This electrostatic attraction between the molecules is only a $1/10^{th}$ or $1/20^{th}$ as strong as a covalent bond, but is still strong enough to explain the special properties water possesses (Carroll, 2002).

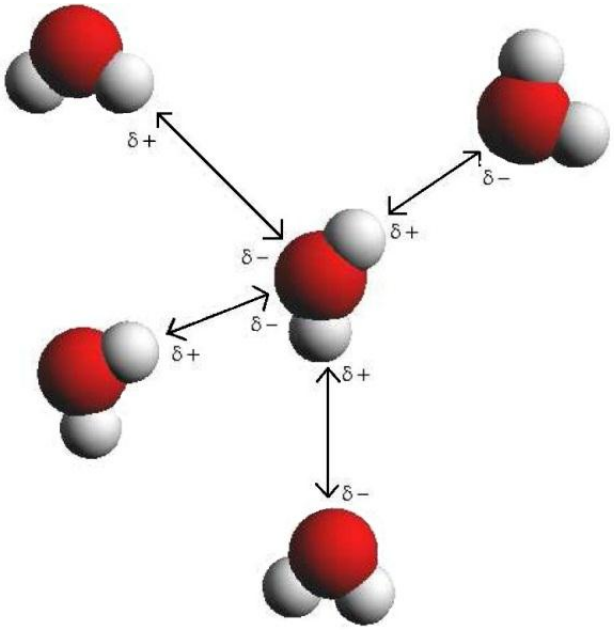

Figure 1-1: Illustration of water molecules and the attraction between them through hydrogen bonding. The center molecule attracts four water molecules by its two positive and two negative poles (Birkedal, 2009).

1.1.2 Natural Gas

Natural gas is a term used mainly for hydrocarbons such as methane, ethane and propane. These hydrocarbons are of interest because of their energy potential as fuels or as a feedstock for petrochemical plants (Carroll, 2002). The term also includes less valuable non-hydrocarbons such as nitrogen, carbon dioxide and hydrogen sulfur. The guest molecules used in this thesis will be the natural gases methane (CH_4) and carbon dioxide (CO_2), where methane is produced for its energy potential, and the greenhouse gas carbon dioxide is injected and stored in the hydrate.

Methane is a natural gas and is denoted CH_4. It is the most important energy component in natural gas, and a significant portion of the world industry depends on methane for fuel (Kvenvolden, 2001). The gas is colorless, with a melting point at -182.5° C, a boiling point at -164° C, and it is the simplest hydrocarbon, being the first member of the alkane series (Daintith et al., 2010). Methane will be in gas

phase at the temperature and pressure regimes used in the experiments conducted in this thesis, as well as in geological reservoir applications. Its mass density and viscosity compared to water is low at reservoir conditions (Espinoza et al., 2011). Methane bound up in natural gas hydrates is either formed from bacterial or thermogenic methane (Yang et al., 2008). The bacterial methane usually forms structure I hydrates, and is generated from bacteria via either reduction from CO_2 or acetate fermentation. Thermogenic methane is generated by organic matters underlying high pressure and temperature and is supplemented with concentrations of ethane, propane and butane, resulting in a structure II type hydrate (Yang et al., 2008).

The carbon dioxide molecule contains one carbon atom and two oxygen atoms in a linear structure and is denoted CO_2. It is a colorless and odorless gas which is soluble in water, and is only in a liquid phase at high pressures (Daintith et al., 2010). CO_2 forms from combustion and biological processes. Its physical and chemical properties are dependent on pressure-temperature conditions. As CO_2 move from standard conditions (15.5° C, 1 atm) to laboratory/reservoir conditions, with temperatures ranging from 4° C to 9° C and a pressure around 80 bar, the CO_2 will change properties and the density will increase. As seen from the phase diagram in Figure 1-2, the CO_2 will be in liquid phase at 83 bars at both temperatures used in this thesis (4° C and 9.6° C).

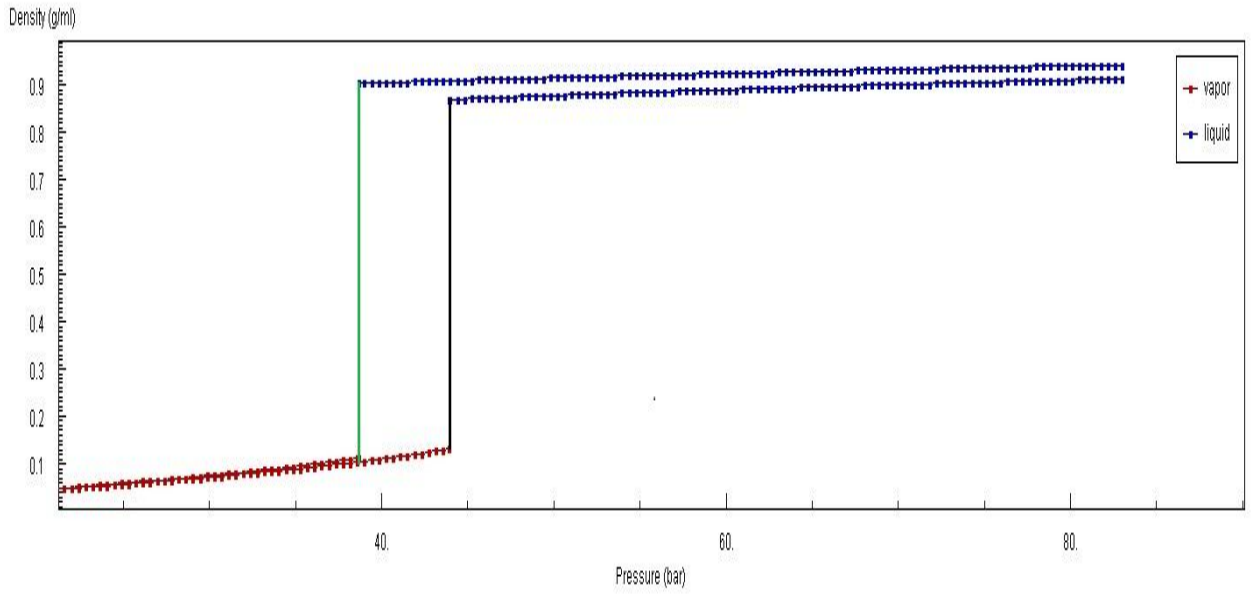

Figure 1-2: Graph showing how the density of carbon dioxide changes as a function of pressure. The green line is at 4° C and the black line is at 9° C (NIST, 2011), proving carbon dioxide is in a liquid state during experiments conducted in this thesis (4° C – 9.6°C, 83 bar).

1.2 Structures, cavities and guest molecules of NGH

Hexagonal ice (ice Ih) is the most common water solid, and forms as a pure component. But when water is exposed to a natural gas under high pressure and low temperature conditions, it will crystalize as a natural gas hydrate where different structures will occur. In this section the different structures, its cavities and the guest molecules present will be reviewed, and are illustrated in Figure 1-3.

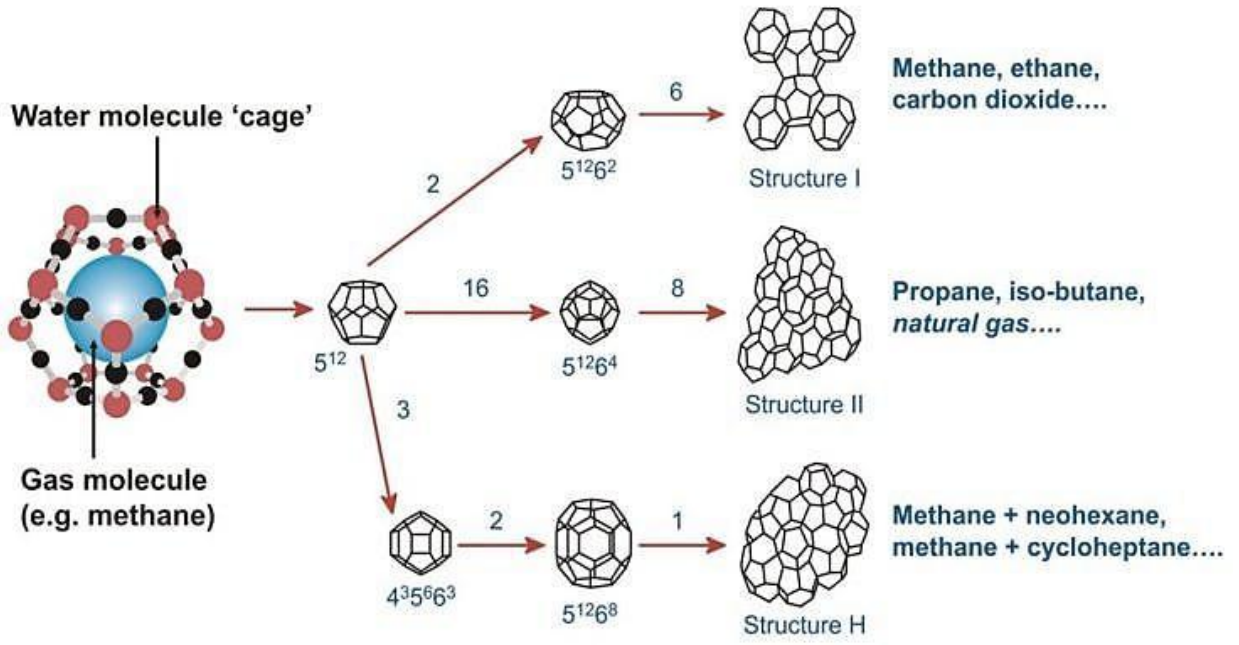

Figure 1-3: An overview over the different natural gas hydrate structures, its associated cavities and guest molecules possible for each structure (HWU, 2013).

1.2.1 Structures in natural gas hydrates

Natural gas hydrates are divided into three main structures, cubic structure I (sI), cubic structure II (sII) and hexagonal structure H (sH). The different hydrate structures have repetitive crystal units built by asymmetric and spherical-like cages of hydrogen bonded water molecules, and are based on and separated by their cavity size and the ratio between large and small cavities (Ersland, 2008). Structure I and structure II are of more interest than structure H in this thesis because they are the structures found in nature. Cubic structure I is the structure present in the hydrate formed in the laboratory experiments conducted in this thesis. There will not be much emphasis on structure H. The difference between structure I and structure II is a result of the variance in how the basic 5^{12} cavity achieves fourfold hydrogen bonds (E.D. Sloan et al., 2007).

Cubic structure I hydrates consist of two pentagonal dodecahedron (5^{12}) and six tetrakaidecahedron ($5^{12}6^2$). 46 water molecules hold together these eight polyhedrons within the cube (E.D. Sloan et al., 2007). Cubic structure II hydrates consist of sixteen pentagonal dodecahedron (5^{12}) and eight tetrakaidecahedron ($5^{12}6^4$) held together by 136 water molecules per unit cell. Hexagonal structure H hydrates are more complex, and has three different cages. The three different structures are illustrated in Figure 1-3. Both structure I and structure II can occur when formed by light hydrocarbon gases like methane. But where structure I can form purely on methane, structure II needs a larger component to stabilize the big cage ($5^{12}6^4$) to maintain its structural stability (Husebø, 2008).

1.2.2 Cavities

The volumetric space where the guest molecule is trapped is referred to as a cavity. Pentagonal and hexagonal faces are essential in the geometries of hydrate cavities. The different structures (sI, sII, sH) are built up by unlike sized cavities consisting of a combination of 12 pentagonal faces and 2 or 4 hexagonal faces. An illustration of a small and large cavity with a residing molecule (CH_4) is found in Figure 1-4. Small molecules residing in small cavities can also reside in large cavities. Large molecules can stabilize structure I and structure II by occupying the large cavities, leaving the small cavities empty. Structure H needs both small and large cavities occupied to be stabilized.

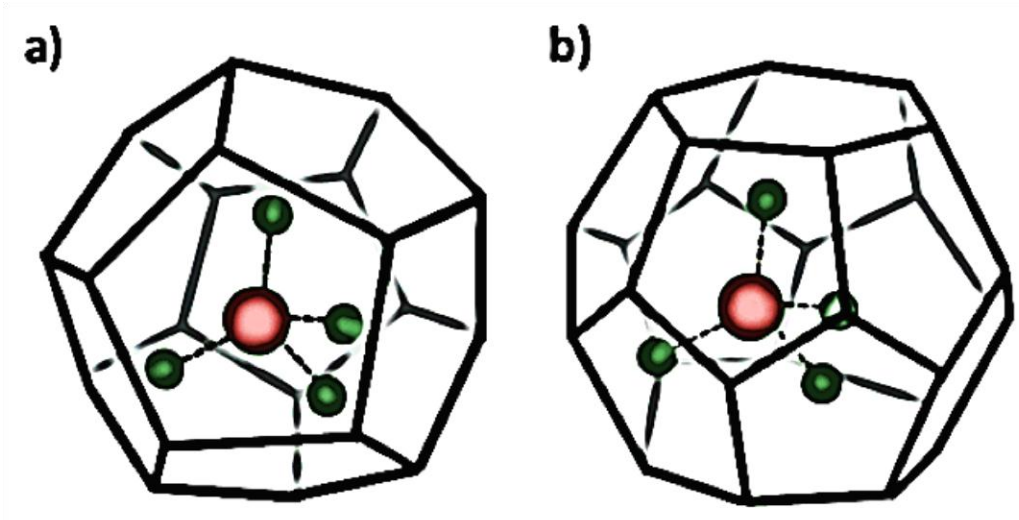

Figure 1-4: (a) Small cavity; pentagonal dodecahedral (5^{12}) and (b) large cavity; tetrakaidecahedron ($5^{12}6^2$). water cages for structure I hydrate with one guest molecule (methane) occupying both cavity sizes (Harrison, 2010).

There are three different types of cavities that engage in structure I and structure II hydrates; 1) Pentagonal dodecahedron, 2) Tetrakaidecahedron and 3) Hexakaidecahedron. The smallest cavity, pentagonal dodecahedron is present in all three structures mentioned in this thesis. An overview showing some properties of sI and sII are found in Table 1.

- Pentagonal dodecahedron is denoted 5^{12}, and is the basic building block and present in all known natural gas hydrate structures (E.D. Sloan et al., 2007). It consists of twelve pentagonal faces with equal lengths and angles and is also referred to as a 12-sided cavity. Due to the fact that pentagons share sides only 20 molecules are required to make the 5^{12} cavity.

- Tetrakaidecahedron is denoted $5^{12}6^2$, and is a cavity which consists of 12 pentagonal faces and 2 hexagonal faces, also referred to as a 14-sided cavity. Each hexagon has six attached pentagons to its edges resulting in two cups. The two cups join in the periphery, resulting in a $5^{12}6^2$ cavity (E.D. Sloan et al., 2007). This cavity hosts molecules smaller than 6 Å in diameter. Ripmeester (personal communication with Sloan, 1988) indicates that this cavity ($5^{12}6^2$) is a preferred cage for almost all structure I hydrates, in which it plays the main stabilizing role (E.D. Sloan et al., 2007).

- Hexakaidecahedron is denoted $5^{12}6^4$, and is a cavity consisting of 12 pentagonal faces and 4 hexagonal faces, also referred to as a 16-hedron. Each hexagon face is completely surrounded by pentagonal faces, and none of the hexagonal faces will share a common edge (E.D. Sloan et al., 2007). The $5^{12}6^4$ cavities can host molecules as large as 6.6 Å, and when large components in natural gas (propane, iso-butane) form single guest hydrates they stabilize this cavity alone in structure II, leaving the smaller cavities empty (E.D. Sloan et al., 2007).

Table 1: An overview of structure I and structure II and their corresponding description and geometries (E.D. Sloan et al., 2007).

Hydrate Crystal Structure	**I**		**II**	
Cavity	Small	Large	Small	Large
Description	5^{12}	$5^{12}6^2$	5^{12}	$5^{12}6^4$
Number Of Cavities/Unit Cell	2	6	16	8
Average Cavity Radius, Å	3.95	4.33	3.91	4.73

1.2.3 Guest molecules

Guest molecules, also referred to as hydrate formers, are the molecules encaged in the structures made by the host, water molecules. Typical guest molecules mentioned in the literature concerning NGH are methane, ethane, carbon dioxide, hydrogen sulfide, nitrogen, propane and iso-butane. Methane is the most abundant guest molecule in NGH found in nature, where one volume of water may encage 207 volumes of methane at standard conditions (Makogon, 1997).

In NGH the cavities expand by 26-32 % compared to ice which expands with 9 % (Makogon, 1997), and they are prevented from collapse by the repulsive presence of their guest molecules. A classification of the different NGH structures are obtained by the determination of the guest molecules encaged, based on its chemical nature, size and shape (E.D. Sloan et al., 2007). Natural gas molecules serves well as guest molecules in that matter that they are not involved in hydrogen bonding and also are hydrophobic (E.D. Sloan et al., 2007).

Structure I hydrate can form by methane, ethane, carbon dioxide and/or hydrogen sulfide, guest molecules with a diameter between 4.2 Å - 6 Å. Structure II is formed by molecules with a diameter less than 4.2 Å, such as nitrogen, or by larger molecules such as propane or iso-pentane with a diameter

between 6 Å - 7 Å. Larger molecules than this (7 Å - 9 Å) can form structure H when accompanied by smaller molecules such as methane (E.D. Sloan et al., 2007). Some compounds change structure at different temperatures and higher pressure, and may result in guest molecules usually filling the large cavities also filling the small cavities. Table 2 shows an overview of relevant guest molecules and their ratio of molecular diameter and cavity diameter, describing where the three different guest molecules may enter. The hydration number is related to the size of the guest molecule and the achieved cage filling of the guest molecule, and in most cases to its nonstoichiometric value. Structure I has a hydration number (N_H) between 5.75–7.4, where N_H =5.75 describes a complete hydration (E.D. Sloan et al., 2007). The hydration number for a complete hydration is calculated by dividing the number of water molecules (46) by the number of cages (6) for structure I. Measurements of methane hydrate composition along the hydrate equilibrium boundary indicate a hydration number at 5.99 (±0.07) (Circone et al., 2005), and is used for calculations later in this thesis.

Table 2: Ration of Molecular Diameters to Cavity Diameters for Natural Gas Hydrate Formers (E.D. Sloan et al., 2007).

		Molecular diameter/Cavity diameter for cavity type			
		Structure I		Structure II	
Molecule	Diameter (Å)	5^{12}	$5^{12}6^2$	5^{12}	$5^{12}6^4$
Nitrogen	4.1	0.804	0.700	0.817	0.616
Methane	4.36	0.855	0.744	0.868	0.655
Carbon dioxide	5.12	1.00	0.834	1.02	0.769

1.3 Thermodynamics of gas hydrates

To reach a phase transition, where water and gas forms to a hydrate, there has to be a thermodynamic driving force. Pressure, temperature and chemical composition sets the premises for the thermodynamic driving force, and if strong enough, hydrate formation will occur. Most of the NGH require high pressure

and low temperature for being within the hydrate stable region, as illustrated in Figure 1-5 below. If the conditions are to the left of the equilibrium lines, hydrate will form or present hydrate will remain stable. If the conditions are on the right side of the equilibrium lines, hydrate formation will not occur or the present hydrate will dissolve. Due to this fact natural gas hydrates are generally found in deep-sea environments or in permafrost where the conditions satisfy pressure and temperature conditions. Figure 1-5 also shows how the equilibrium line changes as different guest molecules are present, illustrating how the different guest molecules are more or less thermodynamically stable than others. A natural gas hydrate formed by a light hydrocarbon, such as methane, requires higher pressure than heavier hydrocarbons, such as ethane and propane, to form at the same temperature. This is also true for a mixture of gases, where a small amount of ethane mixed with methane will require less pressure to form hydrate (Husebø, 2008).

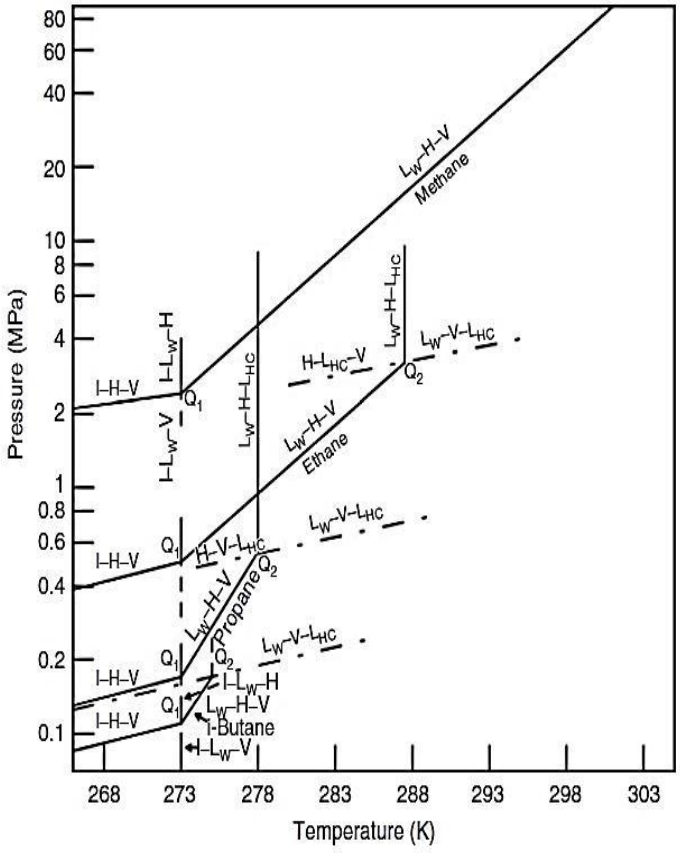

Figure 1-5: Phase diagram illustrating stability regions by equilibrium lines, as a function of pressure and temperature, for the guest molecules/hydrate formers; methane, ethane, propane and butane (E.D. Sloan et al., 2007).

Carbon dioxide and methane are the guest molecules used in this thesis, representing a potential production scheme where the thermodynamics suggest a replacement of CH_4 by CO_2. Both CO_2 and CH_4 can form structure I hydrate, where CH_4 molecules occupy both small and large cages, while CO_2 molecules favor the large cages. Both guest molecules will be stable at sufficient high pressure or low temperatures. However, thermodynamic studies propose that CH_4 hydrates have a higher equilibrium pressure than CO_2 for a range of temperatures (Ersland, 2008). This is illustrated in Figure 1-6 where CO_2 is more stable than CH_4 at any pressures at temperatures below 10° C. This indicates a stronger thermodynamic force in favor of the CO_2 compared to CH_4, causing a spontaneous exchange reaction between the two gases. A mixture of CO_2 and N_2 has shown an increase in the methane recovery. This can be explained by a competition between N_2 and CH_4 for the small cages, whereas $C0_2$ mainly occupy the larger cages (Ersland, 2008), or by melting due to the less stable conditions of nitrogen at a range of pressures. All experiments presented in this thesis have been conducted at temperatures below 10° C and pressures higher than 80 bar, and nitrogen has not been used as an inhibitor for enhanced recovery.

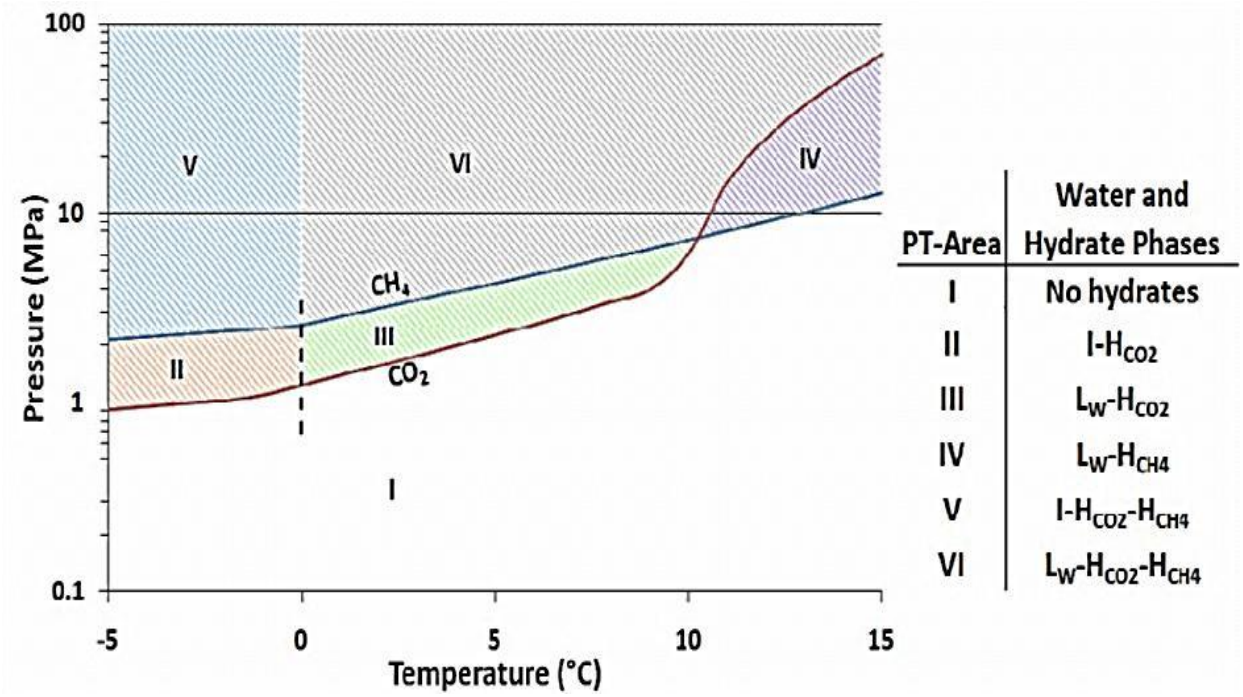

Figure 1-6: Phase diagram showing the stability and instability regions of CO_2 hydrate and CH_4 hydrate (Husebø, 2008) retrieved from CSMGem. The area below the curve represents the unstable region, and the area above the curves represents the stable region. For temperatures below 10° C (a temperature range from 4° C to 9.6° C was used during experiments in this thesis) CO_2 is more stable than CH_4. (I=Ice, L_w=Liquid water, H_{CO2}=CO_2 hydrate, H_{CH4}=CH_4 hydrate).

1.3.1 Hydrate kinetics

When the thermodynamic driving forces are strong enough, the hydrate formation and its kinetics will initiate. This means that Gibbs free energy has to be less than zero, water and hydrate former have to be available and a heat transport during the hydrate formation for removal of the heat of fusion. The hydrate formation can be divided into three stages, initial nucleation, induction time and steady growth. The first step in the hydrate formation is the nucleation, where small clusters will form. Water molecules will then start to arrange and form cages around the guest molecules. This is a random micro scale process that cannot be detected macroscopically. This process takes place in the bottom left corner in Figure 1-7. The next step in the hydrate formation is the induction time. The induction time is the time from where the first crystal nuclei is formed until the first detection of hydrate formation or a detectable amount of moles of hydrate former gas has been consumed and registered, when the system is within hydrate stable conditions. This is a stochastic process, and the time can vary from nanoseconds to months. The induction time measured depends on the thermodynamic force present in the system, and also the sensitivity of the equipment used. Before a critical radius is reached, formation and dissociation will take place randomly. When reaching the critical radius, the final stage will initiate where a steady growth of hydrate will follow. How fast the steady growth is, the hydration rate, is a function of gas consumption with time at constant pressure and temperature, exemplified in Figure 1-7 . The steady growth can be controlled by mass transfer, heat or kinetics (E.D. Sloan et al., 2007).

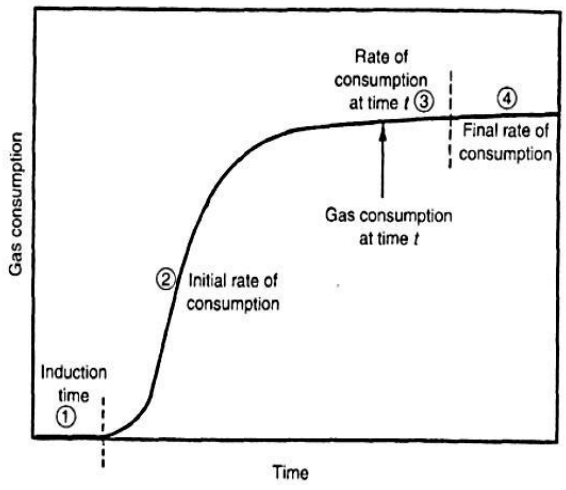

Figure 1-7 Figure showing gas consumption as a function of time during nucleation, induction time and steady growth of hydrate during hydrate formation (E.D. Sloan et al., 2007).

The dissociation process of NGH is of importance regarding gas production from NGH deposits or during flow assurance, preventing pipeline plugging in the industry when transporting gas. The dissociation is an endothermic process, where cooling will occur, and is typically controlled by heat transfer. When moving out of the hydrate stability region, either by adding heat, depressurizing the system, or by injecting inhibitors, dissociation may occur. Inhibitors are commonly used as hydrate preventers in the industry, but in a NGH production scheme depressurization has the most promising outlook regarding hydrate dissociation.

1.4 Natural gas hydrates as a potential energy resource

At the same time as the world demands both more and cleaner energy, the conventional hydrocarbon resources are approaching a decline period. Energy is therefore an important issue today and in the years to come, where a new cleaner energy source is a necessity. NGH could be a potential energy player in the future due to the vast amounts of methane trapped in these reservoirs scattered all over the planet. In addition methane is a cleaner form of energy compared to oil and coal, especially if a CH_4-CO_2 exchange is technically and economically feasible. This could be a step in the right direction to decrease human-made emissions, and mitigate global warming. The effort to investigate NGH as a potential energy resource has been carried out with significant cooperation between countries, governments and academic research sectors with the common goal of being able to produce this potential energy resource. Important challenges still remaining are to identify the location of gas hydrates, assessing the size of the resource, developing viable production methods, and to acquire an understanding of the economics of eventual gas production from NGH (Ruppel, 2011). NGH are today classified as an unconventional energy resource, and is often compared to coalbed gas resources which until recently were considered as an unconventional energy resource. Nevertheless, once coalbed gas was geologically understood, its properties defined and production challenges met, this unconventional energy resource became a conventional resource and accounts for almost 10% of natural gas production in USA (T. Collett, 2005).

1.4.1 Natural gas hydrate resources

There are unquestionable vast resources of natural gas trapped in hydrate deposits distributed worldwide. The estimates vary from $10^{15} – 10^{18}$ m^3 of methane at standard conditions (E.D. Sloan et al., 2007), and indicate an amount twice the equivalent of energy from conventional hydrocarbons (oil, gas and coal). If only a fraction of conservative estimates are recoverable, NGH would play an important role

as a potential energy resource making methane an international commodity in an energy demanding world (Moridis et al., 2008).

NGH reservoirs are found in two regions; 1) Polar areas with continuous permafrost and in 2) Continental margins of all oceans (Kvenvolden et al., 2001). Figure 1-8 shows inferred and known NGH deposits, and how they are distributed worldwide. The map shows that the majority of NGH deposits are distributed in marine environment, and estimates indicate that 99 % of the worldwide NGH is located in ocean sediments (Ruppel, 2011). The great abundance of in-situ NGH are saturated with methane which is concentrated volumetrically by a factor of 164 compared to standard conditions (Moridis et al., 2008), and can be viewed as a concentrated form of natural gas equivalent (E.D. Sloan et al., 2007).

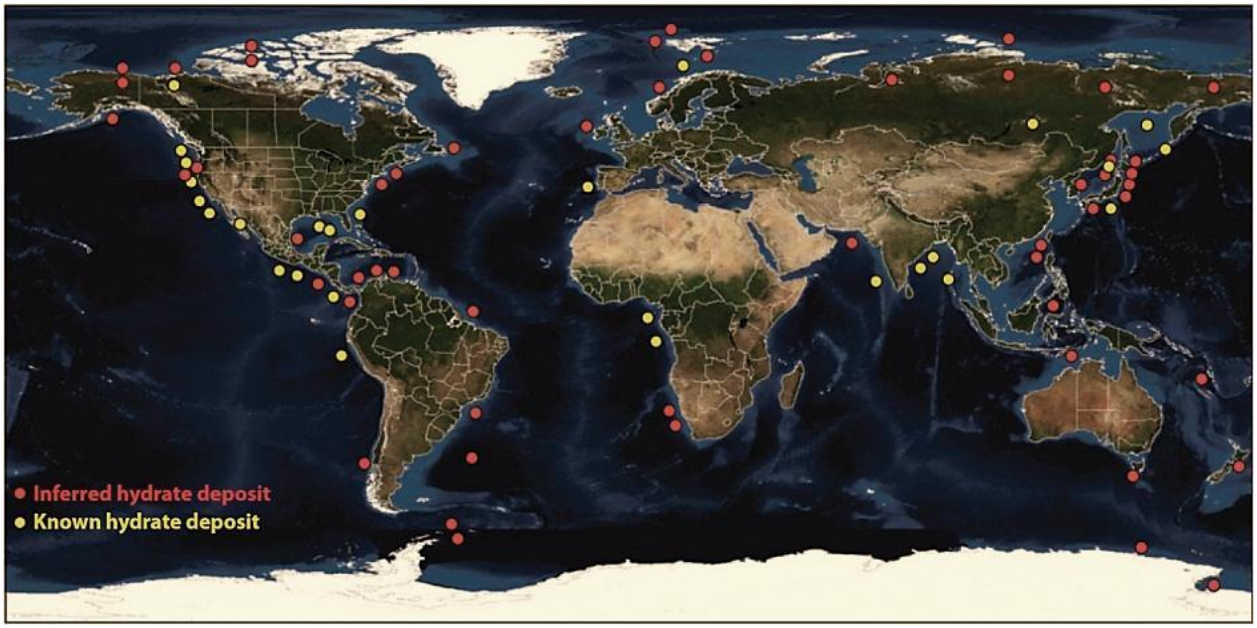

Figure 1-8: A worldwide map of both inferred and known natural gas hydrate deposits. More than 90 documented hydrate occurrences, where the inferred deposits were identified mainly from seismic reflectors and pore water freshening in core samples. Known hydrate deposits are from direct samples from ocean drilling and remote operated vehicle expeditions (Hester et al., 2009).

As shown on the map in Figure 1-8, NGH deposits are abundant on earth. As long as four conditions co-exist hydrate can form in geological structures; 1) reservoir water has to be present with 2) free or dissolved gas under 3) high pressures and 4) low temperatures. In Figure 1-9 is an illustration of the gas hydrate stability zone (GHSZ) from both marine and permafrost regions. As long as water is present and gas migrates upward and into GHSZ, NGH will form. The gas originates from either bacterial or thermogenic methane (Yang et al., 2008). Bacterial methane is generated by bacteria either through

reduction of carbon dioxide or acetate fermentation (Yang et al., 2008), where thermogenic methane is generated from organic matter exposed to high pressure and temperature settings, and is supplemented with concentrations of ethane ,propane and butane (Yang et al., 2008). The geothermal gradient is of great importance, as the heat increases with depth. At temperature and pressure conditions outside GHSZ, gas exists only as free gas or gas dissolved in pore waters (Ruppel, 2011). GHSZ in marine systems is typically around 300-600 meters of water depth and can extend hundreds of meters below the seafloor with temperatures ranging from 2° C - 20° C. Required pressure and temperature conditions predominate within the upper tens to hundreds of meters of seafloor sediments (Ruppel, 2011). Gas hydrate onshore is found in thick permafrost areas. The stability zone is around 100 to 300 meters of depth and can extend hundreds of meters based on the base of permafrost, with temperatures ranging from -10° C to 20° C (Hester et al., 2009). The reservoir rock where natural gas hydrates are observed varies. The gas hydrate can be observed filling pores of coarse grained sediments, nodules distributed in fine grained sediments, as a solid substance in fractures or as a massive unit composed of solid gas hydrate with lack of sediment (Moridis et al., 2010).

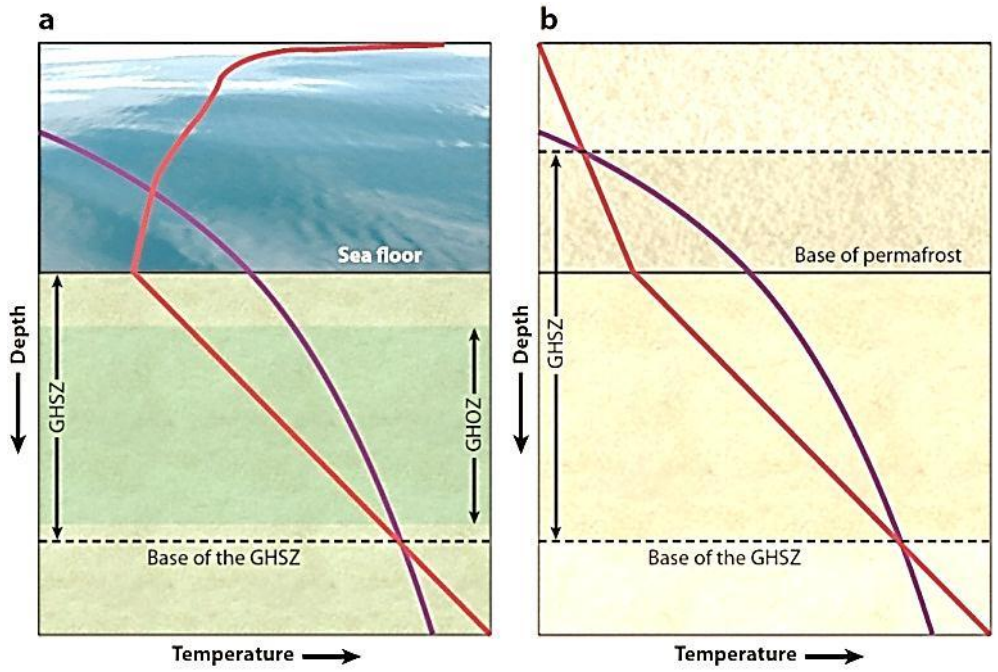

Figure 1-9: Illustration of the gas hydrate stability zone (GHSZ) for both marine and permafrost locations (Hester et al., 2009). The temperature gradient is represented by the red line, and pressure as a purple line. As the depth increases, so will the temperature. Therefore the depth is a limitation for the base of the gas hydrate stability zone due to the temperature gradient, where the pressure sets an upper boundary along with seafloor and base of permafrost.

1.4.2 Classification of hydrate reservoirs

Even though some of the estimates of methane bound up in hydrates are twelve times that of conventional fossil fuels there are many aspects to consider, such as a distinction between in-place, technically recoverable, and economically producible resources when considering hydrates as an energy source (Hester et al., 2009). These factors may be influenced by the characteristics of the NGH reservoir.

Three fields of expertise have been used to identify natural gas hydrates; 1) geological (sediment properties, stratigraphic relationships, gas migration pathways, and recovery and description of gas hydrate samples), 2) geochemical (pore fluid chemistry, and gas compositions), and 3) geophysical (seismic, well logging). Surface seismic has been the most successful method used for reservoir evaluation and resource estimation of natural gas hydrates. Both 2D and 3D seismic have been used to map natural gas hydrate reservoirs around the world in sub-marine environment and below permafrost. It is also used locating upper and lower boundaries, and provides rough estimates of average hydrate saturations.

NGH reservoirs have a wide spread of properties when concerning thermodynamic conditions, geological structures and trapping configurations. A potential energy production from NGH is dependent on these reservoir characteristics, and different categorizations have been proposed. The hydrate resource pyramid shown in Figure 1-10 (Boswell, 2006) demonstrates the distribution of trapped methane among the different global gas hydrate deposits, and also illustrate how there is only a small part of the NGH deposits likely to be considered as commercial energy resources. At the top of the pyramid lie artic sand reservoirs with high permeability and relatively small amounts of gas hydrate. These permafrost associated gas hydrates are most likely to be commercialized due to presence near well-developed infrastructure, such as in the Alaska North Slope. Below these types of reservoirs there are marine sand reservoirs. These sediments are highly permeable with moderate gas hydrate saturations. These deposits are considered as the major target for long-term development of gas hydrate as a resource (Ruppel, 2011). Following are non-sand marine sediments that can be interpreted as less permeable sediments that might host gas hydrate in fractures. Due to the low permeability in these sediments the potential recovery is found in fractures that could theoretically yield significant gas resources. At the bottom of the hydrate resource pyramid lie marine sediments with low permeability. These sediments host most of the gas in place, but are unlikely to become a commercial target for methane production. Energy production

from NGH is dependent on the reservoir characteristics, and considering technical feasibility and economics, permafrost deposits are most suitable at the present time.

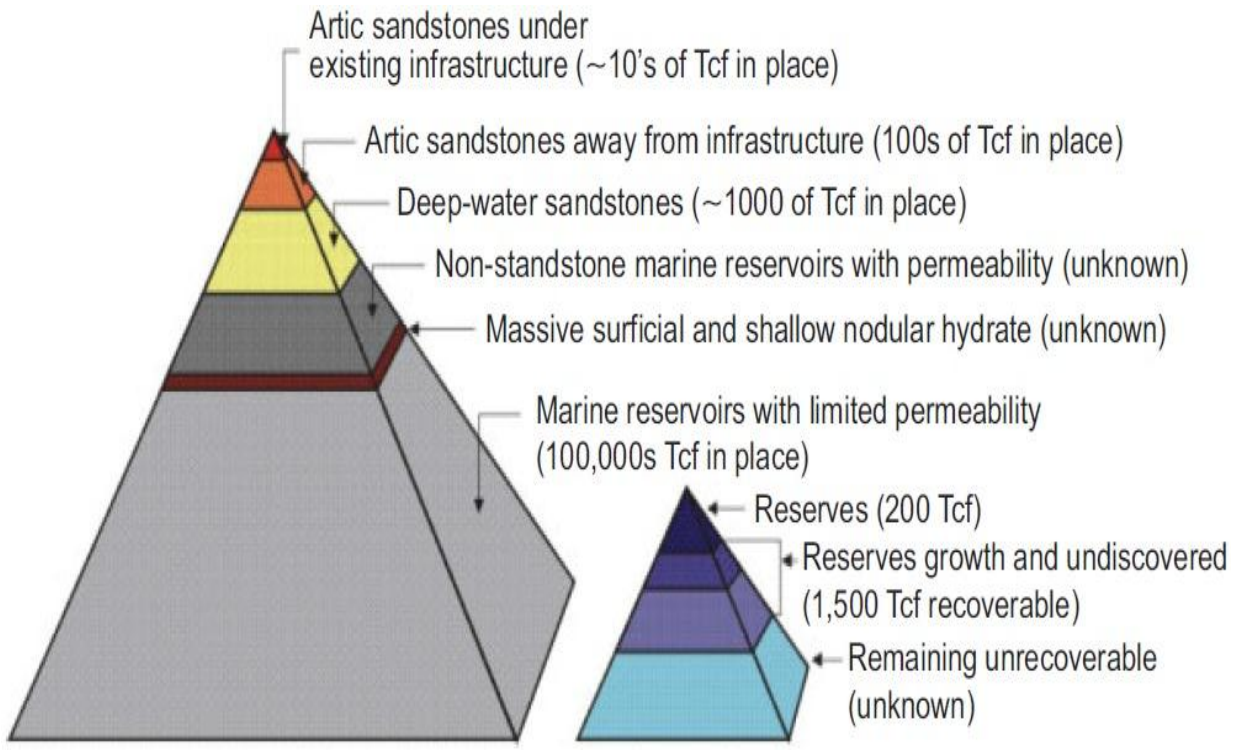

Figure 1-10: The large pyramid represents the natural gas hydrate resource divided into different deposit schemes, and the small pyramid represents conventional gas resources (Boswell, 2006).

An additional way to categorize the potential of the different types of NGH reservoirs are based on concentration and associated with mobile gas and/or fluids present, and does not separate marine and permafrost gas hydrates. This system is divided into 4 classes, and shown in Table 3. Class 1 deposits consist of two layers, a hydrate bearing layer (HBL) and an underlying two-phase layer with mobile gas and liquid water. This type of deposits are a desirable system due to the fact that the base of the gas hydrate stability zone overlaps with the bottom of the HBL (Moridis et al., 2010). Class 2 deposits have a HBL overlying a mobile water zone (Moridis et al., 2010) at, or well within the stability zone. Class 3 deposits have no mobile fluid zone present underlying the HBL (Moridis et al., 2010) at or well within the stability zone. Class 4 deposits are disperse and low saturated (less than 10 %) hydrate deposit with lack of confining geologic strata and are not targets for production. The final class is typical of many oceanic accumulations (Moridis et al., 2010).

Table 3: Classification system of different hydrate reservoirs, based on mobile phases present as well as the presence of confining strata (Hester et al., 2009).

Deposit type	Zone Present	Mobile Phases	Confining Strata
Class 1	Two zones: hydrate-bearing layer (HBL above two-phase zone	Free gas, water	Yes
Class 2	Two zones: HBL above one-phase zone	Water	Yes
Class 3	One zone: HBL	None	Yes
Class 4	One zone: HBL	None	No

1.4.3 Proposed Production Methods

To be able to produce and recover the methane trapped in the structures of the hydrate, the NGH have to either dissolve or be introduced to a more thermodynamically stable hydrate former that will swap place with the methane. Existing technology can be used to produce gas from NGH, and these methods have not changed much since the early 1980´s (Ruppel, 2011). Pressure, temperature and composition are the three variables defining the hydrate stability. By moving out of the stability zone and crossing the equilibrium line, gas recovery from hydrate is possible by dissociation. Depressurization, thermal stimulation and/or chemical stimulation are potential methods;

- During depressurization the pressure is lowered below the equilibrium pressure at the given reservoir temperature. Hydrate dissociation will initiate, and production of liberated gas will initiate. A negative contribution by using this method is vast water and sand production, and the loss of the solid hydrate which may cause geomechanical instabilities. Nevertheless, this is the most promising method today due to the economic advantage since it does not require much added energy.

- Thermal stimulation is done by applying heat. The temperature will cross the equilibrium temperature at the given reservoir pressure. This is done by injection of heated fluids or potentially by direct heating of the formation (Ruppel, 2011). This method is energy demanding

and will lead to relatively slow dissociation. Thermal stimulation is a promising method in combination with depressurization, as it prevents reformation of hydrate and plugging.

- Chemical stimulation through injection of an inhibitor such as glycol or brine, will alter the whole equilibrium line to a shift upwards, and therefore move outside of the hydrate stable region at a certain pressure and temperature. This is not a primary method used to dissociate NGH, but can be used as a supplement. Inhibitors are more commonly used in hydrate prevention during flow assurance.

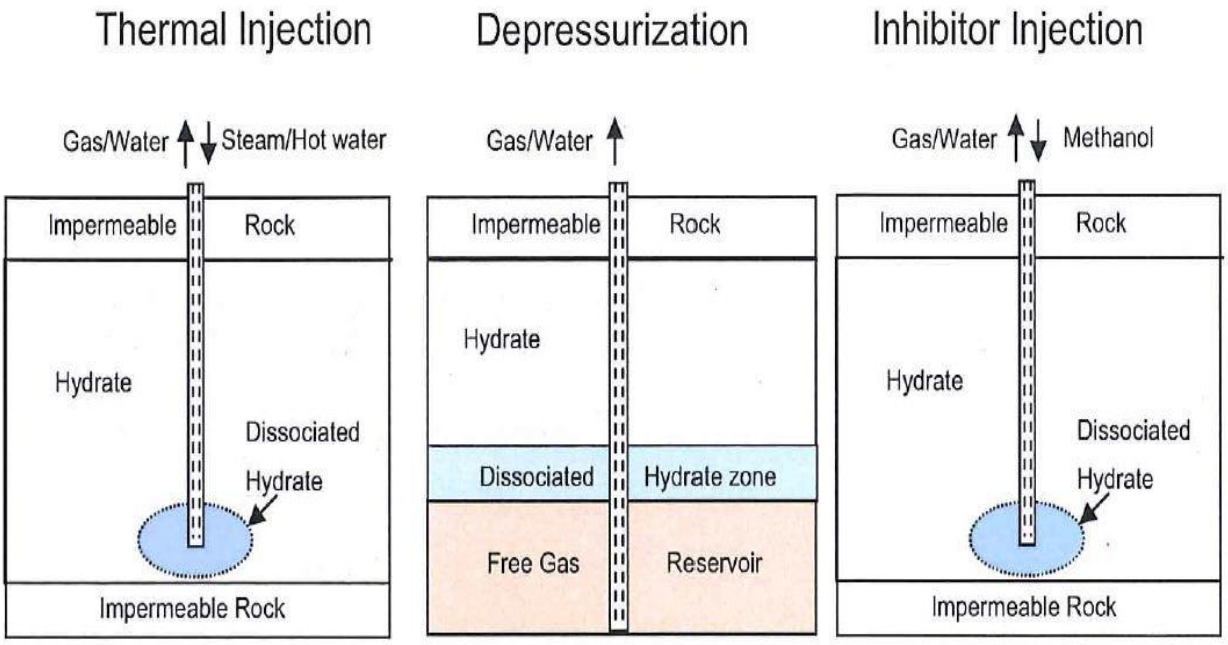

Figure 1-11: A graphic illustration of the three different production methods, thermal stimulation, depressurization and injection of inhibitor, based on dissociation of the present hydrate consequently liberating trapped gas (Makogon, 1997).

Simulation studies have shown that depressurization is the most promising production method in regards to both methane production and economics, where some modeling indicate an energy usage of 15 % of the energy recovered (E. Dendy Sloan et al., 2008). By adding heat you need to apply energy, and inhibitors are expensive. The problem for all of these methods is the vast amount of water and sand production, and the risk of geo-mechanical instability which may cause subsidence and landslides (E. Dendy Sloan et al., 2008).

1.4.4 CH_4-CO_2exchange as a production method

A fourth production method proposed, which this thesis is based on, is through an exchange process where CO_2 is injected into the hydrate bearing layer causing the CH_4 present in the crystalline hydrate lattice to be released and produced. This proposed method is based on the fact that CO_2 is a more thermodynamically stable guest molecule compared to the already present CH_4 (at temperatures below 10° C), resulting in a spontaneous reaction where CH_4 and CO_2 swap places. Figure 1-12 shows a schematic diagram of the exchange between present methane and carbon dioxide in structure I hydrate, and illustrates how CO_2 prefer the medium cages (Ota et al., 2005). This method was considered as an impracticable production method based on laboratory experiments on bulk hydrated samples, where the kinetic was very slow. However, experiments performed on porous media showed enhanced exchange kinetics and efficiency (Schoderbek et al., 2012). There are two main advantages of this production method; 1) a sequestration of carbon dioxide will take place, and 2) the hydrate formation will stay intact, preventing geo-mechanical instabilities and large volumes of produced water during production. The main disadvantage is the recovery rate which is less than by dissociation and access to CO_2.

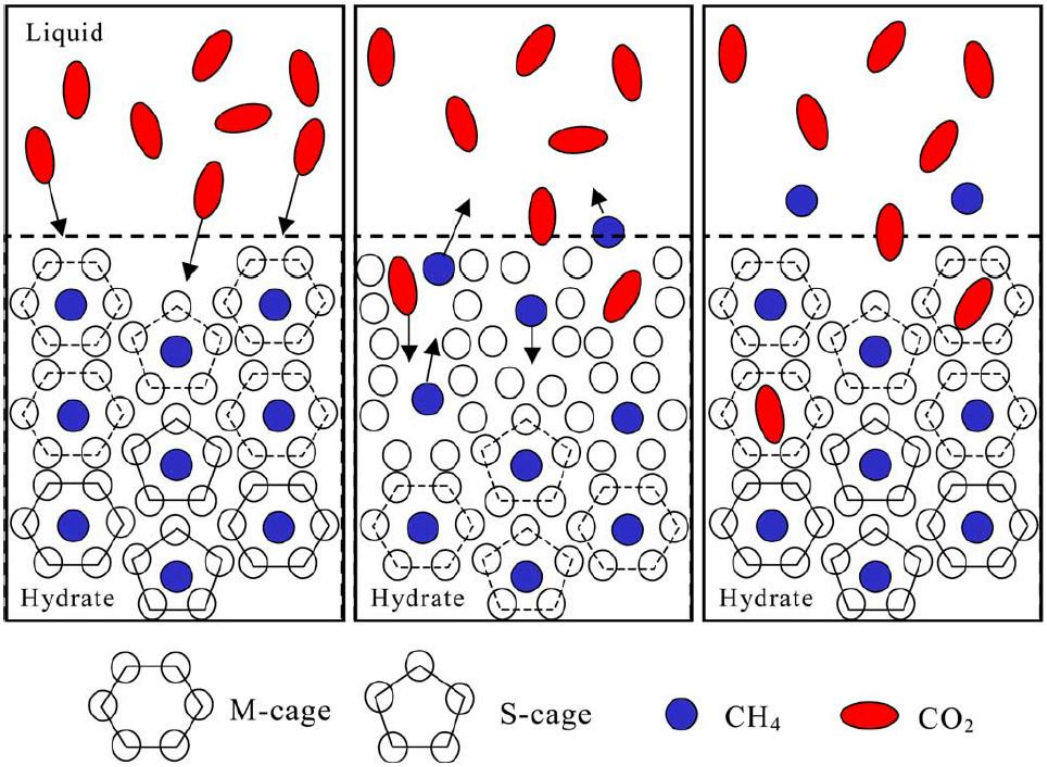

Figure 1-12: Illustration of guest molecule replacement in medium cages and small cages and the methane reoccupation in small cages (Ota et al., 2005)

1.4.5 Monoethanolamine (MEA) and Methyldiethanolamine (MDEA)

In this thesis two inhibitors were used to investigate a possible increased replacement rate and enhanced recovery when introducing liquid CO_2 to the present CH_4 hydrate. Two potential catalysts were used, monoethanolamine (MEA) and N-methyldiethanolamine (MDEA) with the purpose to add heat to the system as the amines react with CO_2 and the present brine. Both are regenerative chemical solvents with importance in the industry as a CO_2 capturing method (Farmahini et al., 2011). MEA and amine solutions, is mostly discussed in the literature as a technique for CO_2 capturing from flue gases to decrease emissions from fossil fuel-fired plants (McCann et al., 2009). To the writers knowledge MEA and MDEA has not before been tested with the purpose of enhancing CO_2 replacement in CH_4 hydrates. Personal communication (2013) with Professor Bjørn Kvamme provided some knowledge and indicated that MEA generates more heat than MDEA, and he also made clear that the reaction between CO_2 and MEA (and the present brine) is an extremely rapid reaction where much heat is generated which could trigger dissociation of methane hydrate. Hence MEA was emphasized in the catalyst experiments presented in this thesis.

1.5 Gas production from hydrate reservoirs

NGH is at the present time not considered an economically feasible resource, but is still subjected to extensive research and development (R&D). National hydrate programs exist in countries like United States, Canada, Japan, India, Taiwan and China (Hester et al., 2009). Energy dependent countries possessing vast hydrate deposits, such as India and Japan, are investing and outspending the United States on hydrate R&D (E. Dendy Sloan et al., 2008). Even though there are many known NGH sites around the world, only a few of them have been exposed to a production scenario. The R&D has mainly been focused on laboratory studies and simulations, and few large scale field tests have been executed. A two year study by the U.S Federal Methane Hydrate Advisory Committee, submitted in 2007, had four following recommendations on future needs for federal supported hydrate research (E. Dendy Sloan et al., 2008):

- A long term production test well in permafrost areas.
- Determinate the economic viability of marine hydrates.
- How hydrates can affect natural climate systems, and the potential of natural hazards
- International collaboration is a necessity for the economy, knowledge, time and expense.

1.5.1 Field studies

Three descriptive NGH fields exposed to a production scenario are; 1) Messoyakha in Russia, 2) Mallik in Canada, and 3) Ignik Sikum on the North Slope of Alaska. All three is located in permafrost regions. They have respectively been recovered by depressurization, thermal stimulation, a CH_4-CO_2 exchange scenario or as a combination of these three methods. A short overview is given below.

The first field producing gas from a NGH is most likely Messoyakha, a conventional gas field located in a permafrost area in West Siberia. After an ordinary gas production during two years (1969-1971), a deviation from the pressure decline was logged (Moridis et al., 2008). During shut-in the average reservoir pressure increased, and the gas water contact remained constant (Grover et al., 2008). An answer to this deviation was explained by an overlying hydrate formation supplying gas, due to dissociation by depressurization, when producing the underlying gas. Estimations indicate that 36 % of the total produced gas originates from the overlying gas hydrate (Makogon, 1997). Due to a lack of information from the field, there are still some questions regarding the validity of this conclusion (T. S. Collett et al., 1998).

The 2002 Mallik program was the first modern and fully integrated field study regarding production from NGH hydrates, and proved that production from hydrates is technically achievable. During a period from December 2001 until March 2002, three wells were drilled in locations with the highest concentrations of gas hydrates found (T. Collett, 2005). Using both controlled depressurization and thermal stimulation, on a 17 meter thick section of highly concentrated hydrate, a five day production was observed (Hester et al., 2009). The depressurization test indicated that the gas hydrates are more permeable and able to flow than previously thought, and due to artificial fracturing this rate was enhanced (T. Collett, 2005). A five day experiment was also conducted where hot water was circulated to increase the reservoir temperature on a 17 meter thick section of highly concentrated hydrate. Gas was produced throughout the test, with a maximum rate of 1500 cubic meters per day (T. Collett, 2005). From the experience and data gathered from this field test, the combination of both depressurization and thermal stimulation would yield the greatest amount of gas (T. Collett, 2005). It is also worth mentioning that this field test was of great interest because of its similarities to marine deposits, which hold the largest NGH reservoirs (B. I. Anderson et al., 2005). Production tests conducted at Mallik in April 2007 and March 2008 using depressurization showed the most promising results by stepwise pressure reduction, as well as less problems concerning sand production (Kurihara et al., 2010).

A field test of great interest, with regards to this thesis is Ignik Sikum #1. The field test was based on a CH_4-CO_2 exchange production method and was executed in 2011 in a permafrost deposit on the North Slope of Alaska with an already existing field infrastructure. The "Upper C" sandstone at Ignik Sikum #1 was selected based on its thick-bedded, homogeneous character, high hydrate saturation and a presence at pressure and temperature conditions close to those used in laboratory studies (Schoderbek et al., 2012). Data based on NMR and multi mineral models indicated a hydrate saturation at approximately 75 % (S_H = 75 %) in the 14 meter thick sandstone reservoir (Schoderbek et al., 2012). The NMR log also indicated that the remaining pore volume was saturated with free water, and not free gas (Schoderbek et al., 2012). This excess water could be problematic when introduced to the hydrate former (CO_2) during the injection. Porosity and permeability could then be affected negatively by additional hydrate in the porous media. Modeling indicated an ideal composition of the injectant to be a gas mixture consisting of 23 % carbon dioxide and 77 % nitrogen (Schoderbek et al., 2012). The co-injection of carbon dioxide and nitrogen was carried out for thirteen days, resulting in a total usage of over 200 000 scf of mixed gas at approximately 1420 psia bottom hole injection pressure (Schoderbek et al., 2012). The production lasted for five weeks, divided into four steps; 1) unassisted flowback, 2) jet pumping above methane hydrate stability pressure, 3) jet pumping near methane hydrate stability pressure, and 4) jet pumping below methane hydrate stability pressure (Schoderbek et al., 2012). As the graph in Figure 1-14 show, there was an increase in the methane production around 24th of March. This was the period where the final process was conducted, lowering the pressure below the hydrate stable pressure. Depressurization may therefore be considered in addition to the CH_4-CO_2 exchange as a part of the production scheme. A total of approximately 998 000 scf of gas was measured and analyzed via the inline gas chromatograph. The produced gas contained 22 000 scf of carbon dioxide, 155 000 scf of nitrogen and 821 000 scf of methane.

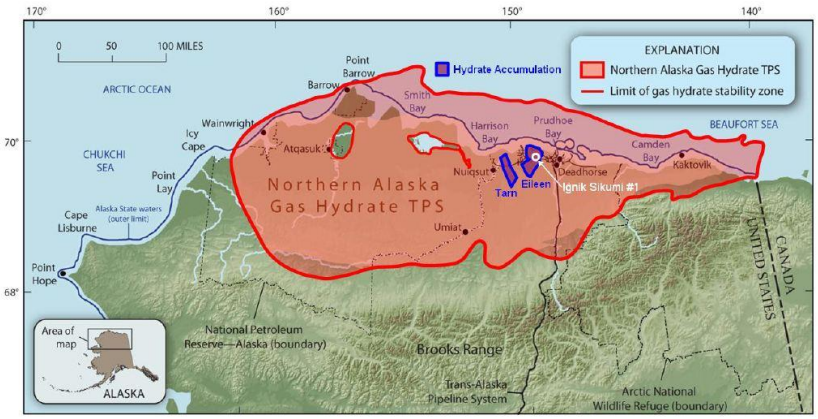

Figure 1-13: North Slope hydrate petroleum system modified from Collett (Schoderbek et al., 2012).

The Ignik Sikumi field test verified that carbon dioxide could be injected into a hydrate filled, water-bearing reservoir, with a methane production as a result (Schoderbek et al., 2012). Figure 1-14 shows the different gas production volumes with time, verifying a methane production, and that vast amounts of CO_2 (50 % of the 48 000 scf of injected CO_2) remained in the reservoir, proving an exchange process took place.

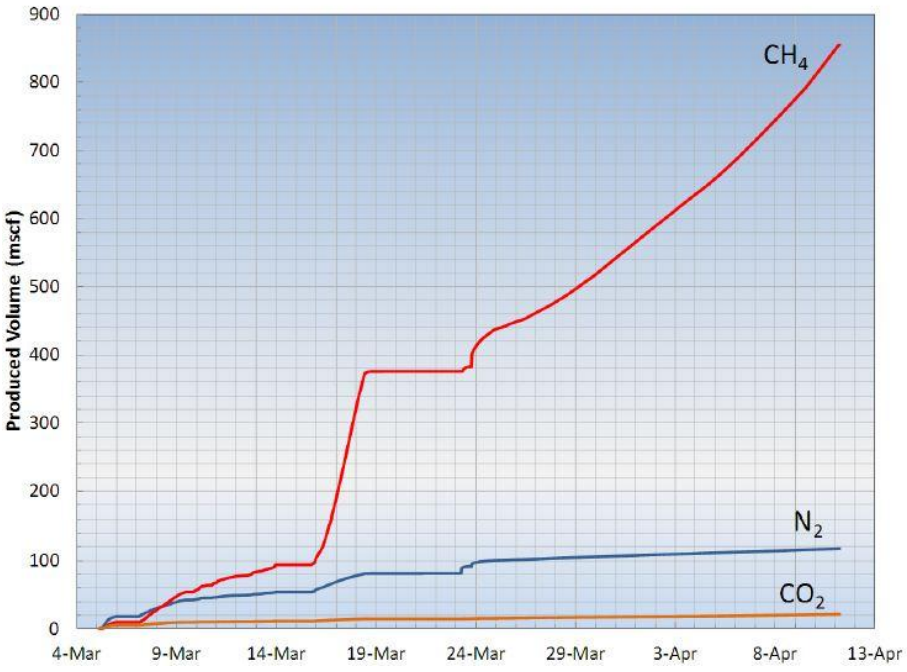

Figure 1-14 : Ignik Sikum production (by flowback/drawdown) curves showing produced volume of methane, nitrogen and carbon dioxide with time (Schoderbek et al., 2012). It is worth mentioning that the final production phase, from 23 March to 11 April, was conducted below methane hydrate stability region.

1.5.2 Rock properties

Understanding how the presence of hydrate in a sediment influences the water and gas flow is critical when predicting gas recovery (Moridis et al., 2010). The ability for fluid flow in a porous media is a rock property and defined by Darcy´s law, and referred to as permeability. Permeability is essential to make pathways available for injection of CO_2 as well as production of methane (Moridis et al., 2010). Permeability measurements in hydrate bearing sediments is complex, and is not conducted in this thesis due to low water and hydrate saturations, resulting in less influence on the permeability. Porosity is defining the pore space vacant between the grains. In this thesis a Bentheim sandstone core was used as a porous media and an average porosity was assumed and used in calculations. The sandstone cores used in this thesis are water-wet, meaning water will spontaneously imbibe into the core, and the capillary pressure will distribute the water within the pore space. All experiments conducted in this thesis had low water saturations at approximately 0.4. Due to the low water saturations an assumption can be made regarding the distribution of brine where the small pores are likely filled with brine and the big pores have brine along the pore wall. The distribution of brine has an impact on the location of hydrate growth within the pore space. Figure 1-15 shows methane hydrate growth within a synthetic porous media.

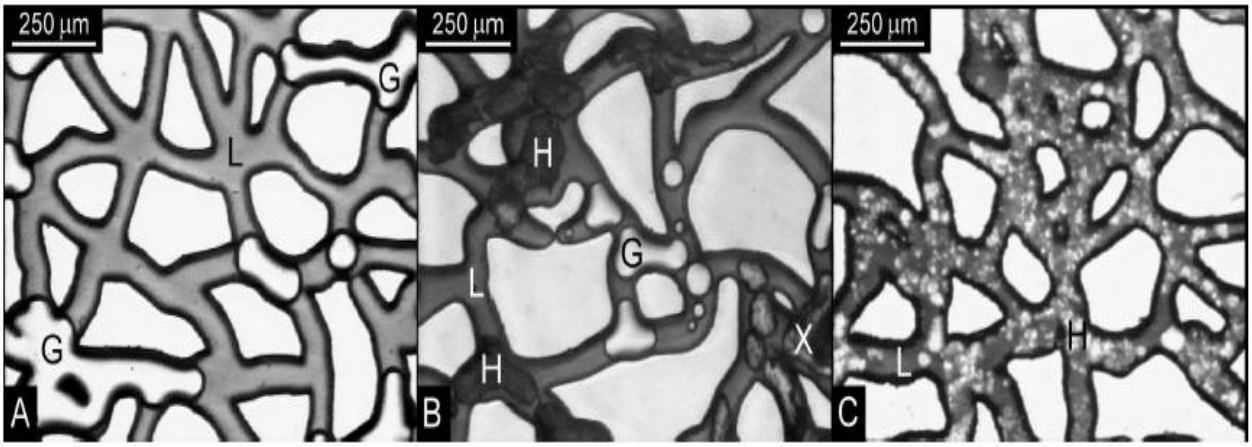

Figure 1-15: Micromodel video stills of methane-water tests (Tohidi et al., 2001). Large white areas are grains. Picture A shows bubbles of methane (G) and liquid water (L) before hydrate formation. Picture B shows formed hydrate (H), liquid (L) and gas (G) within the pore space. (X) illustrates encapsulated gas bubbles prior to complete conversion to clathrate. Picture C shows the hydrate distribution after a period of 2 days.

If the hydrate is located as a solid filling the center of the pore space, it may give support to the matrix and overlying sediments. Deposits showing the most promising production scenarios from NGH are often

poorly consolidated sediments and commonly characterized by limited shear strength (Moridis et al., 2010). Dissolving the NGH during production may trigger pore collapse, subsidence, submarine landslides and release of methane to the atmosphere which are concerns that need to be addressed and understood. Some experiments present data that contradict this association. For the hydrate to have a significant stiffening effect, it has to fill a large volume of the pore space (Tohidi et al., 2001). Experiments, based on p-waves, have shown no loss of stiffness in the granular medium during a CH_4-CO_2 replacement, implying that a sand reservoir would stay mechanically stable after a CO_2 flooding and CH_4 production (Espinoza et al., 2011). Using liquid CO_2 may decrease the stiffness.

1.6 Literature Survey

Theoretical and experimental research has verified that an exchange between the more thermodynamically stable guest molecule carbon dioxide and methane takes place in a stable hydrate. This section will review both earlier and present studies conducted on the subject of CH_4-CO_2 exchange, and within this topic literature concerning temperature effects was sought for. Due to the interaction between the constituents (brine, methane and carbon dioxide), literature concerning solubility, density, and viscosity was valued.

It is now 20 years since the notion that natural gas could be produced from NGH by introducing a more thermodynamically stable hydrate former where the greenhouse gas carbon dioxide was proposed (Ebinuma, 1993). Ebinuma patented a theory where injection of heated carbon dioxide into layers of hydrate bearing sediments would dissociate present hydrate with a following reformation of CO_2 hydrate. Consequently the greenhouse gas would be stored, as well as producing the in-situ natural gas. Ohgaki et al. (1996) were one of the first to carry out experimental work on the topic of CO_2 injection as a CH_4 production technique from NGH. They proved that CO_2 was a preferable hydrate former compared to CH_4, and therefore a more stable guest molecule. The experiment was executed at liquid water conditions, below the methane stability region and above the carbon dioxide stability region. Both Ebinuma (2003) and Ohgaki et al. (2006) based their theory on an unstable natural gas hydrate phase, which is on the contrary from the foundation which this thesis is based on, where the exchange takes place under methane hydrate stable conditions.

Early experiments investigating CH_4-CO_2 exchange from methane hydrate were conducted in hydrate bulk. Experiments proved an exchange rate too slow for a potential production scheme from natural gas hydrates. As experiments were conducted on hydrate within porous media, the exchange rate was increased, due to higher permeability and contacted surface area.

Ota et al. (2005) investigated CH_4-CO_2 replacement by using *in-situ* laser Raman spectroscopy. All experiments conducted by Ota et al. (2005) showed an increase in both amount of CH_4 dissociated ($Q_{CH4,dec}$) and amount of CO_2 hydrate formed ($Q_{CO2,Form}$) with an increase in temperature. Also the experiments showed that both $Q_{CH4,Dec}$ and $Q_{CO2,Form}$ was almost proportionally, indicating that a replacement took place in the hydrate phase. Calculations of activation energies for CH_4 decomposition and CO_2 formation was done by using the slope of the Arrhenius plot. The activation energy for CH_4 decomposition was calculated to 14.5 KJ/mol and CO_2 formation to 73.3 KJ/mol. The rate constant of

decomposition seemed to dominate the CH_4 hydrate decomposition during the replacement, while mass transfer appeared to dominate the CO_2 formation during the replacement. Ota et al indicated that the decomposition of the methane hydrate is dominated by rearrangement of the water molecules in the hydrate, while the CO_2 formation is dominated by diffusion in the hydrate phase.

Graue et al. (2006) verified an exchange process taking place in porous sandstone by using MRI visualization, where no heat was added, in laboratory experiments. The study was carried out in fractured sandstones with a spacer to increase the exposure contact area between methane hydrate and the injected carbon dioxide, as well as providing an accumulation area for the liberated methane. This is shown in Figure 1-16 where methane is visualized in blue, and hydrate and carbon dioxide are invisible. These pictures verify the spontaneous CH_4-CO_2 exchange reaction taking place when methane hydrate is exposed to carbon dioxide (Graue et al., 2006).

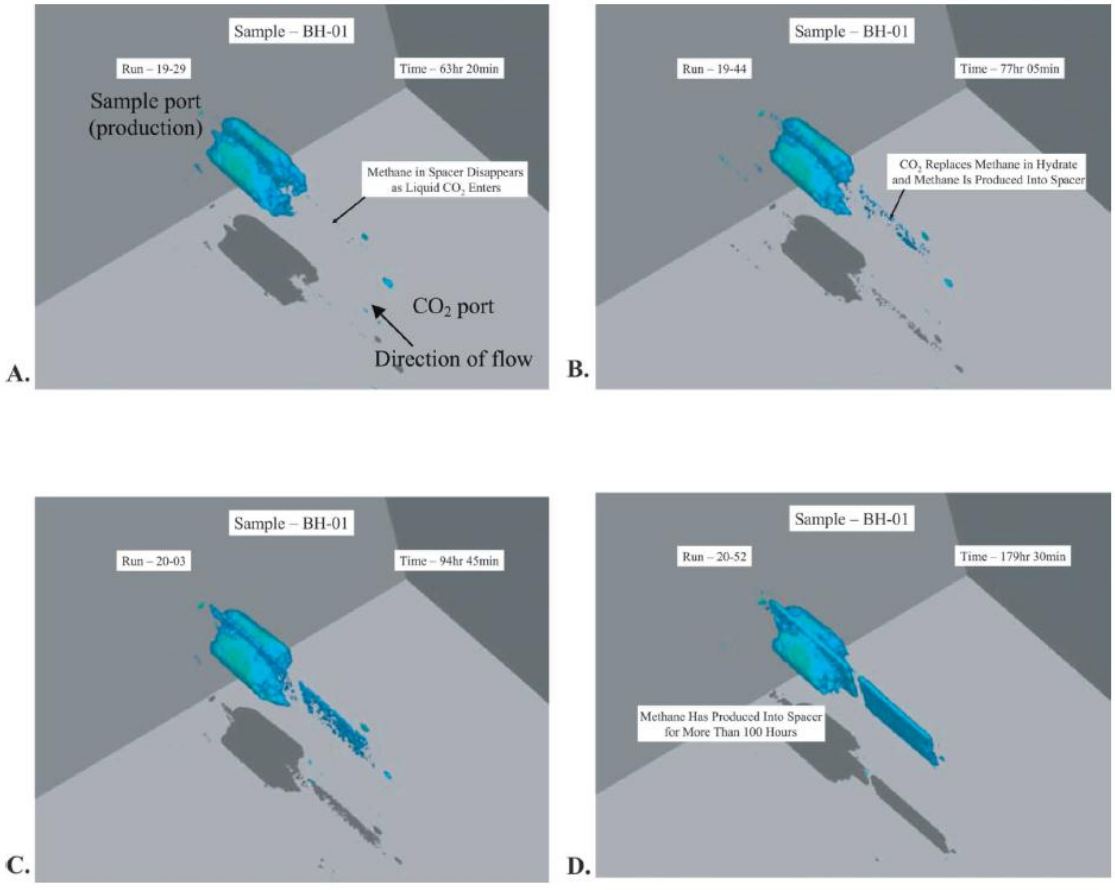

Figure 1-16: Methane production from hydrate into the fractured space originally filled with carbon dioxide (Graue et al., 2006). Blue color is methane, where the solid hydrate and carbon dioxide are not visible for the MRI.

Jung et al. (2010) explored the pressure-temperature region for optimal CH_4-CO_2 exchange, as well as investigating the potential geomechanical implications during exchange with regards to the hydrate bearing sediment (Jung et al., 2010). Their experimental data and theoretical considerations indicate an increased recovery rate near the CH_4 hydrate phase boundary. They also suggest that a CH_4 hydrate reservoir with excess gas should be preferable, compared to excess water, due to an increased permeability to liquid CO_2, a larger hydrate interface, as well as minimal CO_2 clogging.

The difference in chemical potential between CH_4 hydrate and CO_2 hydrate indicates that the CH_4-CO_2 replacement is thermodynamically favorable (Seo et al., 2001). The magnitude of the reaction is controlled by numerous factors and coexisting processes such as; solubility, viscosity, permeability, density differences, invasion patterns, surface of the hydrate phase, fluid expansion after replacement and change in effective stress (Jung et al., 2010). Occupancy of CO_2 molecules in small cages increase with increased pressure, where the CH_4 molecule is slightly smaller and fits more easily in the small cages, and therefore CH_4 hydrate is less pressure sensitive than CO_2 hydrate (Jung et al., 2010).

During hydrate formation (an exothermic reaction) heat is liberated. The heat liberated when CO_2 forms hydrate is between 57.7 and 63.6 kJ/mol (G. K. Anderson, 2003). On the contrary, hydrate dissociation (an endothermic reaction) absorbs heat to manage to disorganize the crystal structure. Heat absorbed during dissociation of CH_4 hydrate varies between 52.7-55.4 kJ/mol (G. K. Anderson, 2004). These figures are based on a complete CH_4 hydrate dissociation, before CO_2 formation.

Water has the highest thermal conductivity of the participants (CO_2, CH_4, and H_2O) and advocates a reduced heat spreading during formation, and therefore promote a local heating where liquid CO_2 displaces water and contacts CH_4 hydrate (Jung et al., 2010). The difference in water viscosity compared to liquid CO_2 is of 1-2 orders of magnitude higher, and subsequently can affect the fluid invasion flow paths. Liquid CO_2 density is pressure dependent, and will be heavier than water in deep sea location and lighter at the continental shelf. Differences in density promote buoyancy effects on fluid flow.

Solubility of the constituents (CO_2, CH_4, and H_2O) has influence on gas transport, hydrate formation, and hydrate dissolution in water not fully saturated with gas (Jung et al., 2010). CO_2 is 10 times more soluble than CH_4 in water, where both solubilities increase when exposed to higher pressure and lower temperatures. These trends invert when hydrate is present, and the amount of dissolved water in CO_2 is not insignificant (Jung et al., 2010). As a result liquid CO_2 can remove water, and therefore dry the sediment. CH_4 is also highly soluble in liquid CO_2. Diffusion of the constituents through solid hydrate is

much slower than through liquids, indicating that CO_2 or CH_4 transport through the solid hydrate will be much slower than through the water. If the exchange process is limited due to diffusion, the surface contact area needs to be increased.

Part 2

Work and Results

2 Experimental Setups and Procedures

This master thesis is based on experimental work conducted in the hydrate laboratory at the University of Bergen. The key purpose of this study was to gather more data to the Hydrate Research Group, and to further enhance the understanding of NGH and the CH_4-CO_2 exchange process as a methane production method. The hydrate laboratory, schematic illustrated in Figure 2-1, consists of three setups; 1) setup A (resistivity) , 2) setup B (baseline) and 3) setup C (temperature). In all setups methane hydrate was formed in porous Bentheim sandstone cores, and then exposed to carbon dioxide injection where the methane and carbon dioxide production was measured. Subsequently the hydrate was melted by depressurization or by thermal stimulation. All three setups are capable to do hydrate formation, CH_4-CO_2 exchange, and hydrate dissociation in one core sample during the same experiment. Several experiments have been conducted, where the focus of this thesis has been to investigate how temperature can affect the exchange rate and methane recovery during the CH_4-CO_2 exchange.

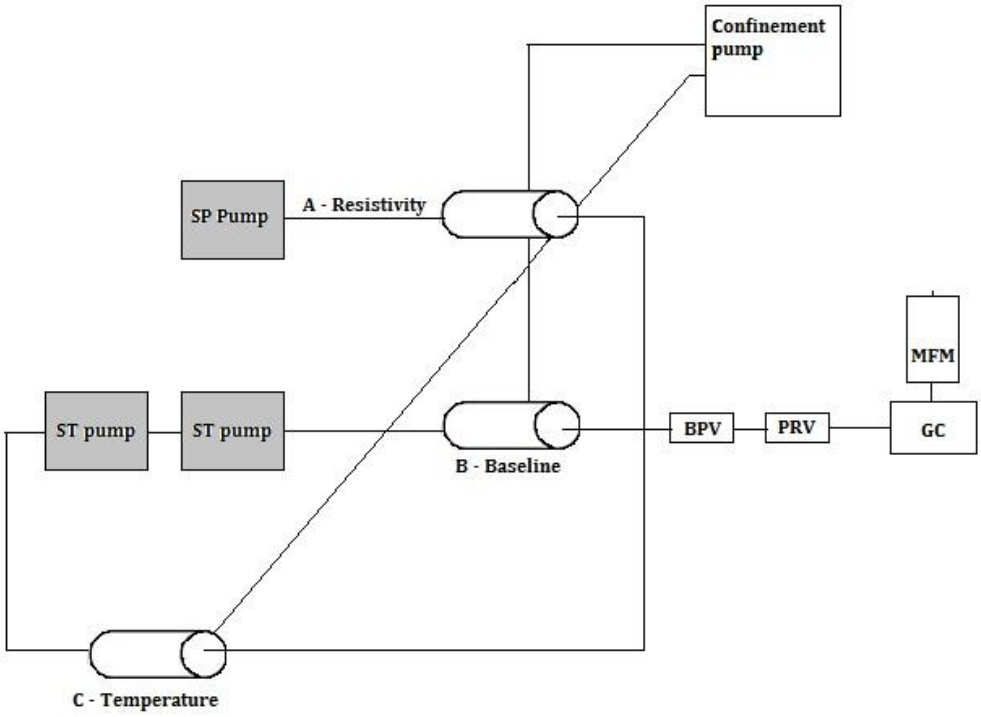

Figure 2-1: A schematic overview of the hydrate laboratory in the University of Bergen. The figure shows the three setups (with implemented cooling jacket), where setup A measures resistivity, setup B is used as a baseline, and setup C is used for temperature experiments. Production line and confinement pump is also illustrated. In this thesis setup C was mainly used.

2.1 Equipment

- Hassler Type Core Holder
- Customized Cooling jacket from UiB workshop
- Sanchez Technologies Stigma 300 Pump (ST pump), with Falcon software
- Thermo Neslab Digital Plus RTE17 refrigerated bath circulator
- Omega Multilogger Thermometer HH506RA
- Edwards RV3 Vacuum pump
- Agilent Technologies 3000 Micro Gas Chromatography (GC)
- Bronkhorst Mini Cori Flow, Digital Mass Flow Meter/Controller (MFM)
- Back pressure valve with nitrogen applied at 86 bar
- Swagelok Pressure Regulator (high pressure to low pressure)
- Swagelok manometers (confining pressure and pressure regulator)
- Haskel pump
- Isco Series D Pump (confinement pressure build up pump)
- Buffer (Confinement pressure)
- 2 Unik 5000 Pressure sensors/transducers
- Duck DPI 610 calibrator
- Slug Injector

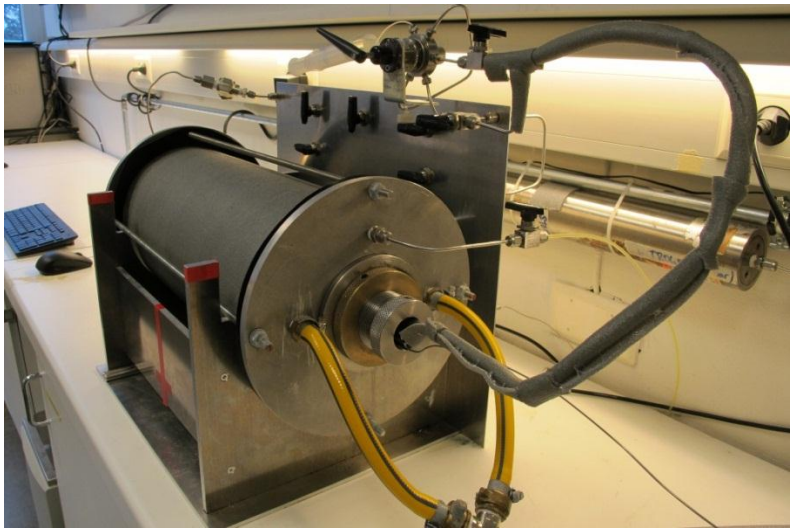

Figure 2-2: Picture of setup C, showing core holder with its surrounding cooling jacket, loop valve, buffer, outlets for anti-freeze and inlet.

2.2 Properties of the porous media

Due to the cost and complexity of retrieving core samples from hydrate reservoirs, an outcrop holding comparable properties to possible production sediments was used in all experiments performed in this thesis. The outcrop was acquired from the Bentheim quarry in Lower Saxony in Germany. It is a clastic sedimentary rock with a generally high porosity (ca. 23 %) and permeability (1.1 D). It holds a grain density of 2.65 g/cm^3 with mineralogy of 95-99 % quarts, and is characterized by its uniform pore geometry with an average pore diameter of 125 microns (Ersland, 2008).

Figure 2-3: Picture of a Bentheim sandstone core used in one of the experiments conducted during this thesis. The core was approximately 14 cm long and 5 cm in diameter.

2.3 Experimental Setup

Time and effort was used on improving the hydrate laboratory with regards to safety, more accurate measurements, as well as ease of use. To achieve this goal, new instruments and solutions were implemented, service on old equipment was carried out, and new tubing systems were implemented where it was needed. These factors had an impact on the quantity of experiments completed in this thesis, as there was some down time. Another limitation regarding numbers of experiments completed

was that all three setups shared one GC and one MFM, resulting in inactivity when other setups were running exchange measurements.

Experiments conducted in this master thesis were primarily carried out on setup C, which is similar to setup A and B. Setup C was modified from an open cooling bath system (illustrated in Figure 2-4), where the Hassler core holder was submerged into an open cooling bath, to a closed system where the Hassler core holder was built in and enclosed by a cylindrical cooling jacket. This conversion was done because of several incidences where the cooling bath ran over, consequently resulting in loss of temperature control in the system.

A Thermo Neslab RTE17 refrigerated bath circulated antifreeze with chosen temperature around the enclosed core holder, ensuring desired core temperature throughout the formation, exchange and dissociation processes. The core temperature was measured by an Omega Multilogger Thermometer at the inlet side with a sensor reaching the core surface. The confinement pressure, with the objective to surpass the pore pressure, was previously held by a Haskel pump running on air, but due to time consumption and inaccuracies it was replaced by a buffer delivering a constant pressure of 120 bar to the confinement. The buffer was prepared by filling approximately 500 ml of N-Decane on the oil delivery side, and then pressurized with nitrogen gas to the desired confinement pressure on the other side. An Isco Series D pump was used to reach the confinement pressure before the buffer was connected to the system. A bypass valve was also implemented, making it possible to inject gas from inlet side and outlet side simultaneously, as well as remove and change present gas (by isolating the core) in the system throughout the experiment. Inlet and outlet pressure transducers monitored the pore pressure, and were positioned so that the core pressure could be measured if both inlet and outlet valves had to be closed. A back pressure valve (BPV), set on approximately 86 bar by nitrogen, released gas when the pore pressure exceeded the set pressure. Due to a maximum pressure limit on the Gas Chromatograph (GC), a pressure regulator was used to control the pressure level from the BPV to the GC. The Swagelok pressure regulator had a high pressure inlet and a low pressure outlet, with an opportunity to adjust the outlet pressure to the preferred pressure level of approximately 1 bar. A Bronkhorst Mini Cori Mass Flow Meter was implemented on all setups to measure the gas produced in order to achieve greater control of the mass produced. Figure 2-4 and Figure 2-5 illustrate respectively the old setup C and the new improved setup C.

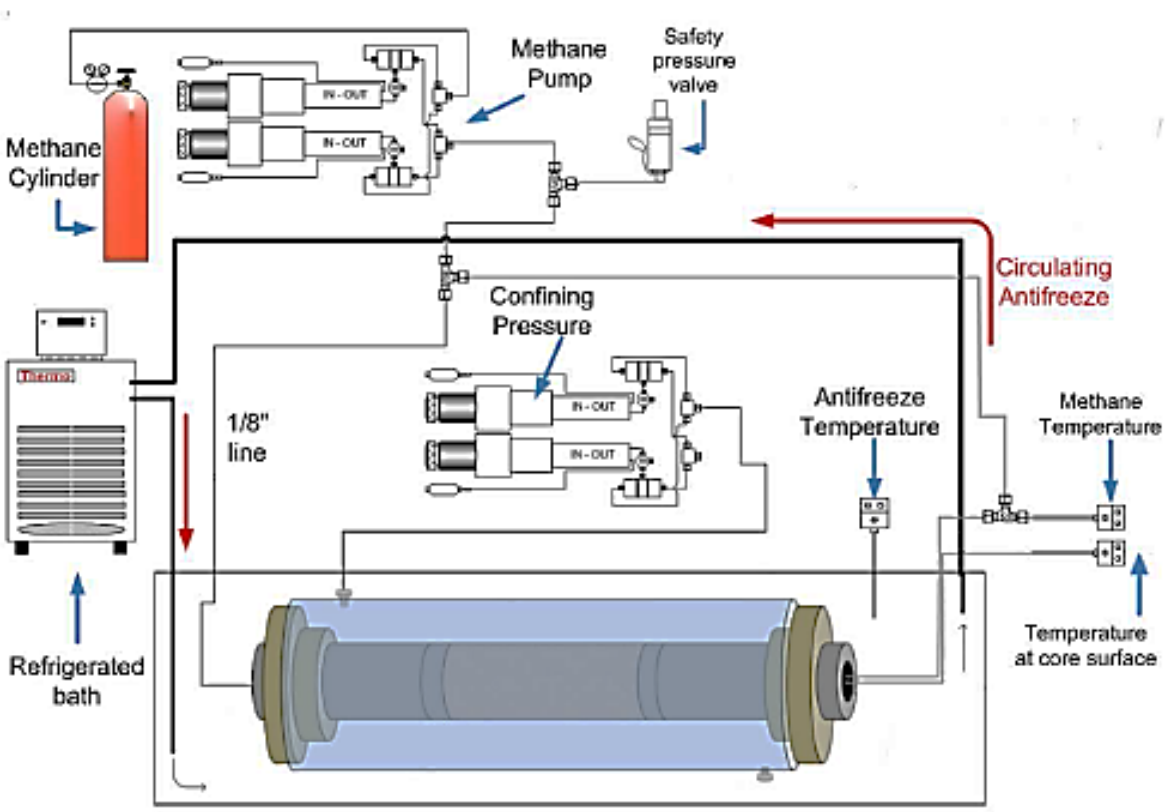

Figure 2-4: An illustration of earlier setup C with an open cooling bath instead of an enclosed cooling jacket and mass flow meter implemented during the modifications conducted in this thesis (Husebø, 2008).

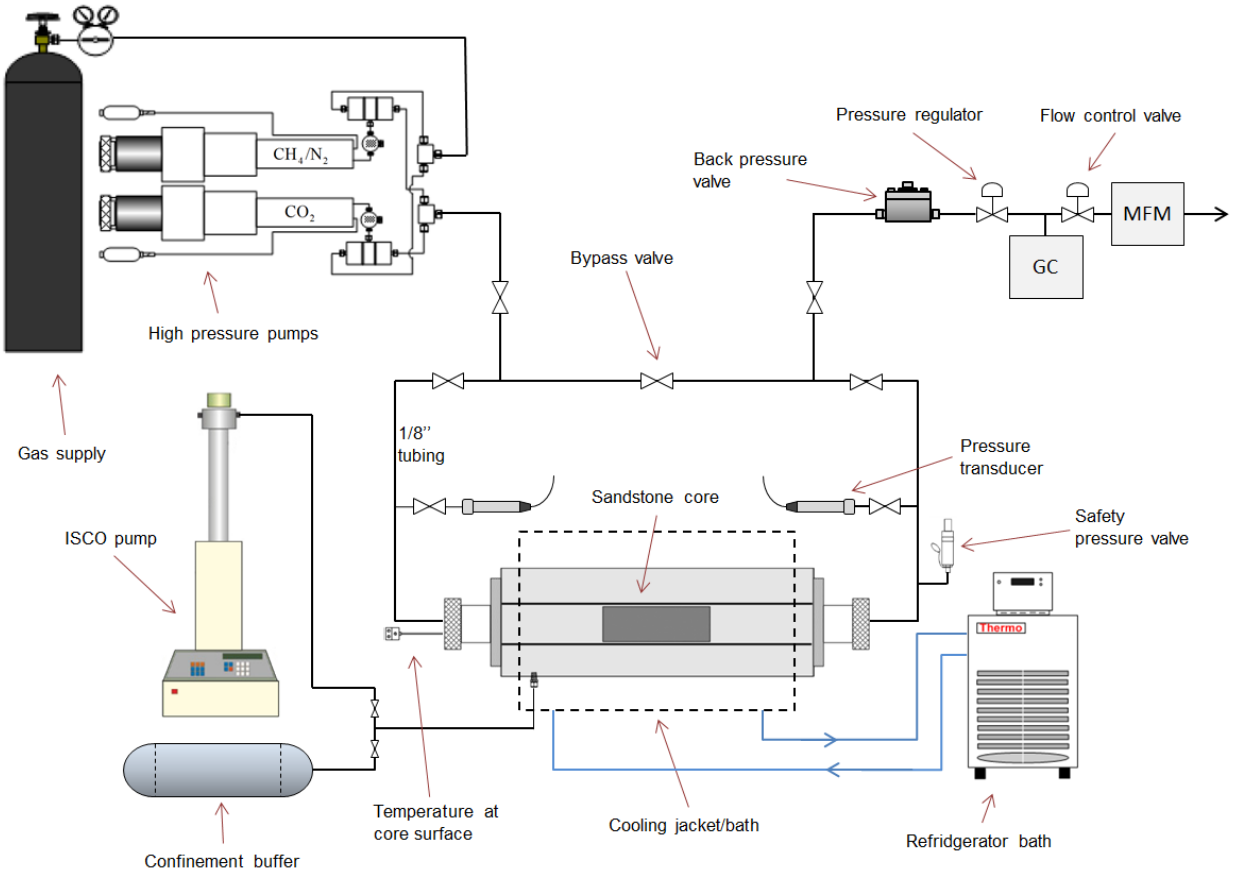

Figure 2-5: An Illustration of the modified and improved setup C used in this thesis. Cooling jacket, mass flow meter and a buffer for holding the confinement pressure were implemented, along with changes regarding tubing and valve systems (Hågenvik, 2013).

2.4 Methods and procedures

Throughout every experiment conducted there was high emphasis on safety due to gas under high pressure. A safety routine was established before any experiments were carried out unaccompanied. Brochures were available at the laboratory and required to read and follow. Safety glasses, lab coats and gloves were used. All parts of the setup which was exposed to high pressure had safety valves installed, ensuring a maximum pressure of 120 bar, as well as a maximum pressure alarm on the pump.

2.4.1 Groundwork for hydrate experiments

When initiating a NGH experiment a porous media had to be prepared. Bentheim sandstone was used in all experiments to mimic the coarse grained sand sediments typically found in Boswell's top pyramid, with properties such as a generally high porosity, permeability and uniform pore geometry. The cores were whole cylindrical plugs with diameter and length of approximately 5 cm and 14 cm respectively. An example of a core used in an experiment is found in Figure 2-3. The core was first and foremost cut to preferred length and diameter, before it was dried in a heating cabinet for a minimum of 24 hours to clean the core from potential impurities. In order to saturate the core it was lowered horizontally into a container with a brine solution mixed to desired composition, covering half of the core, where a spontaneous imbibition ensued, shown in Figure 2-6.

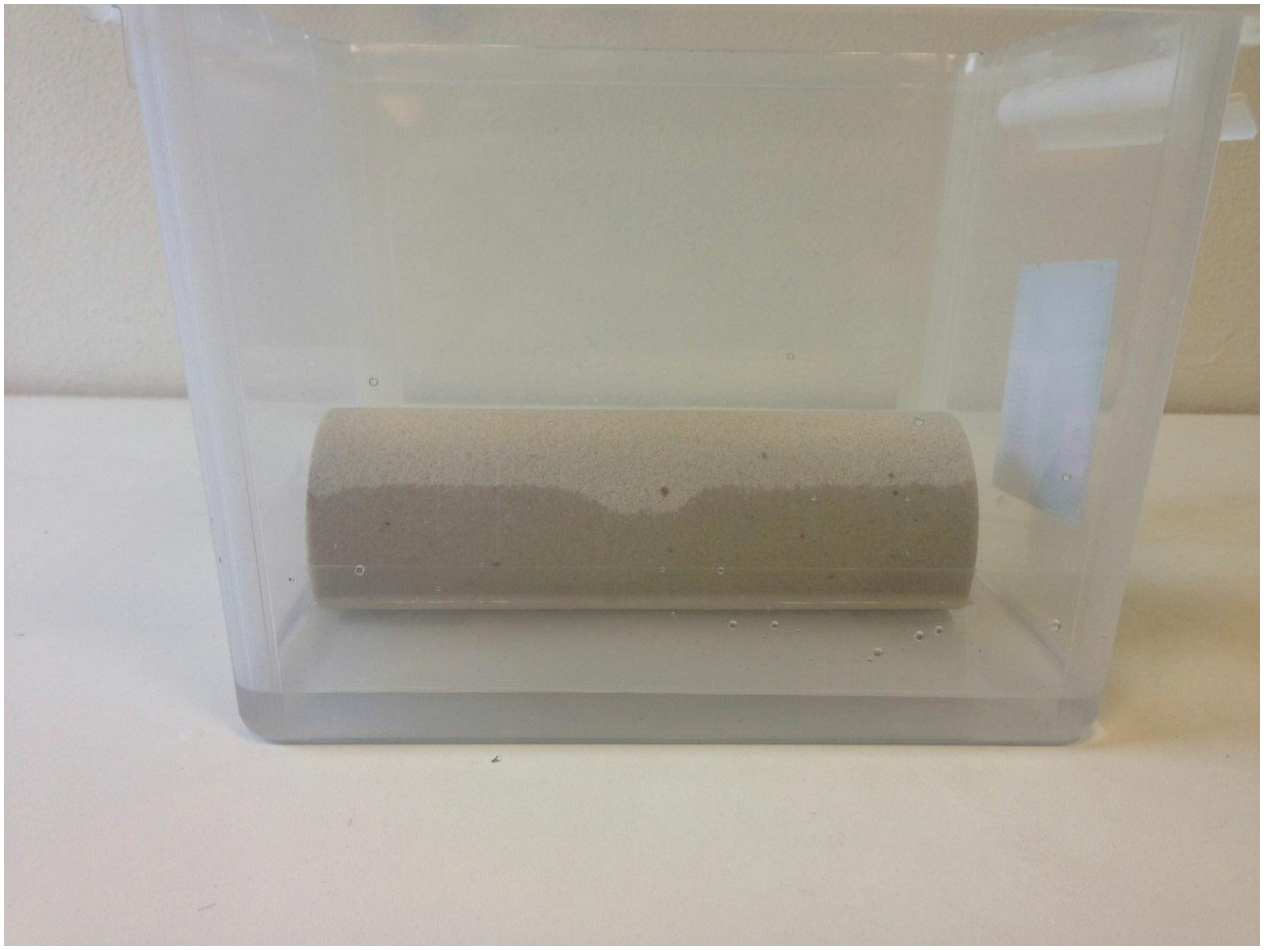

Figure 2-6: Picture of a spontaneous imbibition when saturating a water-wet Bentheim sandstone core. The brine is only covering the bottom of the tray, but due to wettability and capillary pressure the water will imbibe and distribute itself in the porous media.

The saturation goal was calculated by using the average porosity of the Bentheim sandstone core, measuring length, diameter and the weight of dry and wet core. The wanted brine saturation in the core was then achieved by using a vacuum pump and removing the excess water. Before the saturated core was mounted into the Hassler core holder, illustrated in Figure 2-7, it was wrapped in one layer of plastic film and two layers of aluminum foil to protect the sleeve from getting damaged by the injected CO_2.

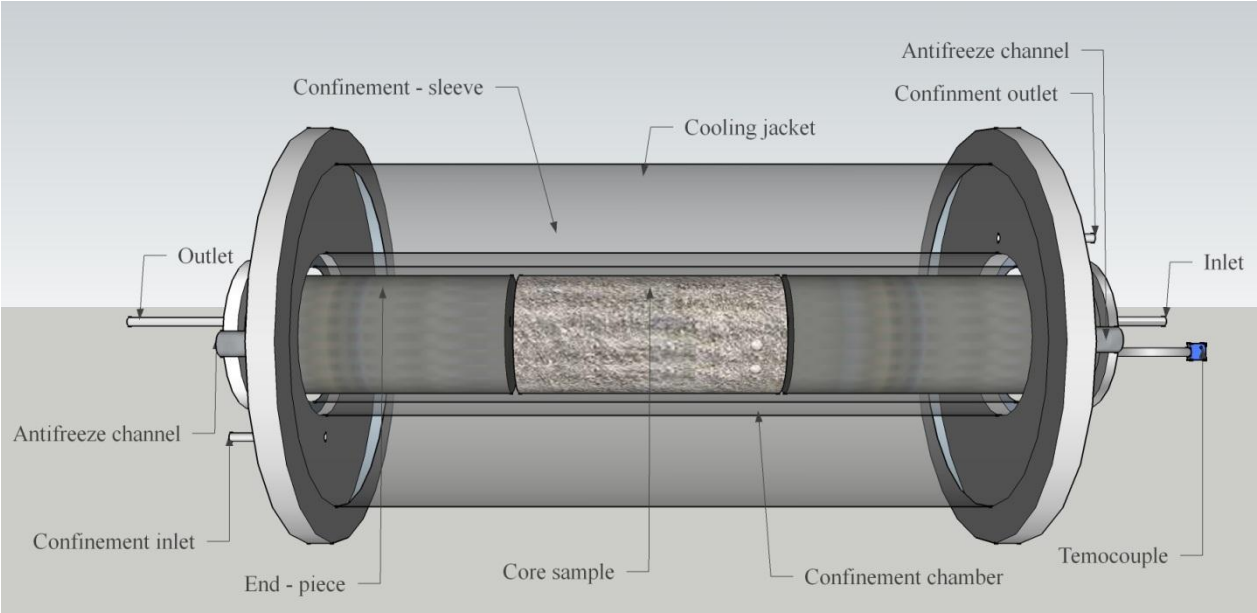

Figure 2-7: A transparent illustration of the core holder and its surrounding cooling jacket, providing an insight on how it is built (Hossainpour, 2013).

2.4.2 Hydrate formation procedure

The prepared core plug was mounted inside the Hassler core holder and both end-plugs were fixed into position isolating the core within the system. Inlet and outlet valves were closed, and vacuum was applied to remove present gas in the remaining system. The CH_4 pressure vessel was then opened, allowing the CH_4 to enter and pressurize both pump and tubing. Inlet and outlet valves were opened simultaneously in the pressure region of 1 bar, consequently exposing the core to methane from both sides with an increasing pressure until reaching the desired conditions, 83 bar at room temperature. Inlet, outlet and by-pass valves remained open throughout the formation process. The pump was set to a constant pressure of 83 bar, while the temperature was lowered from ambient condition to 4° C by decreasing the temperature on the cooling bath. The core temperature was measured by a sensor positioned at the end surface of the core at inlet side. Pressure, temperature and volume (PVT) data were logged, and hydrate formation was detected by the gas consumption observed when reaching a

temperature well within hydrate stable conditions at constant pressure (gas volume change as a function of time). The hydrate formation was concluded complete when the gas consumption rate was stable and close to zero. A leakage rate was calculated by using the slope of the formation curve after reaching completed hydrate formation, where a leakage rate less than 0.05 ml/h was accepted.

2.4.3 CH_4-CO_2 exchange procedure

After completed hydrate formation the core temperature was adjusted to desired condition, and a CH_4-CO_2 exchange process was initiated. The inlet and outlet valves were closed to isolate the CH_4 hydrate saturated core, and the remaining CH_4 was removed from the pump and rest of the system by allowing gas out the ventilation chamber as well as applying vacuum. The pump and system, except the core, was then filled and pressurized by CO_2 until reaching 83 bar. The bypass valve was then closed and inlet and outlet valves were opened. The pump was set to inject CO_2 with a constant rate of 0.02 ml/min (1.2 ml/h), where the CO_2 was injected from inlet side towards the outlet, ensuring a production rate through the GC and MFM. A pressure build-up followed as CO_2 was injected, where the back pressure valve released produced gas when exceeding the BPV pressure set to 86 bar. The pressure regulator was adjusted to an acceptable pressure level (approximately 1 bar) with regards to the limitations of the GC. The produced gas then went through the GC and lastly the MFM, measuring composition and mass of the effluent. By logging mass produced and its composition an estimate of methane produced by injecting CO_2 was attainable. A choke valve controlling the gas flow through the GC could be adjusted to achieve a steady flow and keep the pressure in advance of the pressure regulator at an acceptable level. The tubing from the outlet side of the mass flow meter went to the ventilation chamber, allowing the measured produced gas to emit safely.

Two inhibitors were investigated in this thesis. MDEA and MEA were injected to the system through a loop valve connected on the inlet side, allowing a slug of 250 microliter of MDEA or MEA to enter the system alongside the injected carbon dioxide into the core. One slug of MDEA or MEA was injected in an interval of 15 minutes, and repeated four times. This was repeated several times during the last stage of the exchange process mentioned above. In one experiment setup B was modified to inject MEA from a separate pump directly into the core, before carbon dioxide was introduced.

It is worth mentioning that the CH_4-CO_2 exchange took place within the methane hydrate stability zone as well as carbon dioxide stability zone in all experiments conducted.

2.4.4 Dissociation of CO_2 and CH_4 hydrate

In some of the experiments conducted dissociation was performed either by depressurization or by thermal stimulation. After injection of at least two pore volumes of CO_2, or when the level of the CH_4 produced was low enough during the exchange, a dissociation of the present hydrate could be initiated. A depressurization procedure was followed after PhD Knut Arne Birkedal´s instructions for data input to TOUGH+HYDRATE simulations. The pressure was lowered in several large steps. In correlation with the decreasing pressure, the confinement pressure was decreased avoiding too much stress on sleeve and core plug. The pressure was first lowered to 40 bar from 83 bar. The pump was then emptied to ensure a free volume in the pump for the liberated gas in the next step. The pressure was then lowered to 30 bar as quick as possible. An increased pressure, due to the liberated gas from the dissociating hydrate, forced the the pump to retrieve. When the pressure was way below the stability region for both CH_4 and CO_2, and gas delivery from the hydrate had ended, the experiment was completed and the system could be taken down. In addition to pressure depletion, a thermal stimulation was used as a procedure in several experiments. The temperature was then increased by heating of the anti-freeze, consequently rising the core temperature. The pump was then set to constant pressure (approximately 83 bar). As gas was liberated from the dissociated hydrate, when exceeding the equilibrium temperature and subsequently leaving the hydrate stable region, the pump would receive the gas produced to maintain the constant pressure.

3 Experimental results and discussion

This section will present achieved results from the experiments conducted in this thesis in comparison with past results done within the Reservoir Physics Group at the Department of Physics and Technology, UIB. The results are divided into three progressions; 1) hydrate formation, 2) CH_4-CO_2 exchange and lastly 3) hydrate dissociation either by a depressurization method or by thermal stimulation. All experimental data were collected by computers and their corresponding software programs in the course of each experiment. The collected data were structured and analyzed in Excel before added in an in-house MatLab program customized for presenting and comparing new and earlier results gathered from the Hydrate Research Group (Hauge, 2013). Laboratory work within hydrate research can be time demanding, and also challenging, which can explain the amount of experiments completed during this thesis. Table 4 below gives an overview of the experiments conducted. Results from every experiment will not be presented here due to an emphasis on the experiments that generated relevant data to the topic of this thesis. A total of twelve experiments were conducted, where experiments marked in red were conducted before the laboratory upgrade. CH_4-CO_2 exchange results from these experiments will not be emphasized due to lack of MFM data. In experiment CO_2 -22 and DEP5 plugging hindered completion of CH_4-CO_2 exchange, and therefore only hydrate formation is presented. DEP5 consists of several hydrate formations and dissociations performed on the same core during one experiment where each formation and dissociation is marked as DEP5-1, 2, 3 and 4.

Table 4: An overview of experiments conducted at the hydrate laboratory at UiB. HR-48, CO2-19, and CO2-20 (marked red) are experiments completed before the laboratory upgrade. Therefore there will not be emphasis on these experiments when examining the exchange process in this thesis. The table also show brine salinity, initial water saturations and temperature during exchange.

Experiment	Salinity wt%	S_{wi}	Temperature during exchange (° C)
CO_2 – 19	0.1	0.62	9.6
CO_2 – 20	0.1	0.42	10
CO_2 – 21	0.1	0.41	9.6
CO_2 – 22	0.1	0.38	No exchange due to plugging
CO_2 – 23	0.1	0.41	4.0 (MDEA)
CO_2 – 24	0.1	0.41	4.3 (MEA)
CO_2 – 25	0.1	0.41	4.3 (MEA)
CO_2 – 26	0.1	0.433	9.6
CO_2 – 27	0.1	0.40	4-9 (MEA)
CO_2 – 28	0.1	0.40	No exchange
DEP5-1	0.1	0.43	No exchange due to plugging
DEP5-2	0.1	0.43	No exchange due to plugging
DEP5-3	0.1	0.43	No exchange due to plugging
DEP5-4	0.1	0.43	No exchange due to plugging
HR-48	3.5	0.64	4.2

3.1 Results from Hydrate formation

Hydrate formation was successfully formed in eleven Bentheim sandstone cores with initial water saturations in the region of 0.4 and constant brine salinity of 0.1 wt%, shown in Table 5. The results will be presented in the following section as well as a brief presentation of earlier in-house results with different initial properties. Hydrate formation was achieved by introducing methane gas to the brine saturated sandstone core at a constant pressure set to 83 bar, and then lowering the temperature from ambient to 4° C resulting in a strong thermodynamic driving force which will initiate hydrate growth within an acceptable time frame. In one experiment hydrate formation was attempted at a higher temperature (9.6° C) but still within stable region. In this section hydrate formation results will be shown and discussed.

Table 5: Post hydrate formation properties for all experiments conducted, showing hydrate saturation, remaining water, and moles of methane stored in hydrate for each experiment.

	Hydrate saturation (fraction)	Water remaining (fraction)	CH_4 in hydrate (mol)
CO_2 – 21	0.48	0.03	0.23
CO_2 – 22	0.48	0.00	0.23
CO_2 – 23	0.48	0.03	0.25
CO_2 – 24	0.48	0.03	0.24
CO_2 – 25	0.51	0.00	0.28
CO_2 – 26	0.48	0.05	0.24
CO_2 – 27	0.43	0.06	0.22
CO_2 – 28	0.40	0.08	0.20
DEP5-1	0.46	0.06	0.24
DEP5-2	0.45	0.07	0.23
DEP5-3	0.44	0.08	0.22

Figure 3-1 displays and represents a typical methane hydrate formation curve and is based on data collected from experiment CO_2-22. The methane consumption taking place after roughly 8.5 hours, demonstrated as an increase in the green graph indicates the start of hydrate growth and the following development of hydrate formation. The methane consumption initiates when the water molecules form structures capable to encage present methane molecules, forcing the pump to inject additional methane to keep the pressure constant at 83 bar. The graph clearly shows a steep curve when the hydrate growth first initiates, where 18 ml of methane are consumed during 1.5 hours. This indicates that pressure and temperature conditions are well within the methane hydrate stable region (4° C, 83 bar), proving a strong thermodynamic driving force. Methane consumption as a result from the cooling of the system (due to increased density) and leakage has been accounted for in all results presented.

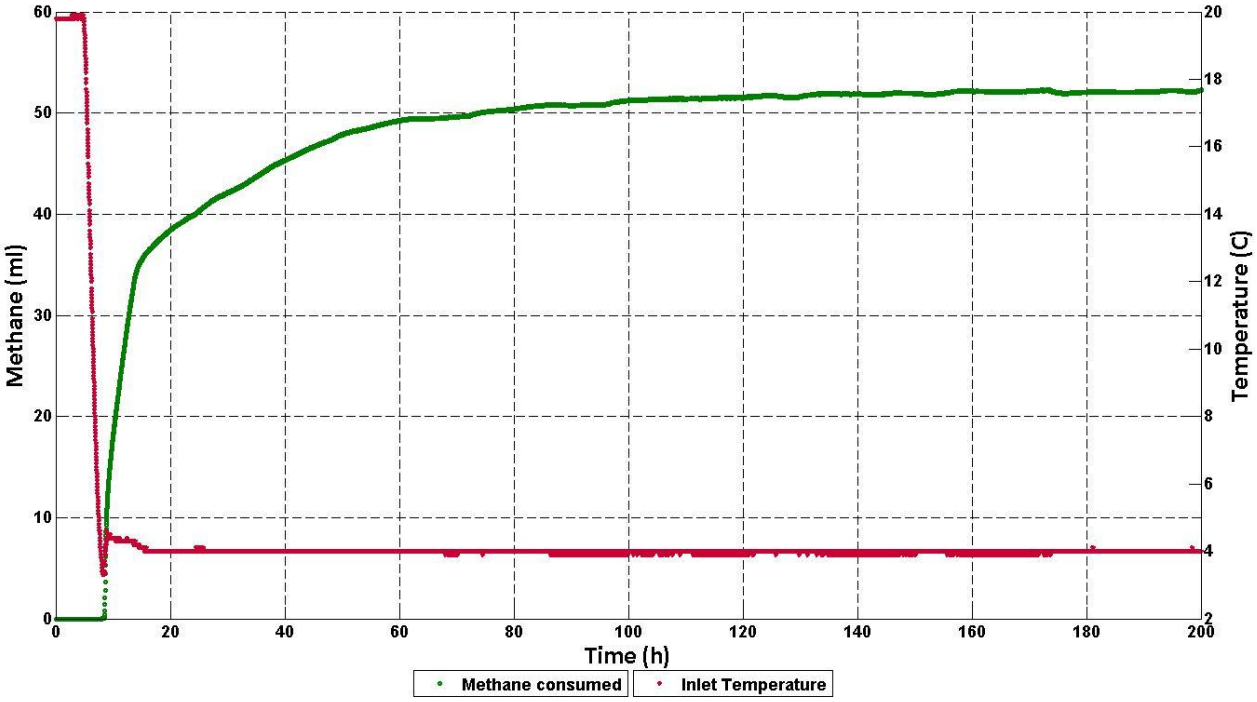

Figure 3-1: Methane consumption (ml) and core temperature (C) as a function of time (h) during the hydrate formation conducted in experiment CO_2-22. The brine salinity was 0.1 wt% with an initial water saturation of 0.38. When reaching a temperature providing strong enough driving force methane consumption initiates, indicating hydrate formation, before the curve evens out indicating the end of hydrate formation.

The first step in the hydrate formation process is the induction time, which is a time that will differ based on laboratory equipment and driving forces present. The induction time in this setup may be considered as the time from when the temperature is within methane hydrate stability region at 83 bar without detecting hydrate growth, which is detected as methane consumption. This time period is illustrated in Figure 3-2 and indicates an induction time during this experiment of approximately 2 hours (based on a methane hydrate stability region from temperatures below approximately 11° C, a temperature retrieved from CSMGem).

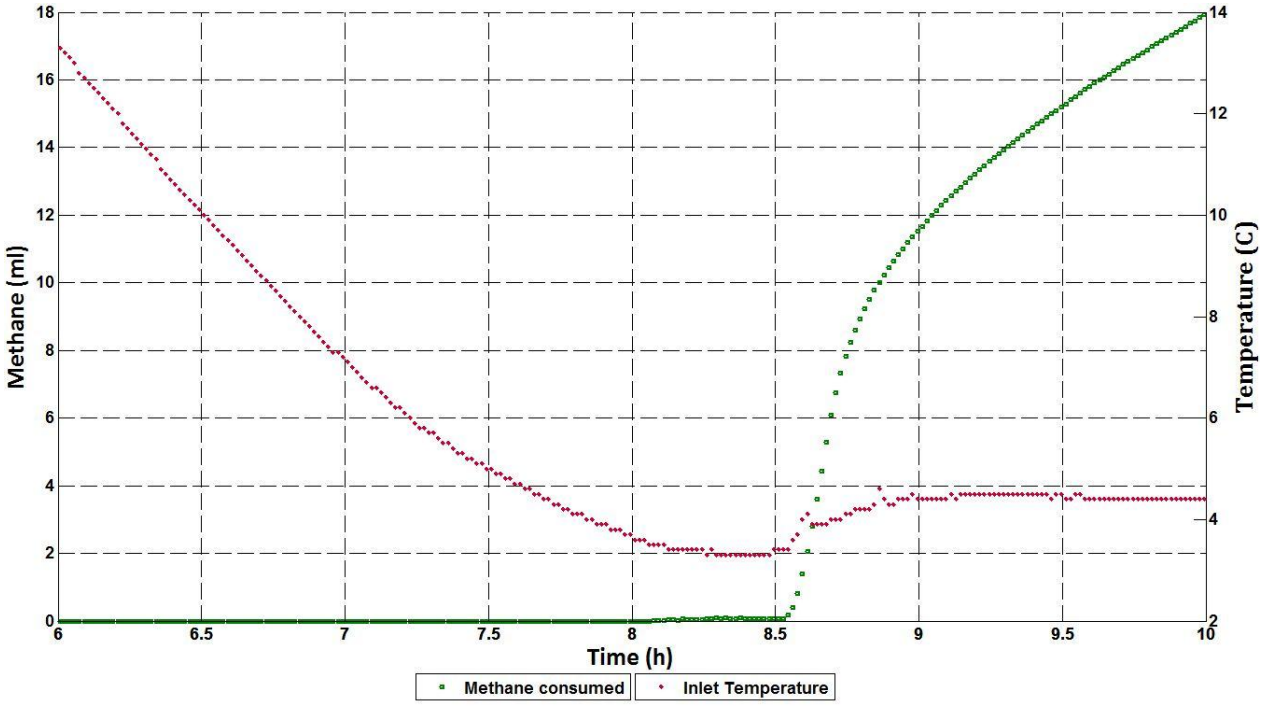

Figure 3-2: The graph show the time period from 6 hours to 10 hours in experiment CO_2-22, where the induction time can be observed as the time from when the temperature is within stable region to the time of methane consumption. Based on CSMGem the stable temperature is approximately 11° C. The experiment had initial properties with brine salinity at 0.1 wt% and initial water saturation at 0.38.

As shown from the graph in Figure 3-1, the methane consumption initiates when the temperature is low enough and subsequently providing a strong thermodynamic driving force. A rapid formation takes place when reaching a temperature of approximately 4° C, seen as a steep curve. After roughly 35 ml of consumed CH_4, the hydrate formation rate decreases. This could be explained by where the hydrate growth is located in the pore space. Due to the fact that the sandstone is water-wet and water saturations are low (approximately 0.4), water will be expected to be located at the grain surface on the pore wall in large pores, as well as filling the small pores. From this statement, as well as a low solubility of methane in water, it is reasonable to assume that the hydrate is formed as a film near the grain surface, between the excess gas and water interface. The hydrate formation rate would then be reduced as the contact between the available water and injected gas is limited by the formed hydrate. As seen from the illustration in Figure 3-3, the formed hydrate will separate the excess gas and the needed brine as the hydrate film grows. The formation rate will then be reduced, and growth is limited by mass transport. The available brine will also become more saline during the hydrate formation, subsequently causing a negative contribution to the hydrate growth, and when reaching 14 wt% becomes in-active water (at experimental conditions). These conclusions are based on a reservoir condition with excess gas. With excess water the hydrate growth probably would be different, where the growth maybe would occur in the center of the pore space with surrounding brine.

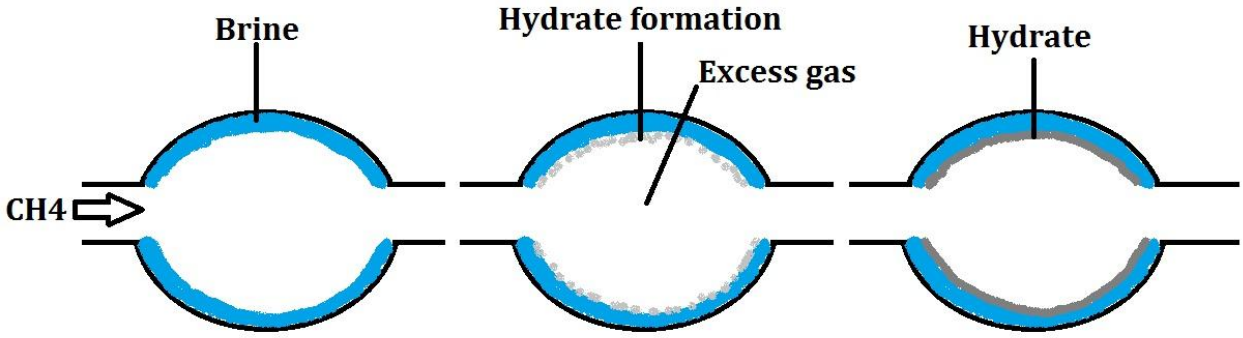

Figure 3-3: 2D Illustration of a possible location of hydrate growth within the pore space in an excess gas situation. Due to the water-wet sand stone core water will be present along the grain surface, and consequently this is where the hydrate will form.

In experiment CO_2-26 the hydrate formation temperature was increased to 9.6° C from customarily 4° C, however still within methane hydrate stable region. This was done to study how temperature affects hydrate formation, and more importantly to further investigate the effect this would have on the following exchange process when formed under equal temperature. As seen in Figure 3-4 hydrate growth did not initiate during a time period of 70 hours within stable conditions with a temperature at 9.6° C and pressure at 83 bar. This is clearly an indication that an increased temperature shift of 5° C within stable conditions contributes negatively to the thermodynamic driving force, consequently increasing the induction time as well as the hydrate formation rate. Hydrate growth could be expected to occur if necessary time had been provided. As the temperature was decreased to approximately 4 °C, the hydrate formation rapidly took place.

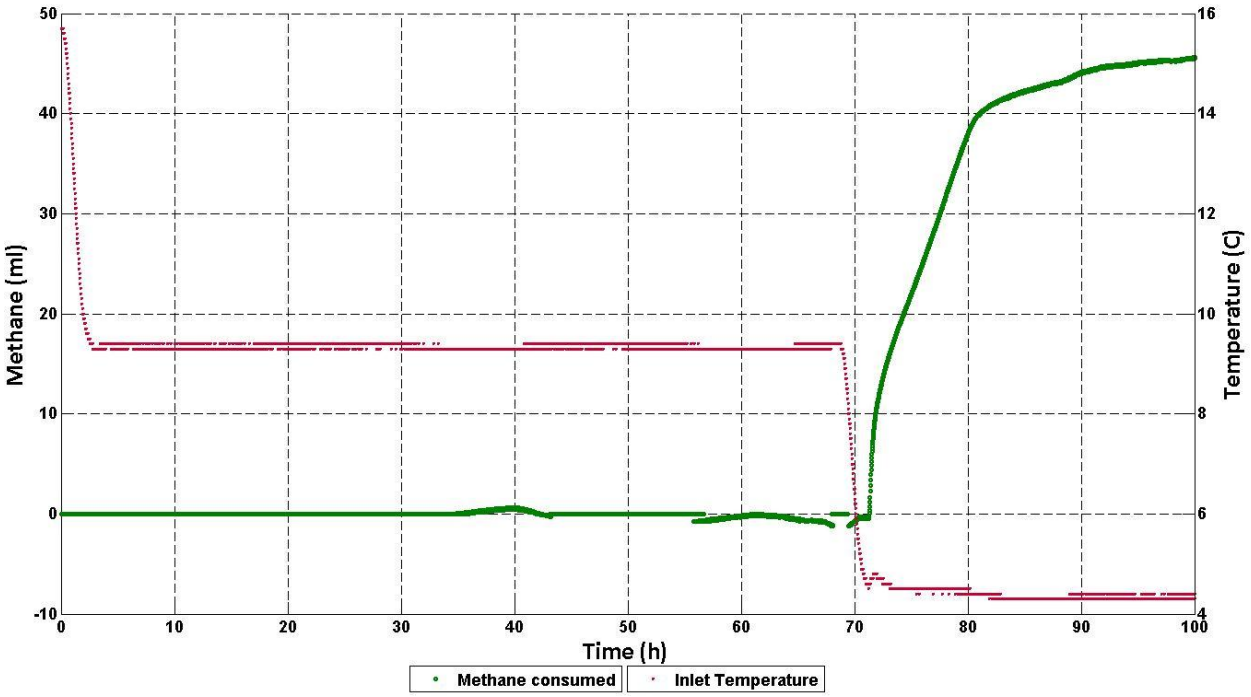

Figure 3-4: The 100 first hours from experiment CO_2-24 showing no hydrate formation at 9.6° C. When the temperature was decreased a rapid hydrate formation initiated, illustrating the thermodynamic driving force.

A plot of all hydrate formations conducted during this thesis is found in Figure 3-5. With some exceptions, all hydrate formations resulted in a methane consumption of 50 ± 5 ml and equal formation rates. Experiment CO_2-25 had methane consumption above 60 ml which can be explained by the core used, which had a larger pore volume than the rest (73.79 ml versus cores with less than 70 ml, and typically 66 ml). Some small differences in initial water saturations (S_{wi}), time, core size, pore volume and temperature can be factors contributing to small differences in methane consumed, but all over there is repetitiveness and consistency in the experiments conducted with equal initial properties. The average methane in hydrates from all conducted experiments is 0.23 mol, and varies between 0.20 and 0.28 mol.

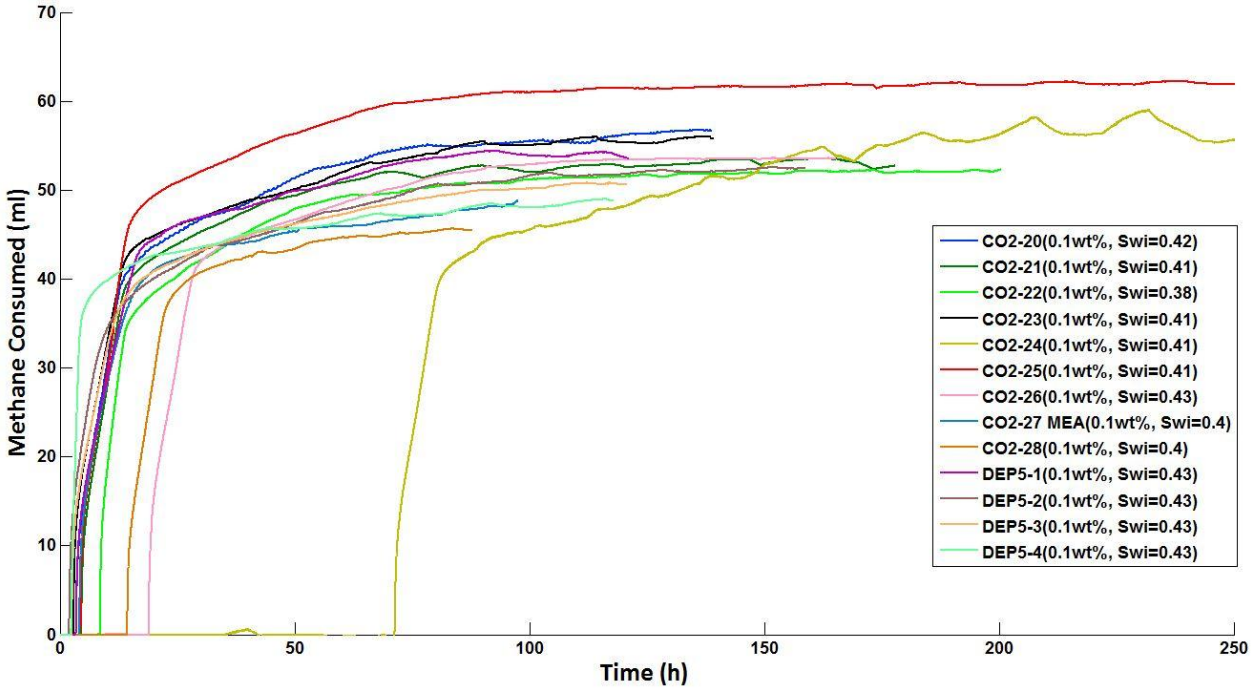

Figure 3-5: Comparison plot showing all hydrate formations conducted during this thesis where all experiments had the same initial properties. Both methane consumption and formation rates are observed to be alike.

Experiment DEP5 was conducted as several hydrate formations and dissociations in one core during one experiment. As seen from Figure 3-6, the methane consumption decreases for each new formation. This could be explained by loss of water during dissociation, resulting in less access to hydrate former. The rapid hydrate formation in DEP5-4 was conducted after hydrate dissociation by thermal stimulation, where the pressure remained constant at 83 bar. The continuous pressure in the system may explain the formation rate seen in the steep graph.

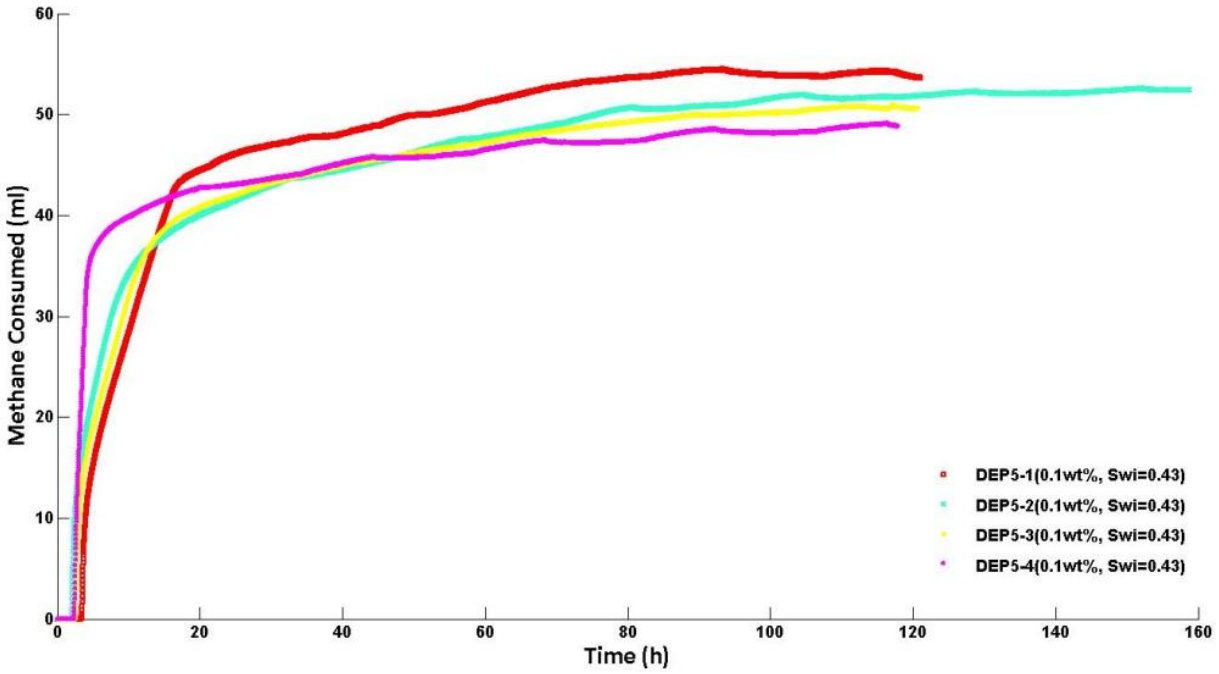

Figure 3-6: DEP5 hydrate formation plot. Four hydrate formations and dissociations were conducted in one experiment. Loss of water causes less methane in hydrate for each formation, and the rapid formation in DEP5-4 could be due to a previous thermal stimulation where pressure remained applied.

To demonstrate how salinity and initial water saturations influence the hydrate formation a plot of experiments conducted within the hydrate group is represented below in Figure 3-7 and Figure 3-8. Salinity varies from 0.1 wt% to 3.5 wt%, and initial water saturation from 0.4 to 0.8. Formation rates and methane consumption, consequently methane in hydrate, varies from 0.3 ml to over 0.7 ml, and illustrate the sensitivity of initial properties. The experiment which consumed the most methane is CO_2-19 with 0.1 wt% salinity and an initial water saturation of 0.62. Earlier in-house research indicates that initial brine saturations have an impact on the initial hydrate formation rate, where the formation rate increases with a decrease in brine saturations (Husebø, 2008). An increase in brine salinity also showed to have a negative effect on formation rates, but not necessarily on the amount of methane consumed

for brine salinities lower than 4 wt% (Husebø, 2008). Usage of water during hydrate formation results in increased brine salinity for remaining brine. At the laboratory conditions a salinity limit of 14 wt% is calculated (CSMGem) for further hydrate growth.

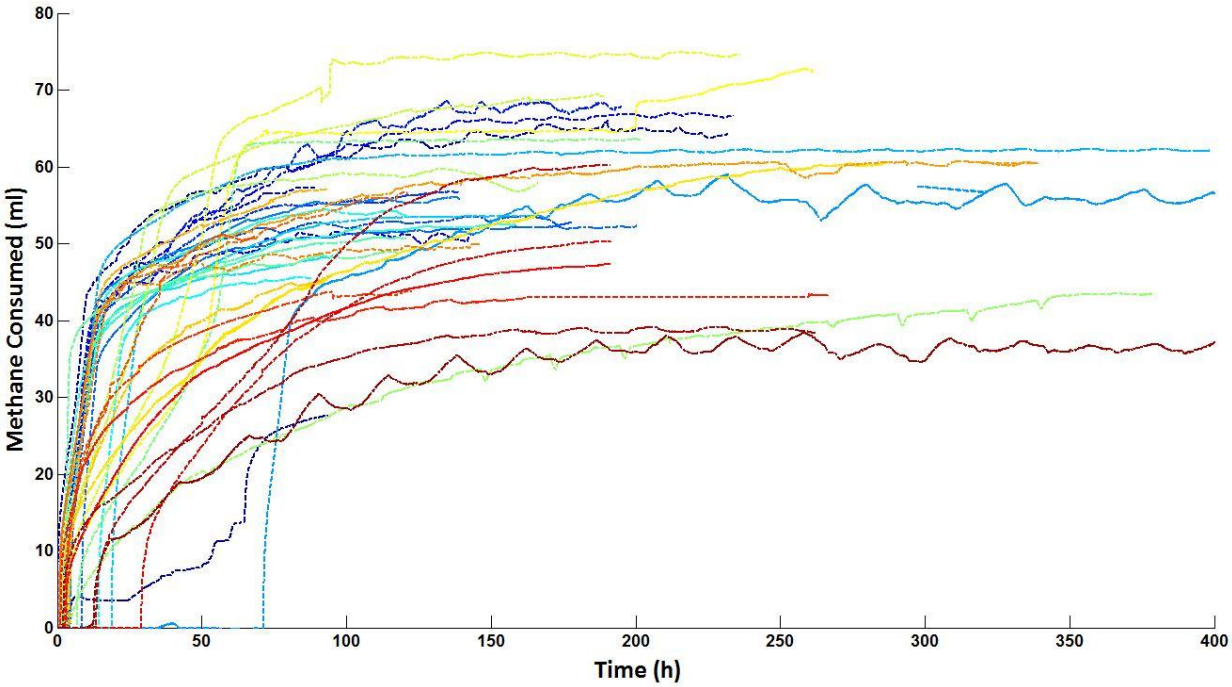

Figure 3-7: Comparison plot of all hydrate formations conducted within the Hydrate Research Group showing variation in both formation rate and methane consumed. Initial brine salinity and water saturation have impact on the hydrate growth.

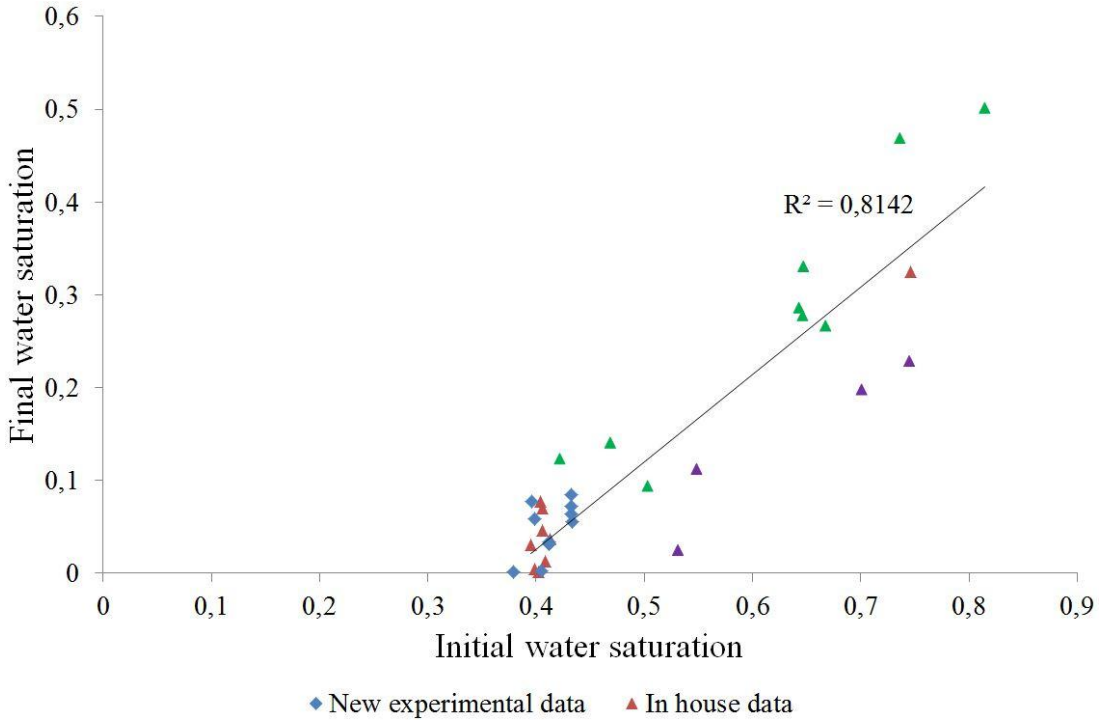

Figure 3-8: Comparison plot of hydrate formation experiments conducted within the Hydrate Research Group at UIB, which illustrate the variations in final water saturations as a function of the initial water saturation and salinity. The green triangles are experiments with salinity of 3.5 wt%, purple is 1 wt%, and red is 0.1 wt%. The blue squares represents experiments conducted in this thesis with a brine salinity at 0.1 wt% and initial water saturation at approximately 0.4.

3.2 Results from CH_4-CO_2 exchange

The main objective of this thesis is to investigate the process taking place when methane hydrate within a porous media is exposed to injected liquid CO_2, where preferably an exchange process will liberate encaged CH_4 and sequestrate CO_2. Experiments were conducted at different temperatures to study a possible change in both exchange rate and methane recovery (amount of methane produced). Theoretically a higher temperature, implying conditions closer to the equilibrium line, could have a positive contribution to the exchange. Table 6 shows an overview over CO_2–CH_4 exchange experiments conducted in this thesis. After giving a short introduction to a typical gas fraction curve as well as a differential pressure curve, there will be a presentation of the results from each experiment conducted, followed by a more in depth discussion.

Table 6: Overview of CH_4-CO_2 exchange experiments conducted in this thesis. Total methane production, methane from hydrate, temperature and use of inhibitors is presented.

	Hours	CH_4 recovery total (Fraction)	CH_4 recovery hydrate (Fraction)	Temperature (C)	Inhibitors
CO_2-21	140	0.37	0	9.6	
CO_2-22		No recovery	No recovery	Plug	
CO_2-23	220	0.51	0.21	4.0	MDEA
CO_2-24	195	0.37	0	4.3	MEA
CO_2-25	190	0.45	0.14	4.3	MEA
CO_2-26	140	0.59	0.35	9.6	
CO_2-27	60	0.89	0.80	4-9	MEA

The methane hydrate remaining in the core after hydrate formation was exposed to a liquid CO_2 injection at a low rate (1.2ml/h), where the composition (gas fractions) and the mass (g) of the produced gas were measured. The data collected from the gas chromatograph (GC) were used to study the composition of produced gas for the duration of the CH_4-CO_2 exchange process. Figure 3-9, a typical gas fraction curve from an experiment, demonstrates how the gas fractions of carbon dioxide, methane and nitrogen evolve as a function of time during the exchange period. The pump and all corresponding tubing, except the core, inlet and outlet tubing, were filled with CO_2 before an injection with a constant rate was initiated (1.2ml/h). As a result, the initial measurements, seen in Figure 3-9, show high gas fractions of CO_2 (close to 1), and low methane fractions (close to 0). The following 15 hours shows a steep increase in methane fractions and a simultaneously decrease in the carbon dioxide fractions. When reaching the vertex, a synchronous decrease in methane fractions and increase in carbon dioxide fractions are observed, before both curves stabilize with high gas fractions of carbon dioxide and low fractions of methane. The first measurements of produced methane are assumed to be free gas from the outlet tubing and core. This can be verified by the increase in production of nitrogen, which necessarily originated from free nitrogen from initial air trapped in the core before pressurizing.

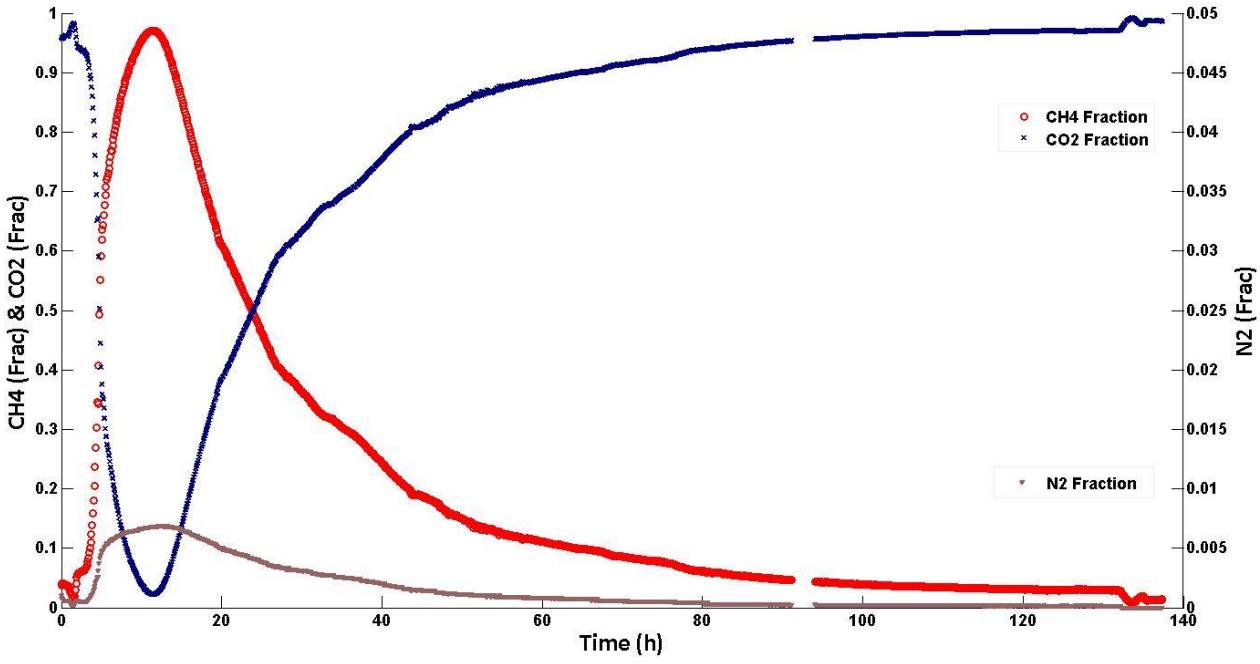

Figure 3-9: GC data showing the gas fractions of methane, carbon dioxide and nitrogen as a function of time from experiment CO_2-26. Red curve represents methane, blue curve represents carbon dioxide and brown curve is nitrogen.

Figure 3-10 shows injection and production pressure as a function of time during the exchange process conducted in CO_2–26. Both graphs trail each other within a close region, implying a low differential pressure throughout the CO_2 injection, proving good permeability in the core for fluid flow. Pressure drops and pressure build ups is a result from the back pressure valve, only allowing gas through when exceeding 86 bar. As illustrated earlier in Figure 3-3, the hydrate is likely present between the free gas and the brine along the pore wall. This type of hydrate may be preferable during an exchange process due to a maintained permeability as well as a high hydrate surface area. The permeability is important for the flow of CO_2, and a high surface area promotes a higher exchange rate due to an increase in contact area between CO_2 and the hydrate. Earlier results validate a decrease in permeability with increased hydrate saturations (Bringedal, 2011).

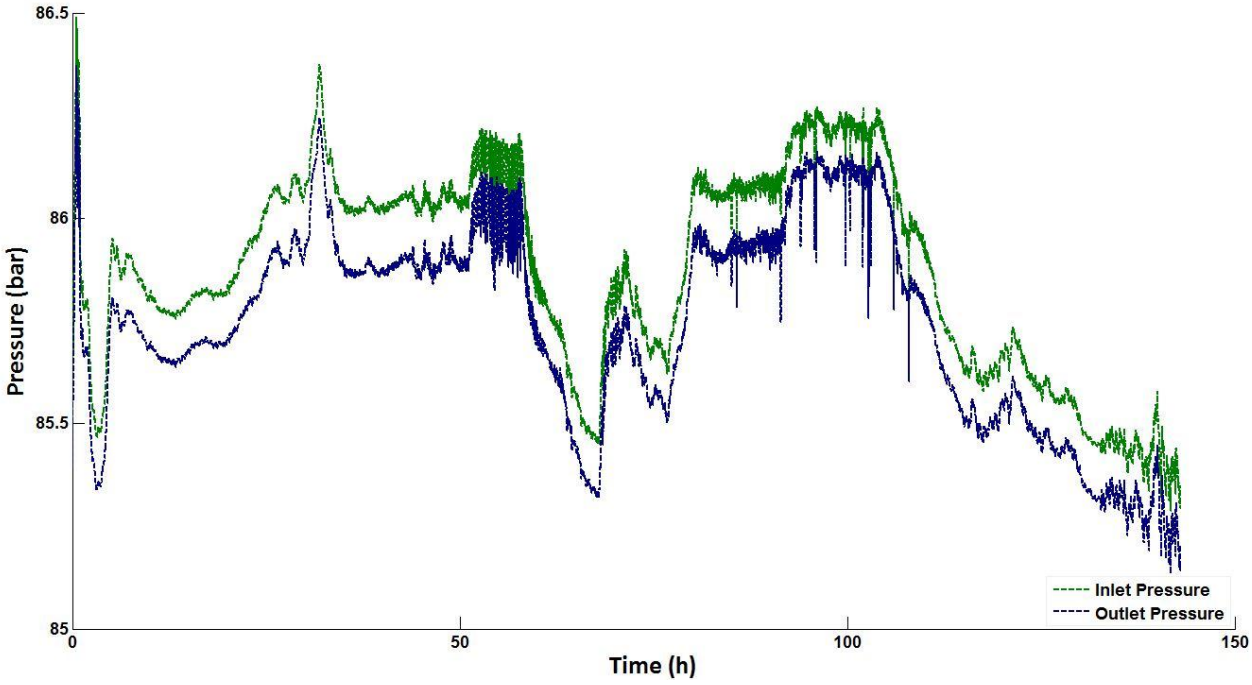

Figure 3-10: Injection pressure and production pressure during CO_2 injection from experiment CO_2 – 26 showing a low differential pressure indicating a high permeability throughout the experiment. The green graph is inlet pressure, and the blue graph is outlet pressure.

3.2.1 Experiment CO_2–21

The temperature during this exchange was set to 9.6° C. The core was prepared with matching initial properties as the rest of the experiments conducted, with a brine salinity of 0.1 wt% NaCl and an initial water saturation of 0.4 (S_{wi}). This is the first experiment conducted after the laboratory upgrade and the result from this experiment is probably not consistent with the rest. The mass flow meter had not been properly installed, and the duration of the experiment was too short (113 hours). Calculations indicate zero methane recovery from hydrate, given all the free methane is produced from the core. The total methane recovery was calculated to 0.35, and shown in Figure 3-11. Nevertheless the exchange rate in this experiment is significantly higher than for all experiments conducted at temperatures around 4° C, as well as equal to the other experiment conducted at 9.6° C (CO_2–26).

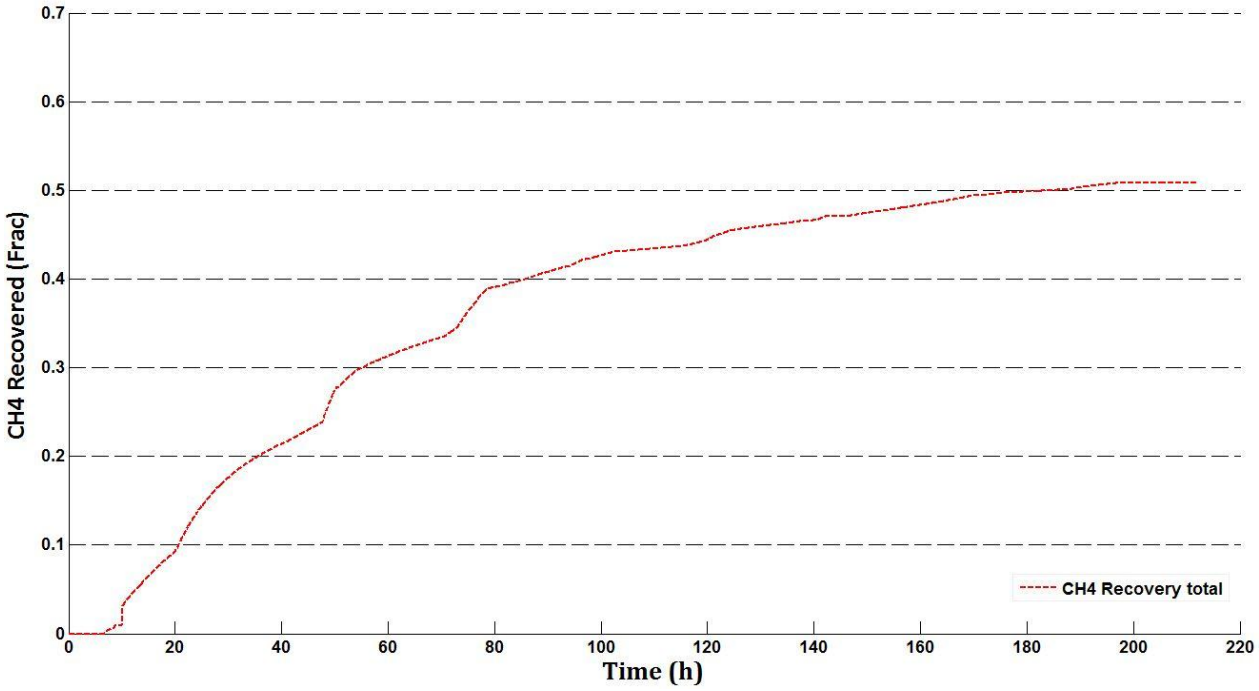

Figure 3-11: A total methane recovery plot from experiment CO_2–21 showing a recovery of 0.35.

3.2.2 MDEA and MEA experiments

In some of the following experiments the catalysts MDEA or MEA was injected. The concept and idea of injecting MDEA or MEA was to gain an *in-situ* temperature increase triggered by the rapid chemical reaction taking place when the additives are introduced to carbon dioxide (and brine), subsequently resulting in an increased methane production due to melting of present hydrate and formation of new carbon dioxide hydrate.

3.2.3 Experiment CO_2–23 (late injection of MDEA)

The temperature during this exchange was set to 4.0° C. The core was prepared with same initial properties as the rest of the experiments conducted with a brine salinity of 0.1 wt% NaCl and an initial water saturation of 0.41 (S_{wi})). After completing an ordinary CO_2-CH_4 exchange with duration of approximately 170 hours, MDEA was co-injected to the system by a loop valve to see if an enhanced recovery would occur. Since the production data is stable after roughly 120 hours (see example of gas fraction curves in Figure 3-9), an increase in methane production due to injection of MDEA would be easily noticeable. This was not observed. There are some uncertainties regarding whether the MDEA and the heat generated from the reaction with CO_2 actually reached the core, as the loop valve was situated in significant distance from the core. The methane recovery from hydrate was calculated to 0.21, with a total methane recovery of 0.51, shown in Figure 3-12.

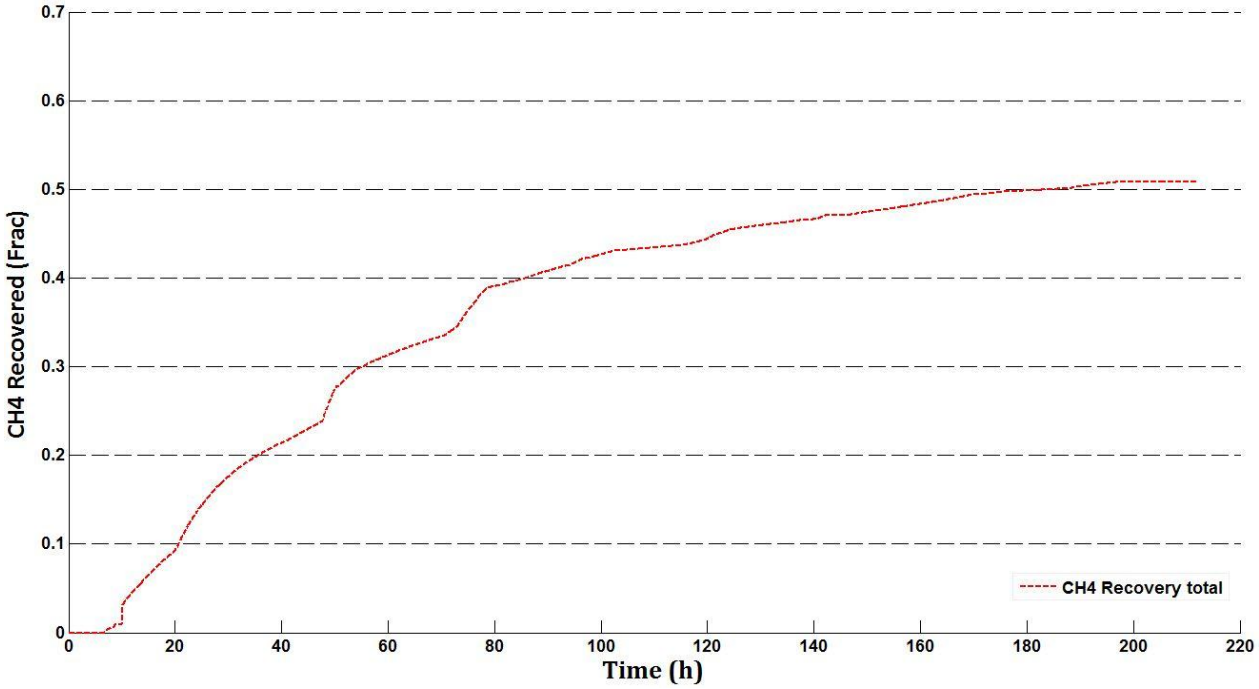

Figure 3-12: Total methane recovery from experiment CO_2–23 showing a recovery of 0.51.

3.2.4 Experiment CO_2 –24 (late injection of MEA)

The temperature during this exchange was set to 4.3° C, where the core was prepared with same initial properties as the rest of the experiments conducted with a brine salinity of 0.1 wt% NaCl, and an initial water saturation of 0.41 (S_{wi})). After completing an ordinary CO_2-CH_4 exchange with duration of approximately 214 hours, MEA was co-injected to the system by the loop valve to see if an enhanced recovery would occur. MEA generates more heat than MDEA when reacting with carbon dioxide, and as the results from the previous experiment CO_2–23 did not prove an increase in methane production, MEA was attempted as a possible improved inhibitor. When MEA was injected by opening the loop valve to the system some excess MEA and carbon dioxide blew out the injection line (inlet at loop valve) due to pressure differences. As this happened sudden heat was sensed. No clear observations or measurements were done verifying an increased methane production after injecting 4 slugs of MEA. A theory explaining this could be that due to the low flow rates and the length of the tubing from where it was injected to the core are of significance, the heat never may have reached the core and its hydrate formation. Difficulties with a defect pressure regulator causing no flow in several periods of the exchange process may have had some influence on the results as well. Methane recovery from hydrate was calculated to zero, with a total methane recovery of 0.37, as shown in Figure 3-13.

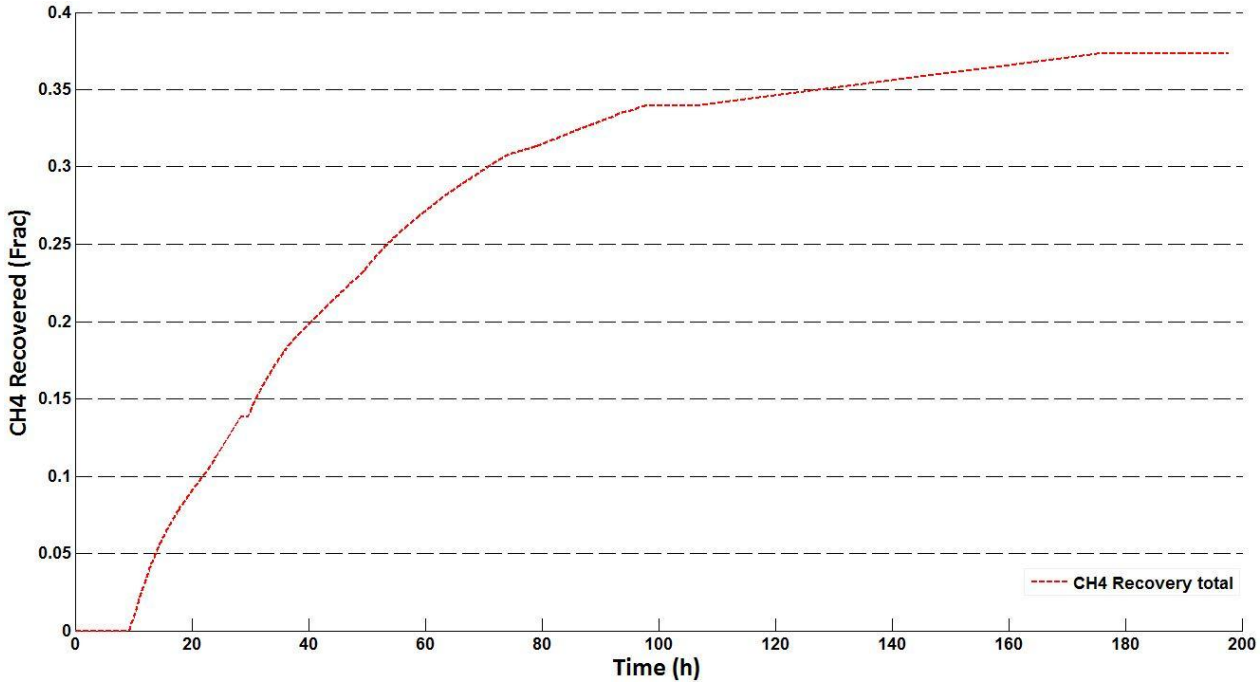

Figure 3-13: Total methane recovery plot from experiment CO_2–24 showing a recovery of 0.37.

3.2.5 Experiment CO_2–25

The temperature during this exchange was set to 4.3° C, and the core was prepared with same initial properties as the rest of the experiments conducted, with a brine salinity of 0.1 wt% NaCl and an initial water saturation of 0.41 (S_{wi})). This experiment was conducted after an upgrade on the GC, resulting in more continuous gas fraction measurements. Methane recovery from hydrate was calculated to 0.14, where the total methane recovery was calculated to 0.45.

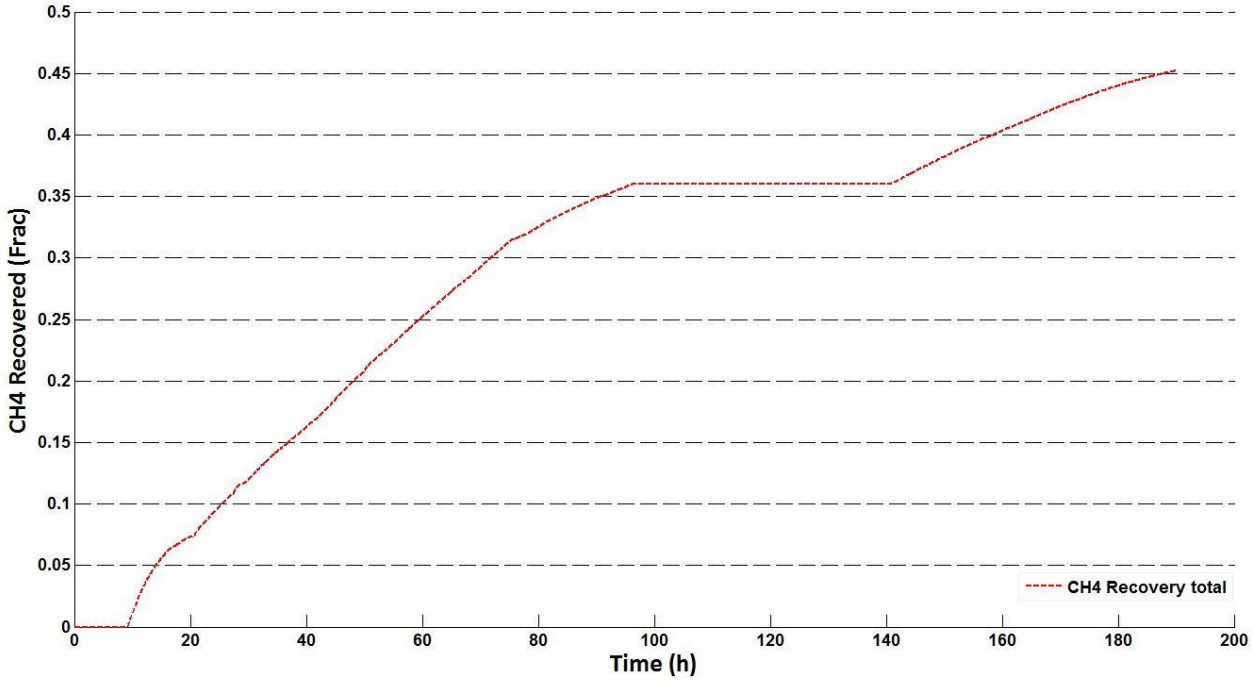

Figure 3-14: A total methane recovery plot from experiment CO_2–25 showing a recovery of 0.45.

3.2.6 Experiment CO_2–26

Temperature during exchange was set to 9.6° C, and the core was prepared with same initial properties as the rest of the experiments conducted with a brine salinity of 0.1 wt% NaCl and initial water saturation of 0.433 (S_{wi})). The gas fraction curves for this experiment are shown in Figure 3-9. This experiment is the most continuous experiment conducted in this thesis, where no problems emerged during the exchange period. Recovery from methane was calculated to 0.35, from a total methane recovery at 0.59 after 142 hours.

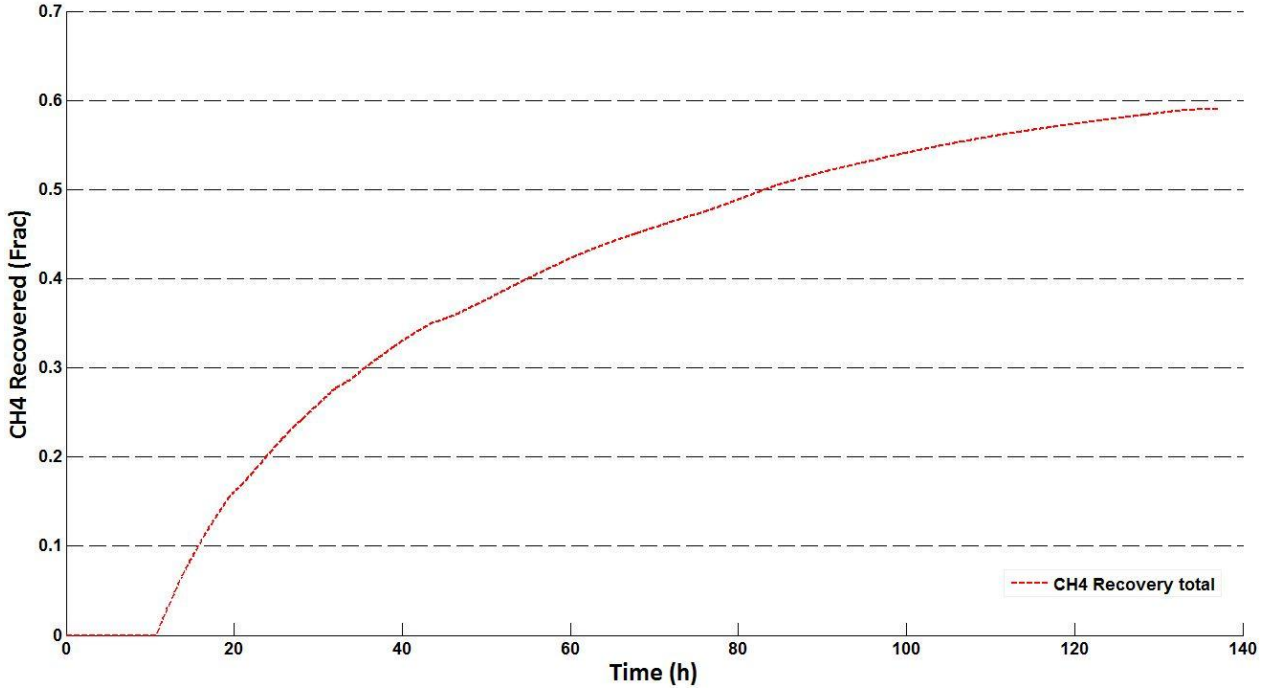

Figure 3-15: Total methane recovery plot from experiment CO_2–26, showing a recovery of 0.59.

3.2.7 Experiment CO_2–27 (separately MEA injection)

The temperature during this exchange varied from 4° C - 9° C in 24 hour cycles due to problems with the cooling bath during the experiment. The core was prepared with the same initial properties as the rest of the experiments conducted with a brine salinity of 0.1 wt% NaCl and initial water saturation of 0.41 (S_{wi}). Due to prior observations regarding MDEA and MEA injections, where transportation of generated heat most likely not reached the core, a new modified setup was prepared. The goal was to achieve a situation where MEA and CO_2 were introduced *in-situ* instead of in the loop valve. The solution was to inject MEA separately, and setup B was modified where the inlet temperature sensor was replaced with an injection line with a separate connecting pump for injection of MEA. By injecting an amount of MEA

before the CO_2 injection commenced, the generated heat should take place *in-situ* and consequently cause some dissociation of hydrate. The MEA was continued injected alongside the carbon dioxide, until approximately 20 ml of MEA was injected. The amount of MEA injected (1/3 of the pore volume) was exaggerated to easier observe the impact. After roughly 18 hours what appeared to be water production was observed in the plastic tubing from GC to MFM. GC data from the same period showed that the gas fraction from the effluent only consisted of methane, as shown in Figure 3-16.

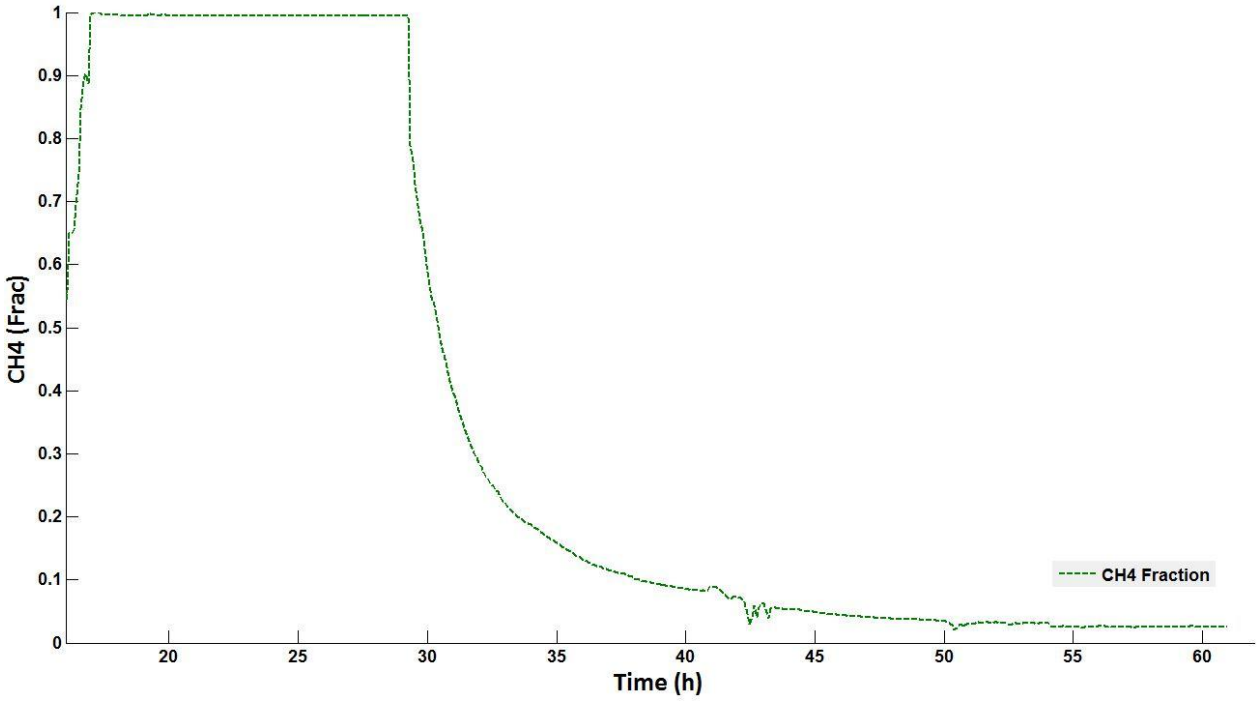

Figure 3-16: A 100 % methane production in a period of approximately 10 hours shown as a methane fraction curve from GC showing methane gas fractions at 1 (only methane produced).

This is indicating methane hydrate dissociation by the generated heat from MEA and CO_2. Water produced through the MFM had a strong impact on the data collected from MFM due to the denser mass of water compared to gas. Calculations of recovery are based on the gas fractions (mol) and the related mass flow (g), and therefore the anomalous (too high mass flow measured in MFM during water production) has been tried accounted for in the recovery calculations. Nevertheless, an overestimation may have been done in this experiment, and the recovery should not be considered as exact. Still the experiment show that MEA could be a potential additive for improving the recovery, as well as the recovery rate, from methane hydrates. Calculations showed a methane recovery from hydrate at 0.8, from a total methane recovery at 0.89 after only 86 hours, as seen in Figure 3-17.

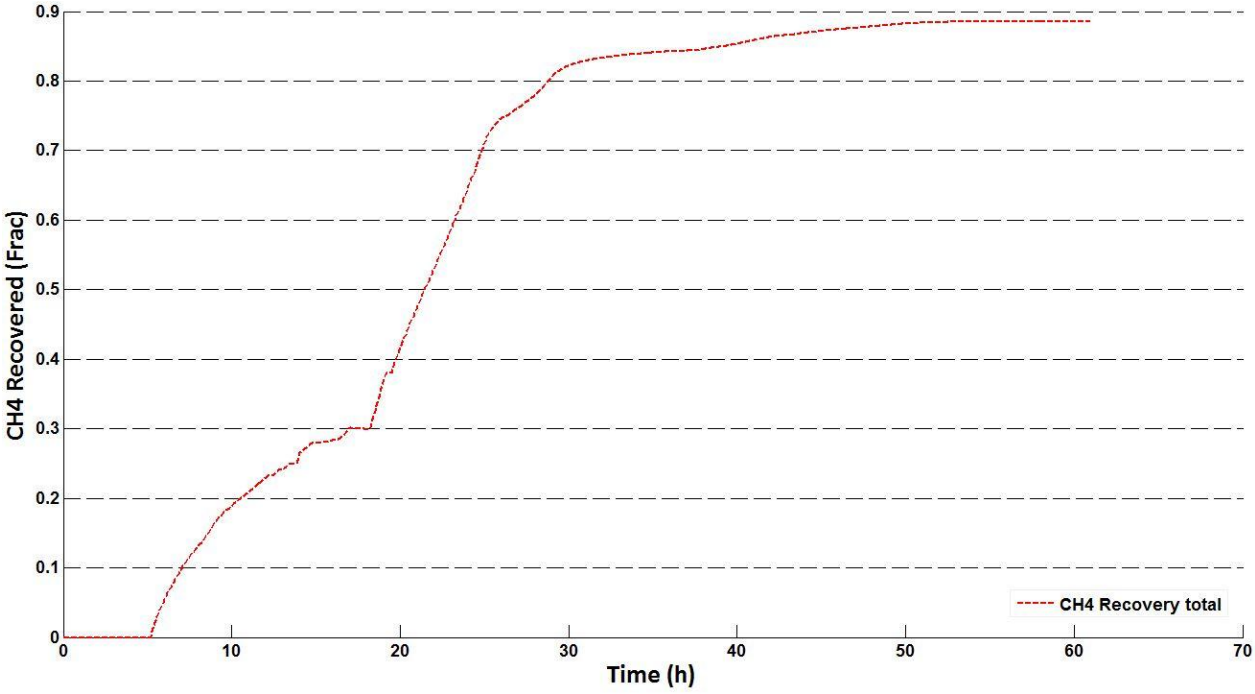

Figure 3-17: Total methane recovery plot from experiment CO_2–27, showing a recovery of 0.89.

3.2.8 Discussion

In the data analysis we assumed that all of the free methane in tubing and pore space was produced. If this assumption is incorrect, where an amount of the free methane will remain in the pore space, there will be an underestimation in the methane recovery results from hydrate presented in this thesis. Two experiments show zero recovery from hydrate, whereas the remaining shows a production of methane higher than the free methane saturation, verifying an exchange of methane and carbon dioxide. Based on this it is likely that some of the free methane remains in the pore space, as it is highly unlikely that the exchange process only takes place occasionally.

As shown in the comparison plot in Figure 3-18 there is a consistency in the exchange rates based on the temperature conditions during the exchange. The experiments conducted at 9.6° C have an exchange rate close to twice the rate observed from experiments conducted at 4° C. One of the experiments conducted at 9.6° C, represented as the red curve in Figure 3-18, shows an increase in the total recovery of methane. In the light of the objective of this thesis the results verify an increase in the exchange rate, as well as indicate an increase in methane recovery from methane hydrates exposed to temperatures closer to the equilibrium line. Consequently 9.6° C is a more favorable production condition than 4° C, which is shown in Figure 3-19, as an increase in the trend line in a plot with temperatures and the corresponding recoveries. This is in agreement with earlier studies done in-house, where an increase in temperature (0.5° C, 4.0° C and 10° C) indicated an increase in recovery (Bringedal, 2011).

There were no observations of an increase in recovery when co-injecting MDEA or MEA with a loop valve, most likely due to loss of heat during the injection. MEA proved to be effective when pre-injected separately into the methane hydrate and then introduced to carbon dioxide. A high recovery rate and recovery (0.89) was observed, most likely due to the generated heat and a following dissociation of the hydrate.

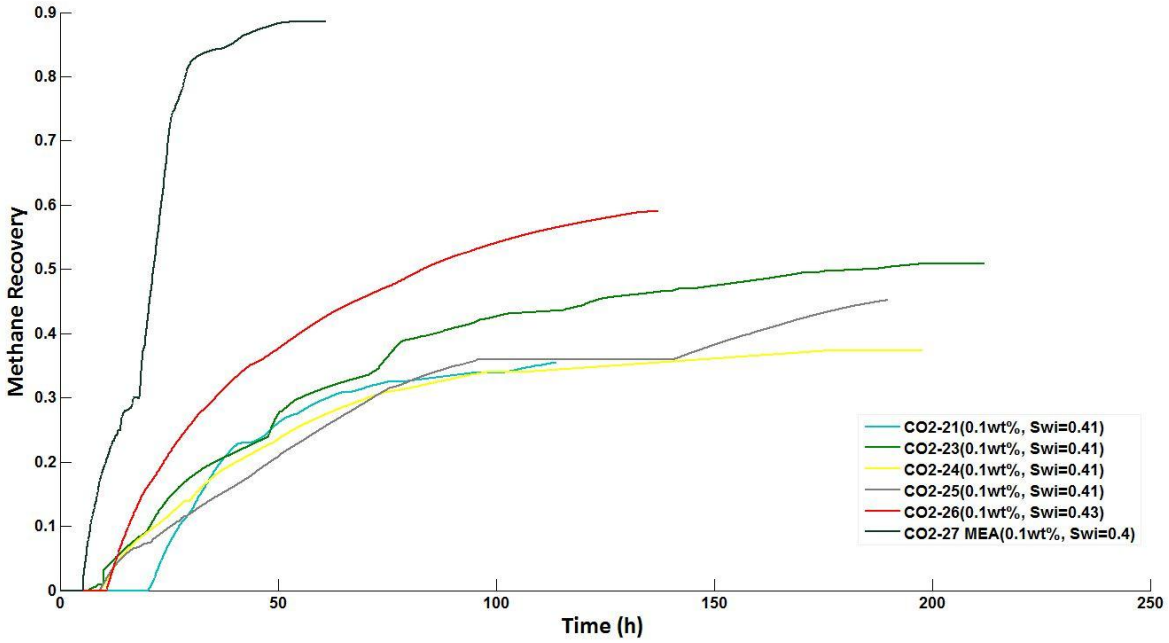

Figure 3-18: Comparison plot of total methane recoveries with time from all exchange experiments conducted in this thesis. CO_2-27. With the exception of CO_2-27 (MEA) there are some indications of consistency in rates and recovery with alike initial properties.

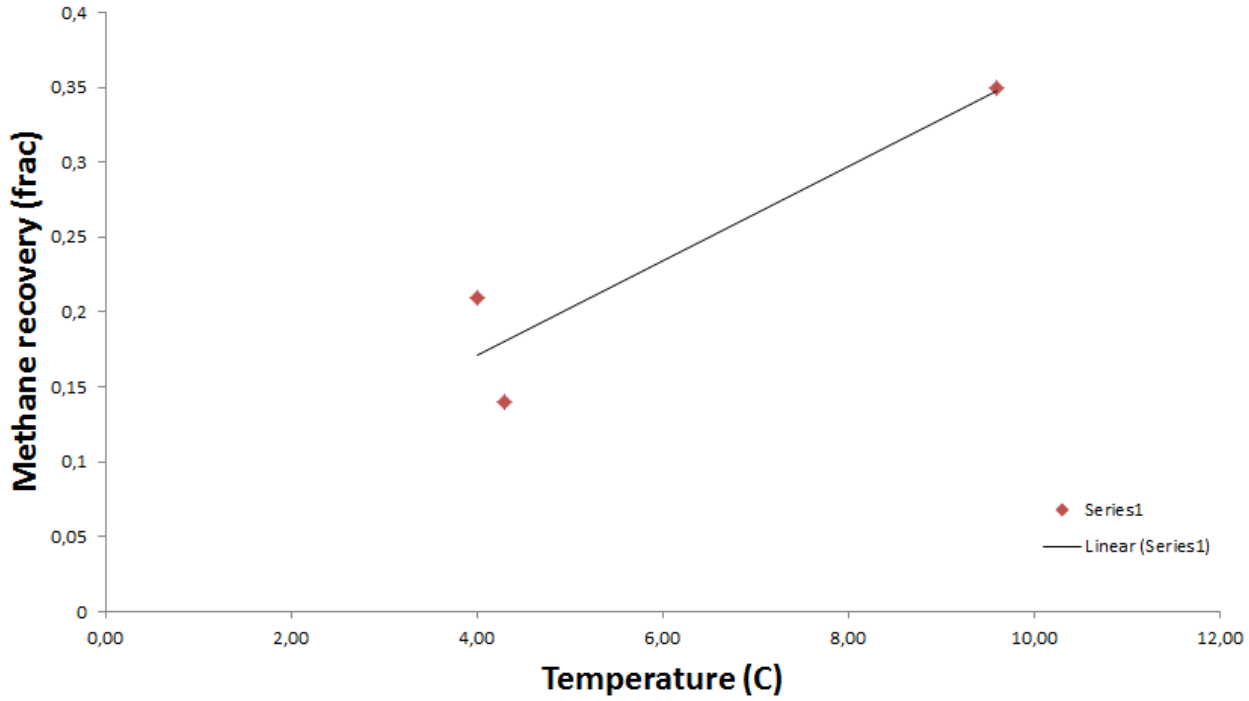

Figure 3-19: Methane recovery from hydrate as a function of temperature. Based on the experiments conducted in this thesis which yielded a recovery from hydrate, there is an indication of increased recovery at higher temperatures, especially when close to the equilibrium line.

Jung et al. (2010) indicate that even though the hydrate is within stable conditions and at equilibrium, there will be an exchange of molecules at the interface of the hydrate and the free gas phase. This means that at the interface of present methane hydrate and the free gas phase the hydrate will constantly form and break down, releasing methane and capturing methane. The rate of this process may be accelerated with an increase in temperature as the hydrate then becomes less stable. When injecting CO_2, forming a CO_2 rich porous medium, released CH_4 molecules may be replaced by CO_2 molecules and subsequently forming new CO_2 hydrate. This reaction will add heat to the system, and could therefore be a source of positive feedback to the exchange by local heating resulting in melting of the neighboring CH_4 cages and an increase of exchange (Jung et al., 2010). The heat liberated during hydrate formation of one mol of CO_2 varies between 57.7-63.6 kJ/mol, whereas the heat absorbed during dissociation of one mol of CH_4 hydrate varies between 52.7-55.4 kJ/mol (G. K. Anderson, 2004) resulting in a positive net heat contribution. In a situation where the pressure and temperature conditions are close to the equilibrium line there is reason to believe that the local heating will have greater impact on the exchange because less heat is required to melt neighboring methane hydrate and consequently there will be an increase in both recovery rate and methane recovery.

Reaction rates will also be dependent on the contact area between CO_2 and CH_4 hydrate (Jung et al., 2010). Hydrate-forming water can dissolve into liquid CO_2 and consequently cause lower hydrate saturation after the replacement of CO_2 and CH_4 in a water limited reservoir (Jung et al., 2010). All experiments conducted in this thesis are executed within an excess gas state. Reservoirs of this nature should be more amenable to an exchange process due to high permeability for CO_2, as well as a larger interface between the CH_4 hydrate and the injected CO_2. There will also be less chance for CO_2 clogging caused by new formation of carbon dioxide hydrate (Jung et al., 2010).

3.3 Hydrate dissociation results

As stated earlier in this thesis, dissociation of hydrates is currently the most promising production technique. Depressurization and thermal stimulation are two possible methods used for dissociation, where the hydrate moves from a stable condition to an unstable condition. Dissociation was conducted in selected experiments in this thesis, and was either initiated after an exchange process was completed or post hydrate formation. The latter was done to investigate dissociation on pure methane hydrate to investigate the shift in equilibrium temperature for pure methane hydrate compared to a mixed hydrate (methane and sequestrated carbon dioxide). Dissociation was performed either by pressure depletion or by thermal stimulation. Hydrate dissociation is an endothermic reaction, thus requiring heat from its surroundings. The heat absorbed during dissociation of one mol of CH_4 hydrate is between 52.7-55.4 kJ/mol (Jung et al., 2010). This is seen in Figure 3-23, where the temperature is reduced by nature and the production rate is decreased as a result. The temperature reduction taking place during dissociation can be problematic, dependent on the heat transfer, where a reformation of hydrate can occur. Thermal stimulation in combination with pressure depletion could prevent this.

When increasing the temperature in a hydrate-bearing system while keeping the pressure constant, a dissociation process initiates as the temperature is crossing the equilibrium temperature at the specific pressure illustrated in Figure 3-21. At 83 bar CSMGem simulation indicates an equilibrium temperature at approximately 11.3° C when exposed to constant pressure of 83 bar. During the temperature stimulation, where the temperature was increased stepwise, the dissociation would occur at the equilibrium temperature as the pressure was held constant. This was conducted on pure methane hydrate as well as methane/carbon dioxide hydrate to further investigate the temperature effect when examining the exchange process.

Data collected from CSMGem gave indications on pressure and temperature equilibrium for pure methane hydrate as shown in Figure 3-20 (pressure) and Figure 3-21 (temperature). As shown in Figure 3-20 the equilibrium pressure for methane hydrate at 4° C is approximately 39 bar, and 70 bar at 9.6° C, indicating that the pressure needs to be reduced below these pressure levels to dissociate. Figure 3-21 shows an indication of the equilibrium temperature for methane hydrate at 83 bar, where approximately 11.3° C is the melting temperature.

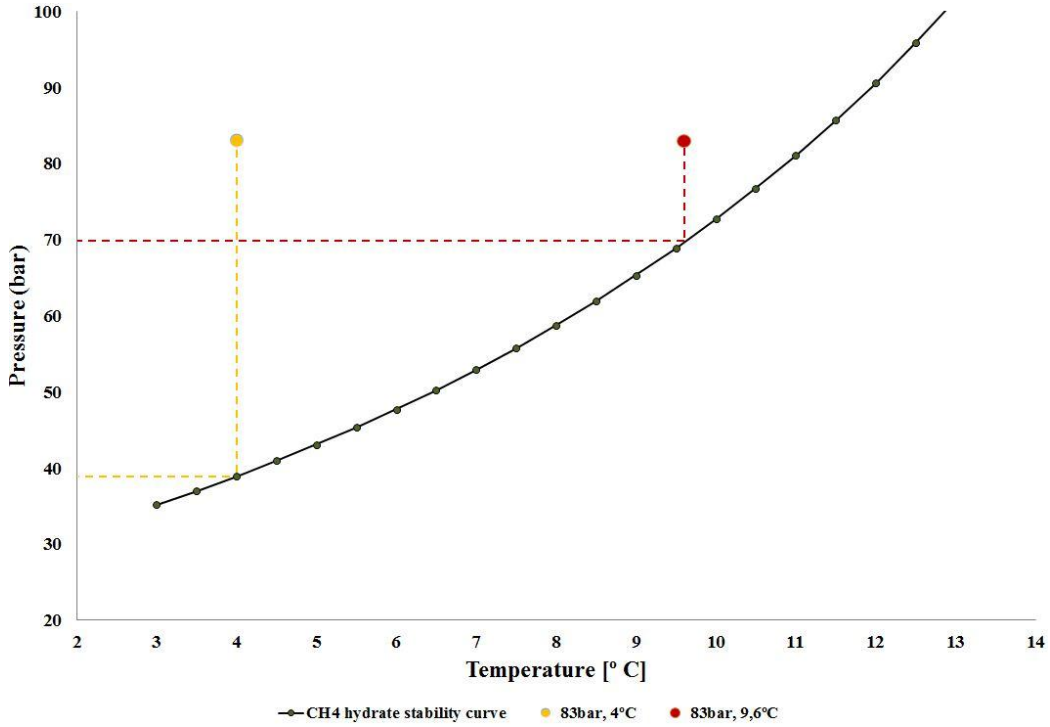

Figure 3-20: CSMGem methane hydrate stability curve, indicating the equilibrium pressure for both methane hydrate at 4° C and 9.6° C respectively approximately 39 bar and 70 bar.

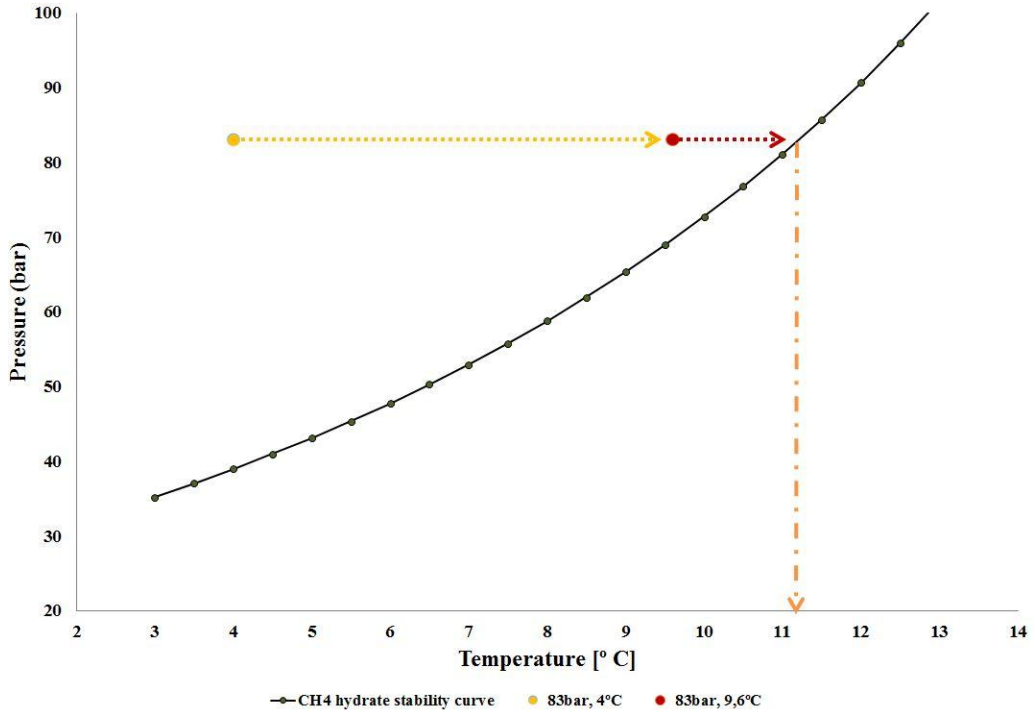

Figure 3-21: CSMGem methane hydrate stability curve indicating equilibrium temperature at 11.3° C a constant pressure of 83 bar.

3.3.1 Depressurization (DEP5-1)

Pressure depletion was conducted primarily to generate data for simulation input needed by PhD Knut Arne Birkedal. A specific depressurization method was followed to match his simulations where only a few large pressure reductions were conducted. The pressure was first reduced from 83 bar to 42 bar within an hour, while keeping the temperature at 4° C. The system was stabilized before reducing the pressure further down to 32.5 bar. Data from CSMGem, shown in Figure 3-20, indicate hydrate equilibrium in the region of 38 bar. Experimental results, presented in Figure 3-22, show dissociation taking place when reaching 32.5 bar, where a volume of 170 ml was produced in a time period of 30 hours. As further pressure reduction was conducted, where the pressure was reduced to 20 bar, a volume of 4 ml was received. The experimental results from this experiment appeared to be in accordance with the numeric results found by Birkedal using simulations from TOUGH+HYDRATE, and are presented in Figure 3-23.

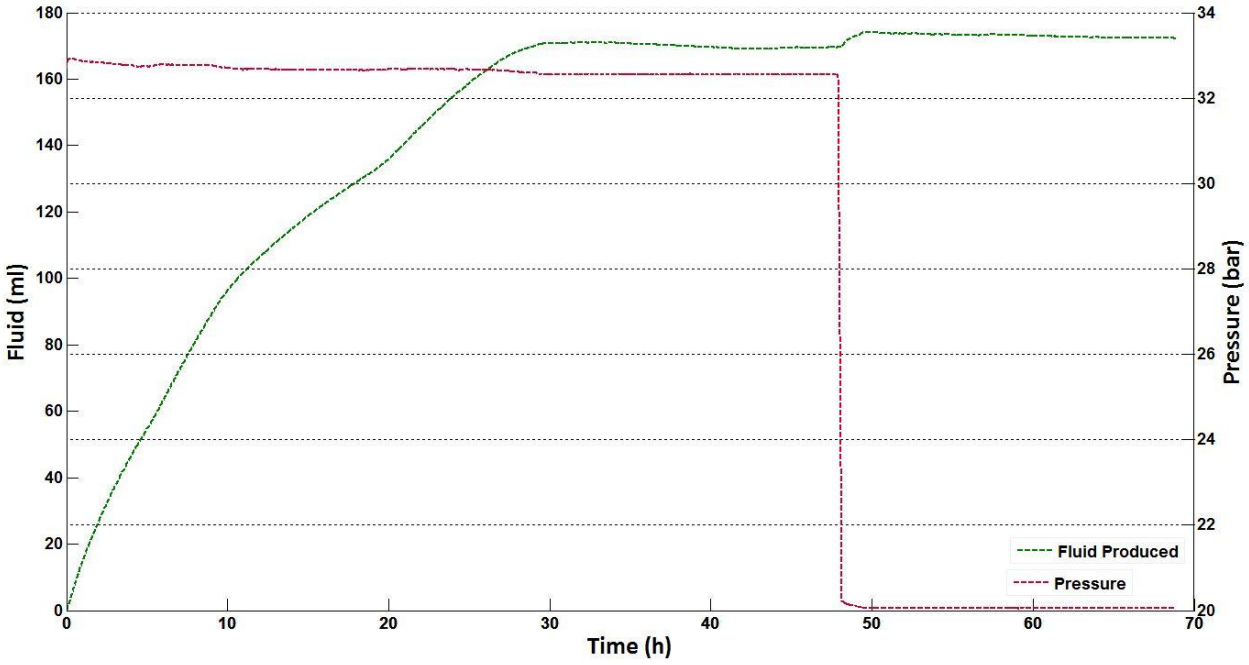

Figure 3-22: Pressure depletion showing volume of fluid production from receiving pump. At approximately 33 bar a dissociation of hydrate initiates.

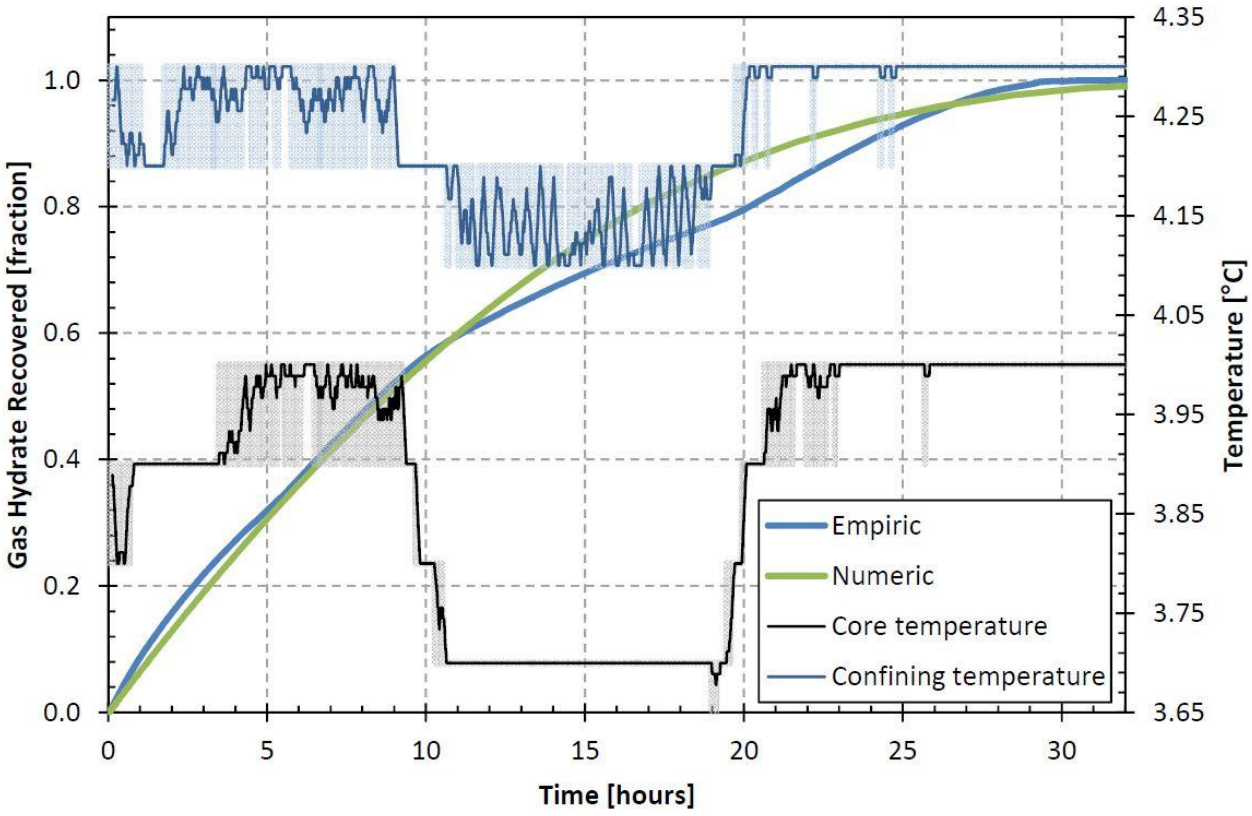

Figure 3-23: Empirical and numerical comparison of hydrate dissociation by depressurization. The empirical data was retrieved from experiment DEP5-1, and numerical simulation by PhD Knut Arne Birkedal (Birkedal et al., 2013).

Birkedal et al. (2013) used TOUGH+HYDRATE code to reproduce experimental data and validate by comparison. Numerical tools are important for evaluation and prediction of conventional hydrocarbon reservoir performance, and could in parallel be an asset for natural gas hydrate research and development. The experimental results were reproduced, as seen in Figure 3-23, confirming the empirical data. Heat transport proved to be a limiting factor for dissociation of hydrate, and the kinetic parameters were more sensitive than anticipated (Birkedal et al., 2013).

3.3.2 Experiment CO_2–26 (Thermal stimulation)

This dissociation experiment was conducted after completed CO_2 injection, and consequently the present hydrate was a mixed hydrate containing methane and carbon dioxide. By increasing the temperature at the cooling bath stepwise, an increase in core temperature occurred resulting in hydrate dissociation when crossing the equilibrium line. As shown in Figure 3-24, the volume produced was a stepwise production following the increased temperature steps. This indicated a hydrate consisting of a mixture of methane and the more thermodynamically stable carbon dioxide, and subsequently a shift in the equilibrium line presented for a pure hydrate shown in Figure 3-21. As the temperature reach 12° C and 16° C a rapid production is observed and could describe a primary melting of methane hydrate and a following carbon dioxide melting.

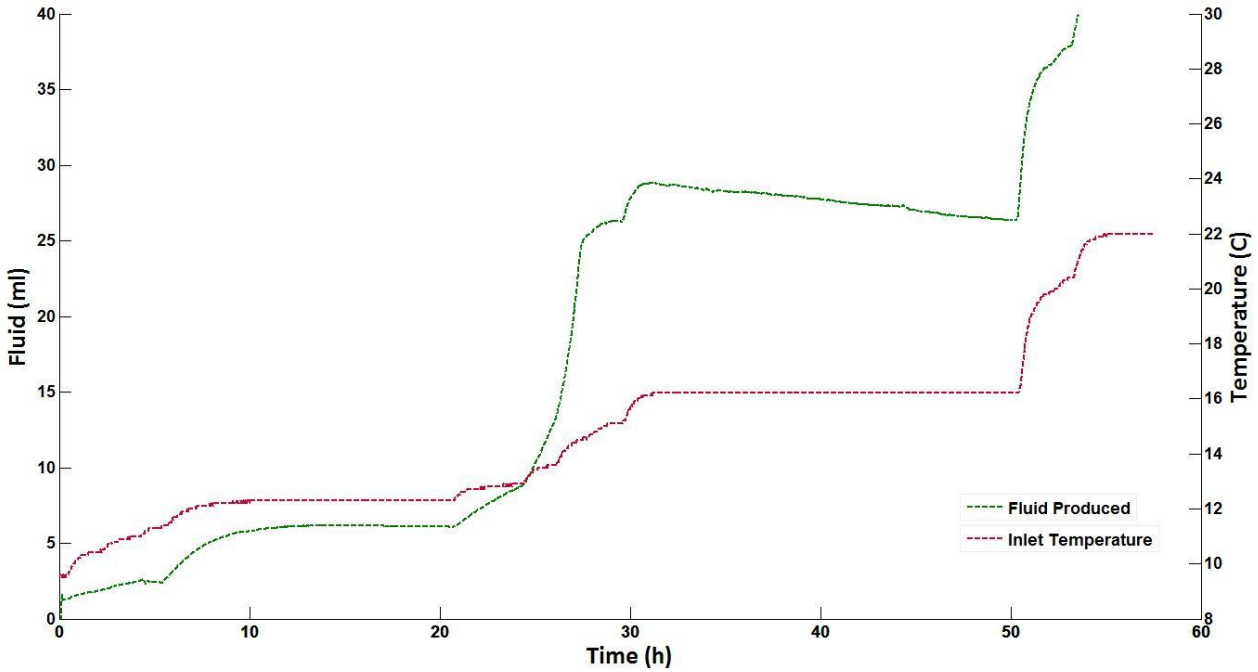

Figure 3-24: Thermal stimulation from a mixed hydrate showing volume produced as the temperature was increased.

3.3.3 Experiment CO_2–28 (Thermal stimulation)

Thermal stimulation was conducted in this experiment to further investigate the dissociation temperature for a pure methane hydrate when applied to 83 bar. Initial core properties were a brine salinity of 0.1 wt% and an initial water saturation of 0.40, equal to CO_2-26, to be able to compare the results. As shown in Figure 3-25 there was an increase in volume produced after reaching an *in-situ* temperature of 10° C, which is over 1° C lower than the simulation program CSMGem indicated, as well as significantly lower than the dissociation temperatures presented from the previous experiment. The dissociation rate before and after reaching 11.3° C is noteworthy. Due to production volume of almost 20 ml after reaching 10° C, this must necessarily be the equilibrium temperature, and can therefore not be explained by gas expansion. But when reaching 11.3° C the dissociation rate is remarkably higher, indicating a far stronger thermodynamic driving force.

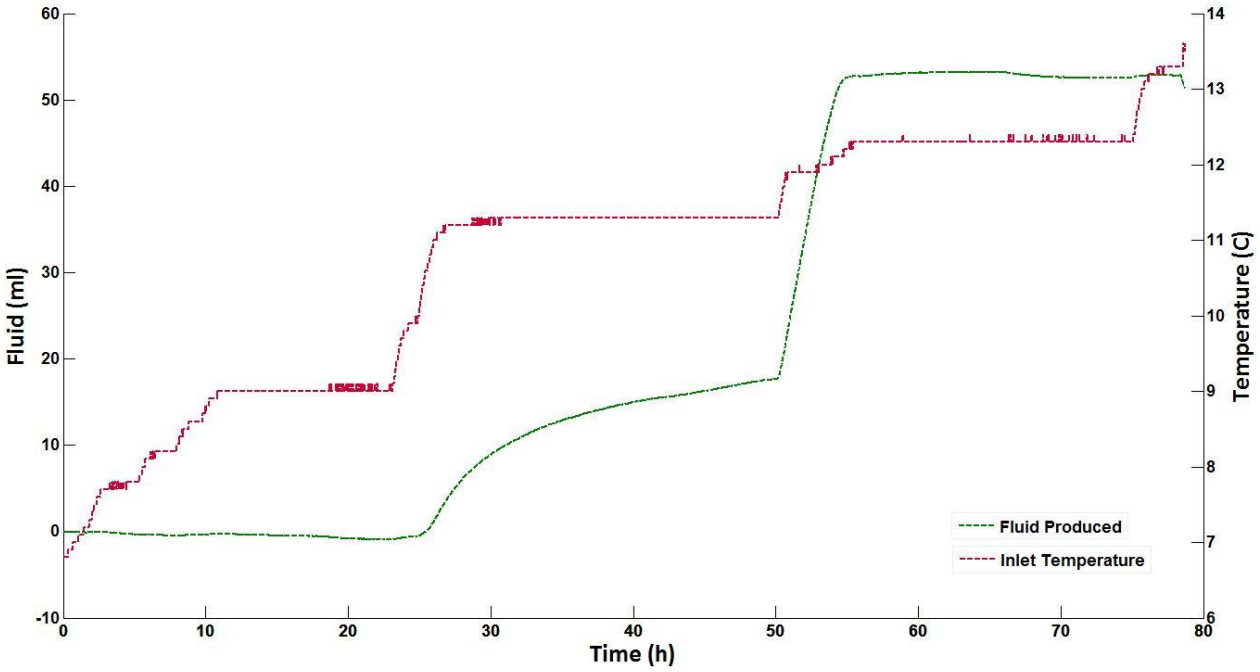

Figure 3-25: Thermal stimulation results, showing volume produced and inlet temperature, from pure methane hydrate in experiment CO_2 – 28 conducted on a pure methane hydrate.

3.4 Uncertainties

The instruments used during the experiments conducted in this thesis are high precision equipment with uncertainties considerably smaller than the experimental uncertainties present. Thus there will not be any emphasis on calculations of instrumental uncertainties, but rather a representation of the validity of the results in regards of an overestimation versus underestimation.

3.4.1 Hydrate formation

An uncertainty regarding hydrate formation is assumptions done during calculations since the pump log of methane consumed is fairly precise. Expansion factor of the hydrate (1.26) and hydration number (5.99) are used to determine remaining water and methane in hydrate, and may contribute to some minor uncertainties. Circone et al. (2005) state based on experimental work that the hydration number could be less for conditions well within stable conditions. If this is the case for the experiments conducted in this thesis (83 bar, 4° C) there would be a slightly overestimation of final hydrate saturation.

The Bentheim sandstone core may be the source of the leading uncertainty regarding hydrate formation due to possible inhomogeneity not accounted for, and can consequently provide incorrect water saturations. Core preparations could also yield a source of errors if the cores were not cleaned and dried properly. Water could also evaporate during the time between the core was saturated until placed in the core holder. Consequently an underestimation of salinity and overestimation of initial water saturation would be done. As seen in Table 5, some of the calculations of remaining water post hydrate formation are zero. This is not the case, and must be an underestimation.

Fluctuations in temperature at the laboratory is also observed to have an impact on gas volume measurements, especially if the pump has a large volume of gas in the pump cylinder, and may also contribute as a source of error. The latter is attempted to correct for in experiments showing these temperature impacts. Leakage is accounted for as the slope of the curve during the hours after completed hydrate formation, and is most likely not contributing to uncertainties of significance. The compaction of gas due to cooling of the system is also accounted for as it is observed as methane consumption before the formation initiates, and therefore accounted for in calculations.

3.4.2 CH_4-CO_2 exchange

Uncertainties from hydrate formation would follow in addition to new sources of errors. During the CH_4-CO_2 exchange there are some uncertainties which may have significant impact on the calculations of

recovery from hydrate. The assumption that all of the free methane present in the core after hydrate formation is produced when injecting liquid carbon dioxide, could potentially be a source of great error when examining the methane recovery from the hydrate. This is seen as zero recovery from hydrate shown in Table 6. Nevertheless is this a source of an underestimation of recovery, implying that the results presented are a confirmation of an exchange between carbon dioxide and methane from hydrate. During the exchange it is also difficult to detect leakage which could result in loss of mass. There are no calculations done regarding sequestrated carbon dioxide in hydrate. This is due to no control of carbon dioxide leakage rate, generating large uncertainties which resulted in physically impossible calculations. This can be explained by the properties of carbon dioxide where diffusion through the sleeve and into confinement oil may have happened.

Part 3

Conclusions and Future Work

4 Conclusion and future work

Founded on the experiments completed during this thesis, and earlier experiments, the following conclusions can be stated:

- Methane hydrate was successfully formed with an average of 0.23 mol of methane in hydrate, where the experiments showed repetitiveness when initial properties were alike.

- Salinity and initial water saturations do have an impact on the hydrate formation rate and final hydrate saturations. An increase in salinity and initial water saturations, S_{wi} >0.6, indicate a decrease in methane consumption and increased residual water saturations.

- Methane hydrate exposed to liquid carbon dioxide proved to yield methane production, where a spontaneous reaction liberates methane and sequestrates carbon dioxide. The recovery from methane stored in hydrate is most likely underestimated, as all the free gas present is assumed produced.

- Temperature seems to have an impact on the exchange rate. When the temperature is closer to the equilibrium line (in experiments set to 9.6° C), where the hydrate is less stable, a higher recovery rate is observed.

- There are indications in the results that the methane recovery also is increased with temperatures close to the equilibrium line where the hydrate is less stable.

- MEA generates heat when it reacts with carbon dioxide. When MEA was pre-injected, with strong indications of melting of methane hydrate, a high recovery rate and recovery was obtained and estimated to 0.89.

- Pure methane hydrate dissociates at temperatures below mixed hydrate, with respectively 10° C and 12° C with a pressure of 83 bar.

Due to the leading uncertainty on the subject of displacement of free methane during the exchange process some experiments on this area could preferably be conducted. By saturating a core with 100 % methane and then flush the core with carbon dioxide at the same conditions as in the CH_4-CO_2 exchange experiments, some indications of displaced methane could be received.

Generate more consistent experiments to improve statistics with regards to temperature effects, salinity and excess water impacts on hydrate formation and the exchange process.

More experiments with use of MEA could also yield interesting results, and should be conducted by separate injection and with less quantity than used in this thesis. A further investigation on the formation of new CO_2 hydrate after melting of hydrate with MEA present would be of importance. If there is no sequestration and preservation of solid hydrate, there is no reason for MEA injection. Depressurization or thermal stimulation could be a method for verifying presence of hydrate after completed recovery.

References

Anderson, B. I., Collett, T. S., Lewis, R. E., & Dubourg, I. (2005). *Using Open Hole and Cased Hole Resistivity Logs to Monitor Gas Hydrate Dissociation During a Thermal Test in the Mallik 5L-38 Research Well, Mackenzie Delta, Canada*. http://www.onepetro.org/mslib/app/Preview.do?paperNumber=SPWLA-2005-SS&societyCode=SPWLA

Anderson, G. K. (2003). Enthalpy of dissociation and hydration number of carbon dioxide hydrate from the Clapeyron equation. *The Journal of Chemical Thermodynamics, 35*(7), 1171-1183. doi: http://dx.doi.org/10.1016/S0021-9614(03)00093-4

Anderson, G. K. (2004). Enthalpy of dissociation and hydration number of methane hydrate from the Clapeyron equation. *The Journal of Chemical Thermodynamics, 36*(12), 1119-1127. doi: http://dx.doi.org/10.1016/j.jct.2004.07.005

Birkedal, K. A. (2009). *Hydrate Formation and CH4 Production from Natural Gas Hydrates - Emphasis on Boundary Conditions and Production Methods.* (Master Thesis in Reservoir Physics), University of Bergen.

Birkedal, K. A., Freeman, C. M., Moridis, G. J., & Graue, A. (2013). Numerical Reproduction of Empirical Methane Hydrate Dissociation and Reformation in Sandstone. *In prep*.

Boswell, R. a. C., T. (2006). The Gas Hydrates Resource Pyramid. *Fire in the Ice (The National Energy Technology Laboratory Methane Hydrate Newsletter), 6*(3), 5-6.

Bringedal, A. L. (2011). *Impacts of Temperature on Methane Production from Hydrates by CO2 injection.* (Master), University of Bergen

Carroll, J. (2002). *Natural Gas Hydrates: A Guide for Engineers*: Elsevier Science & Technology Books.

Circone, S., Kirby, S. H., & Stern, L. A. (2005). Direct Measurement of Methane Hydrate Composition along the Hydrate Equilibrium Boundary. *The Journal of Physical Chemistry B, 109*(19), 9468-9475. doi: 10.1021/jp0504874

Collett, T. (2005). Results at Mallik Highlight Progress in Gas Hydrate Energy Resource Research and Development. *PetroPhysics, 46*(3).

Collett, T. S., & Ginsburg, G. D. (1998). Gas Hydrates In the Messoyakha Gas Field of the West Siberian Basin - A Re-Examination of the Geologic Evidence. *International Journal of Offshore and Polar Engineering, 8*(1).

Daintith, J., & Martin, E. (2010). *A dictionary of science* (6th ed.). Oxford: Oxford University Press.

Ebinuma, T. (1993). *Method for Dumping and Disposing of Carbon Dioxide Gas and Apparatus Therefor*. (US5,261,490 A). Retrieved from http://www.google.no/patents?hl=en&lr=&vid=USPAT5261490&id=_pUaAAAAEBAJ&oi=fnd&dq=ebinuma+1993+hydrates&printsec=abstract#v=onepage&q=ebinuma%201993%20hydrates&f=false.

Ersland, G. (2008). *Studies of flow mechanisms and hydrate phase transitions in fractured rocks*. Norway: University of Bergen, Bergen (Norway); Bergen Univ. (Norway).

Espinoza, D. N., & Santamarina, J. C. (2011). P-wave monitoring of hydrate-bearing sand during CH4–CO2 replacement. *International Journal of Greenhouse Gas Control, 5*(4), 1031-1038. doi: http://dx.doi.org/10.1016/j.ijggc.2011.02.006

Farmahini, A. H., Kvamme, B., & Kuznetsova, T. (2011). Molecular dynamics simulation studies of absorption in piperazine activated MDEA solution. *Physical Chemistry Chemical Physics, 13*(28), 13070-13081. doi: 10.1039/C0CP02238A

Graue, A., Kvamme, B., Baldwin, B. A., Stevens, J., Howard, J. J., Ersland, G., Husebo, J., & Zornes, D. R. (2006). *Magnetic Resonance Imaging of Methane - Carbon Dioxide Hydrate Reactions in Sandstone Pores*. Paper presented at the SPE Annual Technical Conference and Exhibition, San

Antonio, Texas, USA. http://www.onepetro.org/mslib/app/Preview.do?paperNumber=SPE-102915-MS&societyCode=SPE

Grover, T., Moridis, G. J., & Holditch, S. T. (2008). *Analysis of Reservoir Performance of the Messoyakha Gas Hydrate Reservoir*. Paper presented at the SPE Annual Technical Conference and Exhibition, Denver, Colorado, USA. http://www.onepetro.org/mslib/app/Preview.do?paperNumber=SPE-114375-MS&societyCode=SPE

Harrison, S. E. (2010). Natural Gas Hydrates. from http://large.stanford.edu/courses/2010/ph240/harrison1/

Hauge, L. P. (2013). In-house data-base program, University of Bergen (Version 1.6) [MatLab].

Hester, K. C., & Brewer, P. G. (2009). Clathrate Hydrates in Nature. *Annual Review of Marine Science, 1*(1), 303-327. doi: doi:10.1146/annurev.marine.010908.163824

Hossainpour, R. (2013). *Catalysts for Enhanced CO2 - CH4 Exchange in Natural Hydrates* (Mater of Science Master Thesis), University of Bergen.

Husebø, J. (2008). *Monitoring Depressurization and CO2-CH4 Exchange Production Scenarios for Natural Gas Hydrates*: University of Bergen.

HWU. (2013). What are Gas Hydrates. from HERIOT WATT INSTITUTE OF PETROLEUM ENGINEERING http://www.pet.hw.ac.uk/research/hydrate/hydrates_what.cfm?hy=what

Hågenvik, C. (2013). *CO2 Injection in Hydrate Bearing Sandstone with Excess Water*. (Master), University of Bergen.

IEA. (2012). World Energy Outlook 2012.

Jung, J. W., Espinoza, D. N., & Santamarina, J. C. (2010). Properties and phenomena relevant to CH4-CO2 replacement in hydrate-bearing sediments. *Journal of Geophysical Research: Solid Earth, 115*(B10), B10102. doi: 10.1029/2009JB000812

Kurihara, M., Sato, A., Funatsu, K., Ouchi, H., Yamamoto, K., Numasawa, M., Ebinuma, T., NARITA, H., Masuda, Y., Dallimore, S. R., Wright, F., & Ashford, D. I. (2010). *Analysis of Production Data for 2007/2008 Mallik Gas Hydrate Production Tests in Canada*. Paper presented at the International Oil and Gas Conference and Exhibition in China, Beijing, China. http://www.onepetro.org/mslib/app/Preview.do?paperNumber=SPE-132155-MS&societyCode=SPE

Kvenvolden, K. A., & Lorenson, T. D. (2001). *Global Occurrences of Gas Hydrate*. Paper presented at the The Eleventh International Offshore and Polar Engineering Conference http://www.onepetro.org/mslib/app/Preview.do?paperNumber=ISOPE-I-01-069&societyCode=ISOPE

Makogon, Y. F. (1997). *Hydrates of Hydrocarbons*: PennWell Publishing Company.

McCann, N., Phan, D., Wang, X., Conway, W., Burns, R., Attalla, M., Puxty, G., & Maeder, M. (2009). Kinetics and Mechanism of Carbamate Formation from CO2(aq), Carbonate Species, and Monoethanolamine in Aqueous Solution. *The Journal of Physical Chemistry A, 113*(17), 5022-5029. doi: 10.1021/jp810564z

Moridis, G. J., Collett, T. S., Boswell, R., Kurihara, M., & Reagan, M. T. (2008). *Toward Production From Gas Hydrates: Current Status, Assessment of Resources, and Model-Based Evaluation of Technology and Potential*. Paper presented at the SPE Unconventional Reservoirs Conference, Keystone, Colorado, USA. http://www.onepetro.org/mslib/app/Preview.do?paperNumber=SPE-114163-MS&societyCode=SPE

Moridis, G. J., Collett, T. S., Pooladi-Darvish, M., Hancock, S., Santamarina, C., Boswell, R., Kneafsey, T., Rutqvist, J., Reagan, M. T., Sloan, E. D., Sum, A., & Koh, C. (2010). *Challenges, Uncertainties and Issues Facing Gas Production From Hydrate Deposits in Geologic Systems*. Paper presented at the SPE Unconventional Gas Conference, Pittsburgh, Pennsylvania, USA. http://www.onepetro.org/mslib/app/Preview.do?paperNumber=SPE-131792-MS&societyCode=SPE

NIST. (2011). Isothermal Properties for Carbon dioxide from http://webbook.nist.gov/cgi/fluid.cgi?T=4+9+&PLow=0.0&PHigh=83&PInc=&Applet=on&Digits=5&ID=C124389&Action=Load&Type=IsoTherm&TUnit=C&PUnit=bar&DUnit=g%2Fml&HUnit=kJ%2Fmol&WUnit=m%2Fs&VisUnit=cP&STUnit=N%2Fm&RefState=DEF

Ota, M., Morohashi, K., Abe, Y., Watanabe, M., Smith, J. R. L., & Inomata, H. (2005). Replacement of CH4 in the hydrate by use of liquid CO2. *Energy Conversion and Management, 46*(11–12), 1680-1691. doi: http://dx.doi.org/10.1016/j.enconman.2004.10.002

Ruppel, C. (2011). Methane Hydrates and the Future of Natural Gas. *Supplemantary paper 4*. Retrieved from mitei website: http://mitei.mit.edu/system/files/Supplementary_Paper_SP_2_4_Hydrates.pdf

Schoderbek, D., Loyd, K. M., Howard, J., Silpngarmlert, S., & Hester, K. (2012). *North Slope Hydrate Fieldtrial: CO2/CH4 Exchange*. Paper presented at the OTC Arctic Technology Conference, Houston, Texas, USA. http://www.onepetro.org/mslib/app/Preview.do?paperNumber=OTC-23725-MS&societyCode=OTC

Seo, Y.-T., & Lee, H. (2001). Multiple-Phase Hydrate Equilibria of the Ternary Carbon Dioxide, Methane, and Water Mixtures. *The Journal of Physical Chemistry B, 105*(41), 10084-10090. doi: 10.1021/jp011095+

Sloan, E. D., & Koh, C. (2007). *Clathrate Hydrates of Natural Gases, Third Edition*: Taylor & Francis.

Sloan, E. D., Peter, B., Richard, C., Nader, D., Arthur, J., Emrys, J., Kimberly, J., Miriam, K., Devinder, M., Stephen, M., Robert, S., Jean, W., Scott, W., & Robert, W. (2008). *Four Critical Needs to Change the Hydrate Energy Paradigm From Assessment to Production: The 2007 Report to Congress by The U.S. Federal Methane Hydrate Advisory Committee*. Paper presented at the Offshore Technology Conference, Houston, Texas, USA. http://www.onepetro.org/mslib/app/Preview.do?paperNumber=OTC-19519-MS&societyCode=OTC

Strauss, N. (2012). *The Role of the Oil and Gas Industry in the Transition Toward a Sustainable World*. Paper presented at the SPETT 2012 Energy Conference and Exhibition, Port-of-Spain, Trinidad. http://www.onepetro.org/mslib/app/Preview.do?paperNumber=SPE-158270-MS&societyCode=SPE

Tohidi, B., Anderson, R., Clennell, M. B., Burgass, R. W., & Biderkab, A. B. (2001). Visual observation of gas-hydrate formation and dissociation in synthetic porous media by means of glass micromodels. *Geology, 29*(9), 867-870.

Yang, J., Chapoy, A., Tohidi, B., Jadhawar, P. S., Lee, J., & Huh, D. G. (2008). *Thermodynamic Conditions and Kinetics of Integrated Methane Recovery and Carbon Dioxide Sequestration*. Paper presented at the Offshore Technology Conference, Houston, Texas, USA. http://www.onepetro.org/mslib/app/Preview.do?paperNumber=OTC-19326-MS&societyCode=OTC